Title
Topics in Electricity Market Design

Author
Li, Ruoyang

Publication Date
2014

Peer reviewed|Thesis/dissertation

Topics in Electricity Market Design

by

Ruoyang Li

A dissertation submitted in partial satisfaction of the

requirements for the degree of

Doctor of Philosophy

in

Engineering - Industrial Engineering and Operations Research

in the

Graduate Division

of the

University of California, Berkeley

Committee in charge:

Professor Shmuel S. Oren , Chair
Professor Ilan Adler
Professor Duncan S. Callaway

Fall 2014

Topics in Electricity Market Design

Abstract

Topics in Electricity Market Design

by

Ruoyang Li

Doctor of Philosophy in Engineering - Industrial Engineering and Operations Research

University of California, Berkeley

Professor Shmuel S. Oren , Chair

The evolution of policy objectives and emergence of new technologies continually challenge the existing wholesale electricity market design. In the framework of standard market design based on locational marginal pricing (LMP) and two-settlement electricity markets, this dissertation investigates two topics for existing and future power systems – Convergence Bidding (CB) and distribution locational marginal pricing (DLMP). The central theme that connects these two topics is market design – determining how to create proper incentives to compensate market participants that ensures efficiency and reliability of the power grid.

We first empirically test whether the California Independent System Operator's (CAISO) existing two-settlement electricity markets are efficient, and if not, to what extent CB improves market efficiency. We examine the theoretical and empirical tools intended for other financial markets to help us understand the efficacy of CB in the forward and spot electricity markets. In the light of the efficient market hypothesis formalized by Samuelson (1965) and Fama (1970), Jensen (1978) uses the zero-profit competitive equilibrium to describe the condition for market efficiency. This definition of market efficiency directly converts the test of market efficiency into the assessment of return behavior. Following this methodology, we empirically test for market efficiency by evaluating the performance of trading strategies based on market data in the CAISO electric power markets. Our backtest results show that profitable trading opportunities continue to exist in the post-CB period, but the profitability decreases substantially. The decrease in profitability in the post-CB period indicates the improvement of market efficiency, and demonstrates the benefit of CB. The profitability in the post-CB period, however, conveys empirical implications that can be interpreted differently, depending on the level of competition and the level of risk aversion of virtual traders.

We further examine the use of DLMP to improve system efficiency in future power systems. DLMP is a modified form of LMP to alleviate congestion induced by electric vehicle (EV) loads on the distribution network. The distribution system operator (DSO) determines distribution locational marginal prices (DLMPs) by solving the

social welfare optimization for both the conventional household demand and the EV demand with marginal costs exogenously set to LMPs. We show mathematically that the socially optimal charging schedule can be implemented through a decentralized mechanism where retailers and EV aggregators respond autonomously to the posted DLMPs by maximizing their individual net surplus in the perfectly competitive local DSO market. We further investigate the problem of designing pricing mechanism when LMPs are uncertain. A robust DLMP method is developed for EV charging management under price uncertainty. The efficacy of the proposed use of DLMP is demonstrated by means of case studies using the Bus 4 distribution system of the Roy Billinton Test System (RBTS) and the Danish driving data.

To my parents,

Shichang Li and Jingqiong Wu,

to my grandparents,

Huichang Wu, Zhenxiu Chen and Donghai Li,

to Ping Kong.

Contents

List of Figures

List of Tables

Acknowledgments

This dissertation would not have been possible without the help and support of the kind people around me, to only some of whom it is possible to give particular mention here.

First and foremost I offer my sincerest gratitude to my advisor, Professor Shmuel S. Oren for providing me with the opportunity to complete my dissertation. His immense knowledge in optimization, economics, statistics, and electricity markets motivates a spectrum of unique interdisciplinary research opportunities that is not possible to find elsewhere. Even though he is heavily involved in many industry and academic activities, he has been always supportive of my research and available to advise me. He has also given me the freedom to pursue my own research interests without any objection. I am very grateful for his enthusiasm, dedication, and patience, and I simply could not wish for a better advisor.

I would like to thank to my coauthors Professor Qiuwei Wu, and Dr. Alva J. Svoboda for closely collaborating with me and generously sharing their datasets. I am indebted to my committee members Professor Ilan Adler, and Professor Duncan Callaway for agreeing to serve on my committee and making efforts to improve my dissertation on short notice.

I must express my gratitude to my colleagues Anthony Papavasiliou, Tanachai Limpaitoon, Chen Chen, Yong Liang, Felipe Castro, Zhu Yang, Paula Lipka, Clay Campaigne, Wei Qi, and Jiaying Shi, for organizing weekly seminars, providing insightful discussions, and offering constructive criticisms.

I am thankful to an intelligent and friendly group of fellow students in my cohort. They are Qi Zhang, Te Ke, Peng Yi, Long He, Zhao Ruan, Sin Man Choi, Dan Bu, Stewart Liu, and Yang Xu. Thanks also go to Cheng Lyu in my junior batch and Zhiwei Xu from Tsinghua University. I am continually amazed by their passions and achievements, and I always feel lucky to be one of them.

Finally, I thank my family, whom this dissertation is dedicated to, for supporting me throughout my study.

Chapter 1

Overview of Electricity Market

1.1 Electricity Restructuring

Starting in the early 1980s, the electricity sector has been under dramatic restructuring throughout the world, in the pursuit of competitiveness and efficiency. The earliest introduction of wholesale electricity markets and privatization of the power industry took place in Chile in the early 1980s, followed by a series of electricity market reforms in other Latin American nations, including Argentina, Peru, Brazil, and Colombia. The liberalization of the electricity sector in European and Commonwealth countries including Norway, Sweden, Finland, Demark, Great Britain, New Zealand, and Australia, occurred in 1990s.

Since 1992, a series of state and federal initiatives began the deregulation process of the electricity sector in the United States. The Independent System Operator (ISO) was formed to administer regional wholesale electricity markets, and ensure reliability for grid operations. Several regional wholesale electricity markets were established under the management of the ISOs: ISO New England (ISO-NE), New York ISO (NYISO), Pennsylvania-New Jersey-Maryland Interconnection (PJM), Midwest ISO (MISO), Electric Reliability Council of Texas (ERCOT), and California Independent System Operator (CAISO).

The development of wholesale electricity markets increases the reliance on market mechanisms that promote the efficient use of physical resources and transmission facilities. Although basic tasks of wholesale electricity markets remain the same, market designs vary across geographical jurisdictions (Stoft, 2002). This dissertation focuses on the market design based on locational marginal pricing (LMP) and two-settlement electricity markets. LMP is the pricing mechanism proposed by Bohn, Caramanis, and Schweppe (1984) to internalize significant externalities arising from the presence of Kirchhoff's laws that govern the power flow in transmission systems. The concept of LMP is later popularized by the work of Hogan (1992), and becomes the centerpiece of wholesale market design in the United States, Australia, New Zealand and Singapore. Two-settlement electricity markets consist of wholesale forward and spot electricity markets, where the forward electricity market is aimed to provide financial

instruments to hedge against price risk in the spot electricity market. This framework is often referred to as standard market design that is adopted by ISOs in the United States.

The evolution of policy objectives and emergence of new technologies continually challenge the existing wholesale market design. Driven by environmental and climate policy priorities aiming to reduce carbon emissions from the electricity sector, carbon taxes and tradable permits are under consideration for government intervention to correct negative externalities. Market mechanisms that can bridge wholesale electricity markets and emerging technologies are needed to integrate variable renewable generation and induce demand side flexibility. Financial derivatives are expected to introduce risk-sharing mechanisms that improve market efficiency of wholesale electricity markets. This dissertation investigates two topics in wholesale market design for existing and future power systems – Convergence Bidding (CB) and distribution locational marginal pricing (DLMP). For the purpose of this dissertation, the functional description of existing wholesale electricity markets is presented in the context of the CAISO electric power markets.

1.2 Pricing Mechanism

Locational marginal prices (LMPs) are the prices used for the settlement of power purchases and sales in wholesale electricity markets. LMPs are determined by the ISO to maximize social welfare with respect to the physical constraints of the transmission system, and expose producers and consumers to the marginal costs of electricity delivery at different locations. Unlike traditional commodity markets, the wholesale electricity market cannot be cleared with a single clearing-price auction, where the aggregate supply and demand curves are formed and the single clearing price is set to balance the supply and demand. The physical laws governing power flow and the capacity of the transmission lines prevent electricity from flowing freely between producers and customers on the electric power network. When the transmission lines are congested and the import of electricity from cheap producers are constrained, the ISO is forced to use some local but expensive producers for power generation in order to satisfy the demand. As a result, LMPs are high in the downstream areas of the congested transmission lines, and low in the upstream areas. The differences between LMPs in the downstream areas and the upstream areas are congestion rents that reflect the marginal values of the scarce transmission resources. LMPs are calculated for a number of locations on the electric power network. These locations are called nodes, and each node represents the geographic region where physical resources are aggregated.

1.3 Two-Settlement Electricity Markets

This dissertation focuses on the CAISO's market design, where two-settlement electricity markets are implemented. The CAISO's two-settlement electricity markets consist of two interrelated markets: day-ahead (DA) market, and real-time (RT) market. The DA market is a forward market, where energy can be purchased at forward prices, also called day-ahead LMPs (DA LMPs). The RT market is a spot market, where energy can be purchased at spot prices, also called real-time LMPs (RT LMPs). DA LMPs are generally considered more stable than RT LMPs. In the RT market, price spikes are often triggered by unplanned outages of generation plants and transmission facilities, and unpredictable weather, while the DA market is less affected due to a longer planning horizon.

The DA market includes three sequential processes: market power mitigation and reliability requirement determination (MPM-RRD), integrated forward market (IFM), and residual unit commitment (RUC). The MPM-RRD starts the day before delivery. Market participants are allowed to submit supply and demand bids for both physical and virtual trades until the start of the MPM-RRD. In the MPM-RRD, the ISO mitigates bids from physical resources that exercise locational market power, and ensures the availability of physical resources whose outputs are required to maintain local reliability. The results of the MPM-RRD are a pool of bids that is ready for the IFM. In the IFM, the ISO economically clears the supply bids against the demand bids with the transmission constraints enforced, determines DA schedules and DA LMPs, and procures ancillary services. When the CAISO forecast of demand exceeds the total physical supply cleared in the IFM, the additional capacity is procured by the ISO in the RUC to satisfy reliability requirements. Note that the additional resources procured in the RUC are not directly used for production, and hence do not receive DA LMPs. However, there are still costs to keep these resources staying online, namely start-up costs and minimum load costs, as discussed later.

In the RT market, the ISO runs the economic dispatch process every 5 minutes to rebalance the residual demand, which is the deviation between the instantaneous demand and the scheduled demand in the DA market. RT LMPs are determined to settle the residual demand and the supply used to balance the residual demand.

While DA and RT LMPs reflect the cost of energy production, generation plants also incur start-up and minimum load costs which they submit as part of their bids. Start-up costs are the costs that are incurred when generation plants are turned on, and minimum load costs are the costs that maintain generation plants to operate at the minimum load level. The CAISO guarantees that all dispatched resources who submit economic bids will cover their costs in the DA and RT markets. Hence, if a resource does not cover its total cost including start-up and minimum load cost through its energy revenue at DA and RT LMPs, its shortfall is covered by an uplift payment which is allocated to market participants based on a two-tier cost allocation scheme that considers both causation and socialization. The tier 1 uplift costs account for cost causation, and the tier 2 uplift costs account for cost socialization.

1.4 CB in Two-Settlement Electricity Markets

To provide hedging instruments against volatile wholesale spot prices, forward contracts and other financial derivatives have been introduced into these deregulated electricity markets. Financial incentives attract virtual traders to play their critical role in price discovery and market efficiency through exploiting arbitrage opportunities. CB is a financial mechanism that allows market participants, including electricity providers, retailers and virtual traders, to arbitrage price discrepancies between the forward and spot electricity markets. After the introduction of CB in the other five regional wholesale electricity markets, the CAISO has implemented CB on February 1, 2011 under Federal Energy Regulatory Commission's (FERC) September 21, 2006 Market Redesign and Technology Upgrade (MRTU) Order.

CB allows market participants to arbitrage between the DA and RT markets through a financial mechanism, exempting them from physically consuming or producing energy. A virtual demand bid is to make financial purchases of energy in the DA market, with the explicit requirement to sell back that energy in the RT market at the same location. Conversely, a virtual supply bid is to make financial sales of energy in the DA market, with the explicit requirement to buy back that energy in the RT market at the same location. On the physical side, the positions taken in the DA market are offset by the opposite positions in the RT market, which leaves market participants with no physical obligation. In anticipation of DA LMPs being less than RT LMPs, market participants can make profits by using virtual demand bids to effectively buy energy in the DA market and sell it back in the RT market. These virtual demand bids result in the additional demand in the DA market that increases DA LMPs, and the additional supply in the RT market that decreases RT LMPs. This yields the desired outcome of CB – price convergence.

Price convergence is regarded as a benefit to the DA and RT markets. It reduces the incentives for market participants to defer their physical resources to the RT market in expectation of favorable RT LMPs. The improved stability of the DA market is beneficial from reliability perspectives. To ensure reliability of the power grid, the ISO is required to procure sufficient capacity in the RUC, when the total physical supply cleared in the IFM is not enough to meet the CAISO forecast of demand. With physical resources withheld by market participants, the ISO tends to over-procure capacity in the RUC. This raises the RUC uplift costs, and increases the risk of decommiting scheduled resources in the RT market when deferred physical resources show up.

The benefit of CB also comes from the fact that it relieves market participants from using physical resources to arbitrage price differences between the DA and RT markets, also called implicit virtual bidding in some literature. Implicit virtual bidding is the bidding strategy where market participants intentionally defer their physical resources to the RT market to take advantage of favorable RT LMPs, by bidding at prices that are unlikely to be cleared in the DA market rather than their economic costs and benefits. Although implicit virtual bidding can achieve price convergence in the absence of CB, it can also lead to disastrous effects that jeopardize the efficiency

of the DA and RT markets. Without the revelation of the true economic costs and benefits of physical resources, it is difficult for the ISO to allocate resources efficiently and optimally. In addition, the prices at which market participants bid their physical resources largely depend on their own anticipation of DA and RT LMPs, and this introduces uncertainty into the DA market. In some cases, the ISO can either over-schedule physical supply in the IFM that has to be sold back in the RT market, or under-schedule physical supply in the IFM that relies on the procurement in the RUC to balance. These variations decrease the stability of the DA market, and significantly undermine reliability of the power grid.

CB can be conducted at both nodes and trading hubs. In comparison to nodes, trading hubs provide more liquidity to trade large volumes of virtual bids. There are three trading hubs in the CAISO electric power markets, that corresponds to three congestion management zones: NP15, SP15 and ZP26. DA and RT LMPs at the trading hub represent the weighted average of prices at generation nodes within the corresponding congestion management zone. The weights are determined annually based on the seasonal generation in the previous year, and are differentiated by peak and off-peak hours. The virtual bids submitted at the trading hub are distributed to generation nodes in proportion to their weights, and are bound together so that they are cleared as a whole in the DA market.

The credit policy for CB requires that the current exposure of virtual bids submitted by a market participant may not exceed the collateral established with the ISO. The current exposure of virtual bids is calculated by the sum of the product of the quantity and the corresponding reference price of each virtual bid. For one node, the reference price is the 95th percentile value of the historical price differences between DA and RT LMPs. After the settlement of virtual bids, the collateral is adjusted based on the realized profits and losses of virtual bids.

There is no transaction fee imposed on submitted virtual bids, but cleared virtual bids are required to pay uplift costs. The costs allocated to cleared virtual bids include the IFM tier 1 uplift costs, and the RUC tier 1 uplift costs. In particular, cleared virtual demand bids are obligated to pay a proportion of the IFM tier 1 uplift costs, as virtual demand bids tend to increase physical supply procured in the IFM. Cleared virtual supply bids are subject to a proportion of the RUC tier 1 uplift costs, as the ISO tends to under-schedule physical supply in the IFM due to virtual supply bids and increase additional capacity procured in the RUC. The costs allocated to 1 MWh of cleared virtual position are estimated to be between \$0.065 and \$0.085 by the CAISO.

1.5 Scope of the Dissertation

In Chapter 1, we have provided a basic overview of electricity market restructuring and a functional description of existing wholesale electricity markets. This stand-alone chapter is meant to convey background information to readers who do not possess prior knowledge on electricity market design. The material of this chapter is

reproduced in the introduction sections of Chapter 2 and Chapter 3 so that they can stand alone as independent publications.

In Chapter 2, the central question is to address whether the CAISO's existing two-settlement electricity markets are efficient, and if not, to what extent CB improves market efficiency. We examine the theoretical and empirical tools intended for other financial markets to help us understand the efficacy of CB in the forward and spot electricity markets. In the light of the efficient market hypothesis formalized by Samuelson (1965) and Fama (1970), Jensen (1978) uses the zero-profit competitive equilibrium to describe the condition for market efficiency. This definition of market efficiency directly converts the test of market efficiency into the assessment of return behavior. Following this methodology, we empirically test for market efficiency by evaluating the performance of trading strategies based on market data in the CAISO electric power markets. The implications of market efficiency is further discussed in the context of trading performance.

In Chapter 3, we investigate the use of DLMP to improve system efficiency in future power systems. DLMP is a modified form of LMP to alleviate congestion induced by electric vehicle (EV) loads on the distribution network. The distribution system operator (DSO) determines distribution locational marginal prices (DLMPs) by solving the social welfare optimization for both the conventional household demand and the EV demand. Supply busses connecting the distribution system to the transmission grid are treated as generation nodes with marginal costs exogenously set to LMPs for each bus. We show mathematically that the socially optimal charging schedule can be implemented through a decentralized mechanism where retailers and EV aggregators respond autonomously to the posted DLMPs by maximizing their individual net surplus in the perfectly competitive local DSO market. We further investigate the problem of designing pricing mechanism when LMPs are uncertain. A robust DLMP method is developed for EV charging management under price uncertainty. The efficacy of the proposed use of DLMP is demonstrated by means of case studies using the Bus 4 distribution system of the Roy Billinton Test System (RBTS) and the Danish driving data.

In Chapter 4, we summarize all findings and provide concluding remarks.

Chapter 2

Efficiency Impact of Convergence Bidding on the California Electricity Market

2.1 Introduction

The California Independent System Operator (CAISO) has implemented Convergence Bidding (CB) on February 1, 2011 under Federal Energy Regulatory Commission's (FERC) September 21, 2006 Market Redesign and Technology Upgrade (MRTU) Order. CB is a financial mechanism that allows market participants, including electricity suppliers, consumers and virtual traders, to arbitrage price differences between the day-ahead (DA) market and the real-time (RT) market without physically consuming or producing energy. In this chapter, we analyze market data in the CAISO electric power markets, and empirically test for market efficiency by assessing the performance of trading strategies from the perspective of virtual traders. By viewing DA-RT spreads as payoffs from a basket of correlated assets, we can formulate a chance constrained portfolio selection problem, where the chance constraint takes two different forms as a value-at-risk (VaR) constraint and a conditional value-at-risk (CVaR) constraint, to find the optimal trading strategy. A hidden Markov model (HMM) is further proposed to capture the presence of the time-varying forward premium. Our backtesting results cast doubt on the efficiency of the CAISO electric power markets, as the trading strategy generates consistent profits after the introduction of CB, even in the presence of transaction costs. Nevertheless, by comparing with the performance before the introduction of CB, we find that the profitability decreases significantly, which enables us to identify the efficiency gain brought about by CB.

2.2 Market Efficiency and Trading Strategy

Since 1992, the electricity sector in the United States began the process of deregulation in the pursuit of competitiveness and efficiency. The Independent System Operator (ISO) was formed to administer regional wholesale electricity markets, and ensure reliability for grid operations. Several regional wholesale electricity markets were established under the management of the ISOs: ISO New England (ISO-NE), New York ISO (NYISO), Pennsylvania-New Jersey-Maryland Interconnection (PJM), Midwest ISO (MISO), Electric Reliability Council of Texas (ERCOT), and California Independent System Operator (CAISO). To provide hedging instruments against volatile wholesale spot prices, forward contracts and other financial derivatives have been introduced into these deregulated electricity markets. Financial incentives attract virtual traders to play their critical role in price discovery and market efficiency through exploiting arbitrage opportunities. Convergence Bidding (CB) is a financial mechanism that allows market participants, including electricity providers, retailers and virtual traders, to arbitrage price discrepancies between the forward and spot electricity markets. After the introduction of CB in the other five regional wholesale electricity markets, the CAISO has implemented CB on February 1, 2011 under Federal Energy Regulatory Commission's (FERC) September 21, 2006 Market Redesign and Technology Upgrade (MRTU) Order. The central question of this study is to address whether the CAISO's forward and spot electricity markets are efficient, and if not, to what extent CB improves market efficiency.

Recently, Jha and Wolak (2013) have employed hypothesis testing to assess the impact of CB on the CAISO electric power market efficiency. Specifically, they calculate the implied no-arbitrage trading costs for which risk neutral traders will reject the hypothesis that a profitable arbitrage opportunity between the day-ahead (DA) and real-time (RT) market prices (after incurring such trading costs) does exist. They estimate the implied no-arbitrage trading costs, derived from several heuristic trading strategies, before and after the introduction of CB in the CAISO electric power markets. Their estimates show that the implied no-arbitrage trading costs have declined after the introduction of CB which indicates an improvement in market efficiency through price convergence.

We examine the theoretical and empirical tools intended for other financial markets to help us understand the efficacy of CB in the forward and spot electricity markets. The efficient market hypothesis first formalized by Samuelson (1965) and Fama (1970), asserts that at any given time asset prices should always reflect all available information, and change quickly to incorporate new information. Jensen (1978) defines market efficiency in terms of trading profitability – "a market is efficient with respect to [an] information set, if it is impossible to make economic profits by trading on the basis of [this] information set." In particular, if anomalous returns are not high enough for a sophisticated trader to generate consistent profits after allowing for transactions costs, they are not economically significant. The definition of market efficiency by Jensen (1978) directly converts the test of market efficiency into the assessment of return behavior. Following this methodology, we test the efficiency of

the forward and spot electricity markets by developing robust forecasting models and exploring profitable trading strategies. The trading strategy implemented is back-tested using market data in the CAISO electric power markets. Market efficiency is then evaluated in the context of trading performance.

This chapter is organized as follows. Section 2.3 introduces the CAISO's two-settlement electricity markets and the current market design for CB. Section 2.4 presents the formulation of the virtual trader's optimization problem. Section 2.5 presents the regime switching model to capture the time-varying forward premium in electricity markets. Section 2.6 describes the data used in the study. Section 2.7 examines market efficiency and presents some empirical evidence. Section 2.8 discusses the implication of market efficiency. Section 2.9 summarizes the results.

2.3 CAISO Electric Power Markets

Pricing Mechanism

Locational marginal prices (LMPs) are the prices used for the settlement of power purchases and sales in wholesale electricity markets. LMPs are determined by the ISO to maximize social welfare with respect to the physical constraints of the transmission system, and expose producers and consumers to the marginal costs of electricity delivery at different locations. Unlike traditional commodity markets, the wholesale electricity market cannot be cleared with a single clearing-price auction, where the aggregate supply and demand curves are formed and the single clearing price is set to balance the supply and demand. The physical laws governing power flow and the capacity of the transmission lines prevent electricity from flowing freely between producers and customers on the electric power network. When the transmission lines are congested and the import of electricity from cheap producers are constrained, the ISO is forced to use some local but expensive producers for power generation in order to satisfy the demand. As a result, LMPs are high in the downstream areas of the congested transmission lines, and low in the upstream areas. The differences between LMPs in the downstream areas and the upstream areas are congestion rents that reflect the marginal values of the scarce transmission resources. LMPs are calculated for a number of locations on the electric power network. These locations are called nodes, and each node represents the geographic region where physical resources are aggregated.

Two-Settlement Electricity Markets

The two-settlement electricity markets consist of two interrelated markets: DA market, and RT market. The DA market is a forward market, where energy can be purchased at forward prices, also called day-ahead LMPs (DA LMPs). The RT market is a spot market, where energy can be purchased at spot prices, also called real-time LMPs (RT LMPs). DA LMPs are generally considered more stable than

RT LMPs. In the RT market, price spikes are often triggered by unplanned outages of generation plants and transmission facilities, and unpredictable weather, while the DA market is less affected due to a longer planning horizon.

The DA market includes three sequential processes: market power mitigation and reliability requirement determination (MPM-RRD), integrated forward market (IFM), and residual unit commitment (RUC). The MPM-RRD starts the day before delivery. Market participants are allowed to submit supply and demand bids for both physical and virtual trades until the start of the MPM-RRD. In the MPM-RRD, the ISO mitigates bids from physical resources that exercise locational market power, and ensures the availability of physical resources whose outputs are required to maintain local reliability. The results of the MPM-RRD are a pool of bids that is ready for the IFM. In the IFM, the ISO economically clears the supply bids against the demand bids with the transmission constraints enforced, determines DA schedules and DA LMPs, and procures ancillary services. When the CAISO forecast of demand exceeds the total physical supply cleared in the IFM, the additional capacity is procured by the ISO in the RUC to satisfy reliability requirements. Note that the additional resources procured in the RUC are not directly used for production, and hence do not receive DA LMPs. However, there are still costs to keep these resources staying online, namely start-up costs and minimum load costs, as discussed later.

In the RT market, the ISO runs the economic dispatch process every 5 minutes to rebalance the residual demand, which is the deviation between the instantaneous demand and the scheduled demand in the DA market. RT LMPs are determined to settle the residual demand and the supply used to balance the residual demand.

While DA and RT LMPs reflect the cost of energy production, generation plants also incur start-up and minimum load costs which they submit as part of their bids. Start-up costs are the costs that are incurred when generation plants are turned on, and minimum load costs are the costs that maintain generation plants to operate at the minimum load level. The CAISO guarantees that all dispatched resources who submit economic bids will cover their costs in the DA and RT markets. Hence, if a resource does not cover its total cost including start-up and minimum load cost through its energy revenue at DA and RT LMPs, its shortfall is covered by an uplift payment which is allocated to market participants based on a two-tier cost allocation scheme that considers both causation and socialization. The tier 1 uplift costs account for cost causation, and the tier 2 uplift costs account for cost socialization.

CB in Two-Settlement Electricity Markets

CB allows market participants to arbitrage between the DA and RT markets through a financial mechanism, exempting them from physically consuming or producing energy. A virtual demand bid is to make financial purchases of energy in the DA market, with the explicit requirement to sell back that energy in the RT market at the same location. Conversely, a virtual supply bid is to make financial sales of energy in the DA market, with the explicit requirement to buy back that energy in the RT market at the same location. On the physical side, the positions taken in

the DA market are offset by the opposite positions in the RT market, which leaves market participants with no physical obligation. In anticipation of DA LMPs being less than RT LMPs, market participants can make profits by using virtual demand bids to effectively buy energy in the DA market and sell it back in the RT market. These virtual demand bids result in the additional demand in the DA market that increases DA LMPs, and the additional supply in the RT market that decreases RT LMPs. This yields the desired outcome of CB – price convergence.

Price convergence is regarded as a benefit to the DA and RT markets. It reduces the incentives for market participants to defer their physical resources to the RT market in expectation of favorable RT LMPs. The improved stability of the DA market is beneficial from reliability perspectives. To ensure reliability of the power grid, the ISO is required to procure sufficient capacity in the RUC, when the total physical supply cleared in the IFM is not enough to meet the CAISO forecast of demand. With physical resources withheld by market participants, the ISO tends to over-procure capacity in the RUC. This raises the RUC uplift costs, and increases the risk of decommiting scheduled resources in the RT market when deferred physical resources show up.

The benefit of CB also comes from the fact that it relieves market participants from using physical resources to arbitrage price differences between the DA and RT markets, also called implicit virtual bidding in some literature. Implicit virtual bidding is the bidding strategy where market participants intentionally defer their physical resources to the RT market to take advantage of favorable RT LMPs, by bidding at prices that are unlikely to be cleared in the DA market rather than their economic costs and benefits. Although implicit virtual bidding can achieve price convergence in the absence of CB, it can also lead to disastrous effects that jeopardize the efficiency of the DA and RT markets. Without the revelation of the true economic costs and benefits of physical resources, it is difficult for the ISO to allocate resources efficiently and optimally. In addition, the prices at which market participants bid their physical resources largely depend on their own anticipation of DA and RT LMPs, and this introduces uncertainty into the DA market. In some cases, the ISO can either over-schedule physical supply in the IFM that has to be sold back in the RT market, or under-schedule physical supply in the IFM that relies on the procurement in the RUC to balance. These variations decrease the stability of the DA market, and significantly undermine reliability of the power grid.

CB can be conducted at both nodes and trading hubs. In comparison to nodes, trading hubs provide more liquidity to trade large volumes of virtual bids. There are three trading hubs in the CAISO electric power markets, that corresponds to three congestion management zones: NP15, SP15 and ZP26. DA and RT LMPs at the trading hub represent the weighted average of prices at generation nodes within the corresponding congestion management zone. The weights are determined annually based on the seasonal generation in the previous year, and are differentiated by peak and off-peak hours. The virtual bids submitted at the trading hub are distributed to generation nodes in proportion to their weights, and are bound together so that they are cleared as a whole in the DA market.

The credit policy for CB requires that the current exposure of virtual bids submitted by a market participant may not exceed the collateral established with the ISO. The current exposure of virtual bids is calculated by the sum of the product of the quantity and the corresponding reference price of each virtual bid. For one node, the reference price is the 95th percentile value of the historical price differences between DA and RT LMPs. After the settlement of virtual bids, the collateral is adjusted based on the realized profits and losses of virtual bids.

There is no transaction fee imposed on submitted virtual bids, but cleared virtual bids are required to pay uplift costs. The costs allocated to cleared virtual bids include the IFM tier 1 uplift costs, and the RUC tier 1 uplift costs. In particular, cleared virtual demand bids are obligated to pay a proportion of the IFM tier 1 uplift costs, as virtual demand bids tend to increase physical supply procured in the IFM. Cleared virtual supply bids are subject to a proportion of the RUC tier 1 uplift costs, as the ISO tends to under-schedule physical supply in the IFM due to virtual supply bids and increase additional capacity procured in the RUC. The costs allocated to 1 MWh of cleared virtual position are estimated to be between \$0.065 and \$0.085 by the CAISO.

2.4 Portfolio Optimization

Formulation

In the DA and RT markets, the ISO determines DA LMPs $P_t^{DA} \in \mathbb{R}^{24}$ and RT LMPs $P_t^{RT} \in \mathbb{R}^{24}$ for one node on day t, for $t = 1, \ldots, T$. Both P_t^{DA} and P_t^{RT} contain 24 hourly market-clearing prices for 1 MWh of electricity. DA-RT spreads can be expressed as $R_t = P_t^{DA} - P_t^{RT}$. The virtual trader's objective is to maximize the expected payoff of his virtual bids (2.1) with respect to a budget constraint (2.2), by entering virtual positions $x_t \in \mathbb{R}^{24}$ in the DA market and closing those positions in the RT market,

$$\text{(P0)} \quad \max_{x_t} \quad E\left[R_t^T x_t\right] - \tau \|x_t\|_1 \tag{2.1}$$

$$s.t. \quad C\|x_t\|_1 \leq W_0 \tag{2.2}$$

where τ is the costs allocated to 1 MWh of virtual position, C is the reference price for 1 MWh of virtual position, and W_0 is the initial collateral. In this formulation, we implicitly assume that virtual traders behave as price-takers, and that contract can be fractional. $x_t^{(j)} \geq 0$ denotes a virtual supply bid, and we can equivalently view it as taking a long position in the corresponding DA-RT spread, while $x_t^{(j)} < 0$ denotes a virtual demand bid, and we can equivalently view it as taking a short position in the corresponding DA-RT spread.[1] In the budget constraint (2.2), both supply and demand bids must provide collateral separately, as they are not allowed to offset each

[1] $x_t^{(j)}$ is the j-th entry of x_t.

other under the current credit policy for CB. This formulation can be easily extended to multiple-node networks.

Without loss of generality, we assume $W_0 = 1$. The collateral used to establish virtual positions in DA-RT spreads is $y_t = Cx_t$ and the costs associated with 1 dollar of collateral are $\tau^c = \frac{1}{C}\tau$. By viewing DA-RT spreads as payoffs from a basket of correlated assets, the returns on DA-RT spreads are then defined as $R_t^c = \frac{1}{C}R_t = \frac{1}{C}\big(P_t^{DA} - P_t^{RT}\big)$. With these substitutions, (P0) is equivalent to (P1),

$$\begin{aligned} \text{(P1)} \quad \max_{y_t} \quad & E[R_t^{cT} y_t] - \tau^c \|y_t\|_1 && (2.3)\\ \text{s.t.} \quad & \|y_t\|_1 \le 1, && (2.4) \end{aligned}$$

which is a portfolio optimization problem in the presence of linear transaction costs. The budget constraint (2.4) requires that the absolute value of weights must sum up to one. This is different from the standard portfolio optimization problem where long and short positions can be netted out. We can further formulate a chance constrained portfolio selection problem, where the chance constraint takes two different forms as a value-at-risk (VaR) constraint and a conditional value-at-risk (CVaR) constraint, to find the optimal trading strategy.

Portfolio Optimization under a VaR Constraint

VaR is a modern way of measuring the risk of a portfolio, based on computing probabilities of large losses of the portfolio. Mathematically, $\text{VaR}(z;\eta) = \inf\{\gamma | P(z \le \gamma) \ge \eta\}$ is the level η-quantile of the random variable z denoting the losses. To put it another way, the confidence level η is the probability that losses do not exceed or equal to $\text{VaR}(z;\eta)$. (P1) can be reformulated as a portfolio optimization problem (VAR0(γ,η)) under a VaR constraint (2.6),

$$\begin{aligned} \text{(VAR0}(\gamma,\eta)\text{)} \quad \max_{y_t} \quad & E[R_t^{cT} y_t] - \tau^c \|y_t\|_1 && (2.5)\\ \text{s.t.} \quad & \text{VaR}(-R_t^{cT} y_t;\eta) \le \gamma && (2.6)\\ & \|y_t\|_1 \le 1 && (2.7) \end{aligned}$$

where γ is the predetermined upper bound for the VaR of the portfolio.

Assuming R_t^c follows a multivariate Gaussian distribution $\mathbf{N}(\mu_t, \Sigma_t)$, $-R_t^{cT} y_t - \gamma$ follows a multivariate Gaussian distribution $\mathbf{N}(-\mu_t^T y_t - \gamma, y_t^T \Sigma_t y_t)$. Thus, the tail probability is $P(-R_t^{cT} y_t \le \gamma) = \Phi(\frac{1}{\sqrt{y_t^T \Sigma_t y_t}}(\mu_t^T y_t + \gamma))$, where Φ is the cumulative distribution function of the standard multivariate Gaussian distribution. By substituting the tail probability into (2.6), it yields $\Phi(\frac{1}{\sqrt{y_t^T \Sigma_t y_t}}(\mu_t^T y_t + \gamma)) \ge \eta$, and (VAR0$(\gamma,\eta)$) can be rewritten as (VAR1(γ,η)),

$$\begin{aligned} \text{(VAR1}(\gamma,\eta)\text{)} \quad \max_{y_t} \quad & \mu_t^T y_t - \tau^c \|y_t\|_1 && (2.8)\\ \text{s.t.} \quad & \mu_t^T y_t + \gamma \ge \Phi^{-1}(\eta) \|\Sigma_t^{\frac{1}{2}} y_t\|_2 && (2.9)\\ & \|y_t\|_1 \le 1. && (2.10) \end{aligned}$$

As shown in Table 2.3 and Table 2.4, DA-RT spreads are negatively skewed in most of the hours, which cannot be modeled properly by a normal distribution. Without assuming normality, VaR cannot be written in a closed form, and there is no guarantee that VaR is convex. Nemirovski and Shapiro (2006) propose a computationally tractable approximation of the non-convex VaR constraint. Therefore, we can replace the VaR constraint (2.6) with the Chebyshev bound (2.134) yielding (VAR2(γ,η)),[2]

$$\begin{aligned}
(\text{VAR2}(\gamma,\eta)) \quad \max_{y_t} \quad & \mu_t^T y_t - \tau^c \|y_t\|_1 && (2.11)\\
\text{s.t.} \quad & -E[(R_t^{cT} y_t + \gamma)] + (\eta E[(R_t^{cT} y_t + \gamma)^2])^{\frac{1}{2}} \leq 0 && (2.12)\\
& \|y\|_1 \leq 1. && (2.13)
\end{aligned}$$

Note that the Chebyshev bound (2.134) is a conservative approximation of the VaR constraint (2.6), which implies that the confidence level realized is higher than the confidence level intended η.

Portfolio Optimization under a CVaR Constraint

Since VaR is incapable of addressing the distribution of losses beyond VaR$(z;\eta)$, CVaR is introduced by Rockafellar and Uryasev (2000) as an alternative risk assessment technique to account for losses in the tail of the distribution. For continuous distributions, CVaR is defined as the conditional tail expectation exceeding VaR$(z;\eta)$, CVaR$(\text{z},\eta) = E[z|z \geq \text{VaR}(\text{z},\eta)]$. In this case, the optimization problem can be stated as follows,

$$\begin{aligned}
(\text{CVAR0}(\gamma,\eta)) \quad \max_{y_t} \quad & E[R_t^{cT} y_t] - \tau^c \|y_t\|_1 && (2.14)\\
\text{s.t.} \quad & \text{CVaR}(-R_t^{cT} y_t;\eta) \leq \gamma && (2.15)\\
& \|y_t\|_1 \leq 1. && (2.16)
\end{aligned}$$

VaR and CVaR can be characterized by function $g_\eta(z,\rho) = \rho + \frac{1}{1-\eta} E[(z-\rho)_+]$ in the following forms,

$$\begin{aligned}
\text{CVaR}(z,\eta) &= \min_{\rho} g_\eta(z,\rho), && (2.17)\\
\text{VaR}(z,\eta) &= \arg\min_{\rho} g_\eta(z,\rho). && (2.18)
\end{aligned}$$

Thus, by substituting the CVaR constraint (2.15) with (2.17), (CVAR0(γ,η)) becomes

$$\begin{aligned}
(\text{CVAR1}(\gamma,\eta)) \quad \max_{y_t} \quad & E[R_t^{cT} y_t] - \tau^c \|y_t\|_1 && (2.19)\\
\text{s.t.} \quad & g_\eta(-R_t^{cT} y_t, \rho) \leq \gamma && (2.20)\\
& \|y_t\|_1 \leq 1. && (2.21)
\end{aligned}$$

[2]See Appendix B for details.

2.5 Regime Switching Model

Spot Price and Forward Price

In deregulated electricity markets, the prominent features of electricity spot prices include, mean-reversion, seasonality, and spikes. The causes of these features can be traced to the inherent characteristics of electricity. As the supply function of power generation becomes much steeper above a certain capacity level, the marginal production cost increases substantially with the aggregate demand. The consumer demand is highly inelastic and varies widely from season to season, resulting in seasonal variations in the levels of electricity spot prices. The difficulty of storing electricity further limits the feasibility of holding inventories to arbitrage and smooth price discrepancies across time periods. In some extreme cases, price spikes occur when the power system is not flexible enough in response to forced outages of power plants and unexpected contingencies in the transmission networks within a short time frame. Price spikes are frequently seen during the summer, when the demand is high.

Regime switching models seem to be natural candidates to study the dramatic alternations in the behavior of electricity spot prices. Deng (2000) proposes several mean-reversion jump-diffusion models with parameters varying in different regimes to capture the systematic alternations of electricity spot prices among different equilibrium states of supply and demand. Mount, Ning, and Cai (2006) investigate the predictability of price spikes in electricity markets using daily on-peak average spot prices and loads. They adopts a probabilistic model with two regimes, where the state variables are the load and the reserve margin. However, the prediction accuracy decreases substantially when forecasts of the state variables are used.

In electricity forward markets, there is a wide range of tradable instruments with maturities varying from a day, a week, a month, to a year. Here we mainly present studies that focus on modeling forward prices that are settled one day ahead of delivery by regime switching. De Jong (2006) provides statistical evidence that the regime switching model outperforms the generalized autoregressive conditional heteroskedasticity (GARCH) model and the stochastic Poisson jump model. The consistent test results from various day-ahead spot markets in Europe and the United States make a convincing case for the use of regime switching models to capture price dynamics in electricity markets.[3] Haldrup and Nielsen (2006) analyze market data in Nord Pool with a regime switching model that features long memory. They find that the regime switching model is superior to the non-switching model in terms of out-of-sample forecasting performance. Some other successful applications of regime switching models to electricity forward prices are presented in Huisman and Mahieu (2003), Rafał Weron (2009), and Janczura and Rafal Weron (2010).

[3]The day-ahead spot market or the spot market in Europe is similar to the DA market in the United States, where the delivery of electricity for each of the 24 hours is settled one day in advance.

Time-Varying Forward Premium

The forward premium is defined as the difference between the forward prices and the expected spot prices. In electricity markets, the 24 hourly forward premia FP_t on day t take the form,

$$FP_t = E_{t-1}[P_t^{DA} - P_t^{RT}] = E_{t-1}[R_t]. \tag{2.22}$$

There exists extensive literature on the time-varying property of the forward premium – a situation where the forward premium varies through time to reflect economic risk. The time-varying forward premium is observed and well documented in exchange rates and traditional commodity markets. In one of the seminal papers, Fama (1984) first attributes the behavior of forward exchange rates to a time-varying forward premium, and finds that the variation in the forward premium accounts for a substantial proportion of the variation in forward exchange rates. In addition to Fama (1984), other papers focusing on explaining the determination of the time-varying forward premium include Fama and French (1987), Bekaert and Hodrick (1993), Backus, Foresi, and Telmer (2001), and Baillie and Kilic (2006).

Recently, there is a growing literature investigating the time-varying forward premium in electricity markets. These studies present empirical evidence that supports the risk-factor-related time variation in the electricity forward premium. Bessembinder and Lemmon (2002) develop a general equilibrium model for forward prices, where the difference between the equilibrium forward price and the expected wholesale price can be explained by risk-related factors that reflect the net hedging pressure of producers and consumers. The risk-related factors are approximated in terms of the central moments of the distribution of wholesale spot prices. To be specific, the electricity forward premium is negatively correlated to spot price volatility, but positively correlated to spot price skewness. The model is empirically verified by using data from the PJM power market and the California Power Exchange (CALPX) at a monthly level.[4] The one-month forward price is estimated by the average of one-month forward prices prior to the delivery month. They also point out that in a frictionless market with risk-neutral outside speculators, the forward prices would converge to the expected spot prices. Based on a data set of hourly spot and forward prices in the PJM power market, Longstaff and A. W. Wang (2004) find evidence that supports the structural model presented in Bessembinder and Lemmon (2002) at an hourly level. They also conclude that the forward premium is fundamentally related to the risk premium required by market participants to compensate for uncertainty.

Shawky, Marathe, and Barrett (2003) conduct studies on the spot and future price relationship, based on the contracts traded on the New York Mercantile Exchange and delivered at the California-Oregon Border. They find the forward premium of electricity is larger than those of other commodities. An exponential GARCH specification is employed to model the time-varying volatility clustering in the forward

[4] The CalPX was founded in 1998. It declared bankruptcy and permanently ceased market operations during 2000-2001 California energy crisis. During its existence, the CALPX administered market transactions, while the CAISO ensured the reliable management of transmission network.

premium time series. Cartea and Villaplana (2008) propose a model to forecast wholesale electricity prices in different states identified by two observable state variables – demand and capacity. By testing their model in the PJM, England and Wales, and Nord Pool markets, they present empirical results that the forward premium exhibits a seasonal pattern. The forward premium is high during the months of high demand volatility. Benth, Cartea, and Kiesel (2008) provide a framework to explain the forward premium with two market factors – the levels of risk aversion of buyers and sellers, and the market power of producers relative to that of consumers.

As mentioned, the existing literature extensively studies the time-varying forward premium by statistical models with observable state variables, namely the volatility and skewness of spot prices, the level of risk aversion, market structure, and demand and supply capacity. The choice of state variables is largely predetermined and varies across different electricity markets, which limits the possibility to arrive at a generalization. From a different perspective, the time-varying forward premium can be subject to regime shifts, where the behavior of the forward premium exhibits dramatic changes. Lucia and Schwartz (2002) propose a factor model with unobservable state variables, for the purposes of derivative pricing. These unobservable state variables can be further interpreted as latent market regimes. However, their model is primarily aimed to forecast the forward curve – forward prices with different maturities, rather than the forward premium. To the authors' best knowledge, there is no paper on modeling the electricity forward premium with unobservable states. Our study therefore is intended to fill this gap by introducing a hidden Markov model (HMM) to model the regime shifts in the electricity forward premium.

Model Description

A HMM can be presented as a dynamic bayesian network model in which the underlying state transition follows a Markov process. Each state has a probability distribution over the possible observations. The state is assumed to be invisible to the observer, but the observation is visible. Therefore some information about the sequence of states can be inferred from the sequence of observations. In the context of CB, $\{S_t, R_t\}_{t=1}^T$ is a discrete-time stochastic process, where the sequence of states $\{S_t\}_{t=1}^T$ is an unobserved Markov chain.[5] Given $\{S_t\}_{t=1}^T$, the observed sequence of DA-RT spreads $\{R_t\}_{t=1}^T$ is a sequence of conditionally independent random variables with the conditional distribution depending on $\{S_t\}_{t=1}^T$ only through the current state of the chain S_t. In this study, we assume the conditional probability density function of R_t, given the occurrence of S_t, follows a Gaussian mixture distribution. This HMM variant is also called Gaussian mixture hidden Markov model (GMHMM). The GMHMM is illustrated in Figure 2.1.

We assume there exist M different states in the GMHMM and N different clusters in the Gaussian mixture distribution. The equation for DA-RT spreads R_t given the

[5]We use upper case letters to denote random variables, and lower case letters to denote realizations of random variables.

cluster z_t, for $z_t = 1, \ldots, N$, can be expressed as,

$$R_t = \mu_{z_t} + \Sigma_{z_t}^{\frac{1}{2}} \epsilon_t, \tag{2.23}$$

where μ_{z_t} denotes the conditional mean given the cluster z_t, Σ_{z_t} denotes the conditional covariance given the cluster z_t, and ϵ_t denotes the noise. Both μ_{z_t} and Σ_{z_t} can take different values depending on the realization of the cluster z_t. The noise term ϵ_t follows a standard multivariate Gaussian distribution $\epsilon_t \sim \mathbf{N}(0, I_{24})$. The cluster z_t follows a multinomial distribution, and occurs with probability $P(z_t|s_t) = c_{s_t,z_t}$, conditioned on the state s_t, for $s_t = 1, \ldots, M$ and $z_t = 1, \ldots, N$. The transition from the present state s_t to the future state s_{t+1} is governed by a transition probability matrix, and the transition probability is $P(s_{t+1}|s_t) = a_{s_t,s_{t+1}}$, for $s_t, s_{t+1} = 1, \ldots, M$.

The GMHMM offers a flexible framework where both the inferences of unobservable states and the estimations of forward premium statistics can be obtained from market data. We denote the historical DA and RT LMPs by p_t^{RT} and p_t^{DA}. Let $r_t = p_t^{DA} - p_t^{RT}$ denote the historical DA-RT spreads. The forward-backward algorithm and the expectation-maximization algorithm documented in Appendix A are adopted to compute the posterior marginals of state variables and update maximum likelihood estimators respectively, given a sequence of DA-RT spreads r_t. Maximum likelihood estimators are denoted as $\Theta = \{\pi_k, \mu_{k,h}, \Sigma_{k,h}, a_{k,l}, c_{k,h} : k, l = 1, \ldots, M, h = 1, \ldots, N\}$.

In-Sample and Out-of-Sample Test

We implement the in-sample and out-of-sample test to measure and evaluate the performance of the trading strategy using historical data. In both tests, the two chance constrained portfolio selection problems (VAR2(γ, η)) and (CVAR1(γ, η)) can be approximated and solved with sampling for a given GMHMM. To illustrate the sampling procedure, we calculate the expected value of a function in general form $f(R_t)$.

In the in-sample test, the whole sequence of DA-RT spreads, $r_1, \ldots, r_T$, is used to train the parameters of GMHMM Θ on day t. The expected function value of DA-RT spreads $f(R_t)$, conditioned on the whole sequence of DA-RT spreads, can be derived

as,

$$
\begin{aligned}
E[f(R_t)|r_1,\ldots,r_T] &= \sum_{s_t=1}^{M} E[f(R_t)|s_t,r_1,\ldots,r_T]P(s_t|r_1,\ldots,r_T) && (2.24)\\
&= \sum_{s_t=1}^{M} E[f(R_t)|s_t]P(s_t|r_1,\ldots,r_T) && (2.25)\\
&= \sum_{s_t=1}^{M}\sum_{z_t=1}^{N} E[f(R_t)|z_t,s_t]P(z_t|s_t)P(s_t|r_1,\ldots,r_T) && (2.26)\\
&= \sum_{s_t=1}^{M}\sum_{z_t=1}^{N} E[f(R_t)|z_t]c_{s_t,z_t}P(s_t|r_1,\ldots,r_T), && (2.27)
\end{aligned}
$$

where $E[f(R_t)|z_t]$ can be simulated since R_t follows a multivariate Gaussian distribution given the cluster z_t, c_{s_t,z_t} is the maximum likelihood estimator of the cluster probability obtained by the expectation-maximization algorithm, and $P(s_t|r_1,\ldots,r_T)$ is the posterior state probability computed by the forward-backward algorithm.[6]

In the out-of-sample test, only the sequence of available DA-RT spreads up to day t, $r_1,\ldots,r_{t-2}$, is used to train the parameters of GMHMM Θ on day t. We exclude r_{t-1}, because virtual positions for day t must be taken in the morning of day $t-1$, when RT LMPs for the rest of the day are still unavailable for the calculation of r_{t-1}.

The probability of being in the state s_t, conditioned on the sequence of available DA-RT spreads up to day t, can be derived as,

$$
\begin{aligned}
P(s_t|r_1,\ldots,r_{t-2}) &= \sum_{s_{t-2}=1}^{M} P(s_t,s_{t-2}|r_1,\ldots,r_{t-2}) && (2.28)\\
&= \sum_{s_{t-2}=1}^{M} P(s_{t-2}|r_1,\ldots,r_{t-2})P(s_t|s_{t-2},r_1,\ldots,r_{t-2}) && (2.29)\\
&= \sum_{s_{t-2}=1}^{M} P(s_{t-2}|r_1,\ldots,r_{t-2})P(s_t|s_{t-2}), && (2.30)
\end{aligned}
$$

where $P(s_t|s_{t-2})$ is the probability of going from the state s_{t-2} to the state s_t in 2 time steps. The n-step transition probability satisfies the Chapman - Kolmogorov equation, and thus (2.30) can be rewritten as,

$$
P(s_t|r_1,\ldots,r_{t-2}) = \sum_{s_{t-2}=1}^{M} P(s_{t-2}|r_1,\ldots,r_{t-2}) \sum_{s_{t-1}=1}^{M} P(s_t|s_{t-1})P(s_{t-1}|s_{t-2}). \quad (2.31)
$$

[6] $P(s_t|r_1,\ldots,r_T)$ is denoted by $\lambda_k(t)$ in Appendix A.

The expected function value of DA-RT spreads $f(R_t)$, conditioned on the sequence of available DA-RT spreads up to day t, can be derived as,

$$\begin{aligned} E[f(R_t)|r_1,\ldots,r_{t-2}] &= \sum_{s_t=1}^{M} E[f(R_t)|s_t,r_1,\ldots,r_{t-2}]P(s_t|r_1,\ldots,r_{t-2}) && (2.32)\\ &= \sum_{s_t=1}^{M} E[f(R_t)|s_t]P(s_t|r_1,\ldots,r_{t-2}) && (2.33)\\ &= \sum_{s_t=1}^{M}\sum_{z_t=1}^{N} E[f(R_t)|z_t,s_t]P(z_t|s_t)P(s_t|r_1,\ldots,r_{t-2}) && (2.34)\\ &= \sum_{s_t=1}^{M}\sum_{z_t=1}^{N} E[f(R_t)|z_t]c_{s_t,z_t}P(s_t|r_1,\ldots,r_{t-2}), && (2.35) \end{aligned}$$

where $E[f(R_t)|z_t]$, c_{s_t,z_t} and $P(s_t|r_1,\ldots,r_{t-2})$ can be computed in the same way as mentioned in the in-sample test.

One distinction between the two tests lies in the fact that virtual positions constructed in the out-of-sample test only relies on the distribution of past DA-RT spreads, while the distribution of both past and future DA-RT spreads are used to determine virtual positions in the in-sample test. By using the predicted distribution of DA-RT spreads, the out-of-sample test produces a robust and credible assessment of the trading strategy. The in-sample test contributes to the evaluation of the trading strategy by allowing us to obtain the most efficient portfolio of virtual positions and achieve the best attainable performance, under the true distribution of DA-RT spreads.

2.6 Data

The data for this study consist of the historical DA and RT LMPs at the CAISO NP15 EZ Gen Hub before and after the implementation of CB. The data in the pre-CB period include the historical DA and RT LMPs from January 1st, 2010 to December 31st, 2010, and the data in the post-CB period include the historical DA and RT LMPs from January 1st, 2012 to December 31st, 2012. For each day, the data contain DA and RT LMPs for each of the 24 hours during that day. The CAISO NP15 EZ Gen Hub is one of the trading hubs in the CAISO electric power markets, and covers the current CAISO congestion management zone NP15.[7]

[7] The majority of Pacific Gas and Electric Company's load is located in NP15.

2.7 Numerical Results

Summary Statistics for the DA and RT Markets

Table 2.2 reports summary statistics for post-CB DA and RT LMPs in dollars per megawatt hour. As can be seen, the means of post-CB DA and RT LMPs are low for the early morning hours, and high for the peak late afternoon hours. Post-CB DA and RT LMPs exhibit large variation during peak hours. For each hour, the volatility of post-CB RT LMPs is higher than the volatility of post-CB DA LMPs, due to large price spikes in the RT market.

The same statistics for pre-CB DA and RT LMPs are presented in Table 2.1 in dollars per megawatt hour. Similar features are observed as Table 2.2.

Table 2.4 presents summary statistics for post-CB DA-RT spreads in dollars per megawatt hour. Post-CB DA-RT spreads can also be viewed as realized or ex post forward premia. The mean of post-CB DA-RT spreads varies throughout the day. Large negative spreads are observed during peak hours. The volatility of post-CB DA-RT spreads is higher during peak hours than during off-peak hours. Post-CB DA-RT spreads are negatively skewed in most of the hours, because price spikes occur frequently in the RT market during the summer.

The same statistics for pre-CB DA-RT spreads are presented in Table 2.3 in dollars per megawatt hour. The overall mean of post-CB DA-RT spreads is closer to zero than the overall mean of pre-CB DA-RT spreads, which indicates better price convergence after the introduction of CB.

Table 2.7 and Table 2.8 show the seasonal means and standard deviations of post-CB DA-RT spreads in dollars per megawatt hour. Both exhibit strong seasonal patterns, especially for peak hours. In particular, the means of post-CB DA-RT spreads for 5 p.m. range from a low of -$23.82 during the period from May to July to a high of $3.55 during the period from November to January. The large negative mean values of post-CB DA-RT spreads are observed during the period from May to July, as a result of the price spikes that occur regularly throughout the summer in the RT market. The lowest overall mean of post-CB DA-RT spreads is observed during the period from May to July, and the highest overall standard deviation of post-CB DA-RT spreads is also observed during the same period. This seasonal variation is consistent with the Bessembinder and Lemmon (2002) model in that downward hedging pressure is imposed on the forward premium by the variance. The strong seasonal patterns raise the need to incorporate a time-varying property in the forward premium model, and support the use of the GMHMM characterized by the time-varying conditional mean and variance. It is also worth noting that off-peak hours do not display significant seasonal effects as peak hours do. The means and standard deviations of post-CB DA-RT spreads in off-peak hours show relatively small variation across different periods, compared with those in peak hours.

The same statistics for pre-CB DA-RT spreads are presented in Table 2.5 and Table 2.6 in dollars per megawatt hour. Similar features are observed as Table 2.7 and Table 2.8.

Summary Statistics for the GMHMM

Several heuristic procedures for model selection are applied to determine the number of states and the number of clusters in the GMHMM. We choose the number of states $M = 2$ to avoid the overfitting problem commonly encountered in learning a large state-space HMM. A simple model also allows us to provide clear economic interpretations for different states, which are discussed later. One common method of choosing the appropriate number of clusters is to graph the within cluster sum of squared error against the number of clusters in Figure 2.3. The appropriate number of clusters can be defined as the number at which the reduction in the within cluster sum of squared error slows significantly. As demonstrated in Figure 2.3, to increase the number of clusters reduces the the within cluster sum of squared error, but at 3 clusters the marginal gain drops suggesting that additional clusters do not have a substantial impact on the within cluster sum of squared error. It produces an "elbow" in the graph at 3 clusters. Hence, we choose the number of clusters $N = 3$, according to this "elbow criterion". After model selection, statistical inference and estimation can then be conducted by applying the forward-backward algorithm and the expectation-maximization algorithm on historical data. In particular, note that maximum likelihood estimators presented in this section are estimated using the whole sequence of DA-RT spreads to obtain a complete picture of the property of the forward premium across seasons. In Figure 2.2, similar features are observed as Figure 2.3.

The transition probabilities of the post-CB GMHMM are shown in Table 2.13. The transition probability from one state to itself is over 90%, which implies that the alternations between states occur at a relatively low frequency in the underlying state transition process. It captures the fact that the forward premium time series exhibits seasonal patterns and evolves slowly from season to season. Table 2.15 shows summary statistics for DA-RT spreads of the clusters of the post-CB GMHMM in dollars per megawatt hour.[8] Each cluster is represented by a multivariate Gaussian distribution characterized by its mean vector and covariance matrix. For most of the hours, the means are positive in cluster 1, and negative in cluster 2 and cluster 3. The standard deviations in cluster 2 are uniformly larger than those in cluster 1, indicating a higher level of volatility. However, cluster 3 behaves very differently from the other two clusters, and can be interpreted as a cluster where DA-RT spreads are highly volatile, especially during several specific peak hours, including 7 a.m. and 2 p.m. to 5 p.m. During these peak hours, the means in cluster 3 are lower than -$400, while the lowest mean value in cluster 1 and cluster 2 is -$37.59 during the corresponding hours. The standard deviations in cluster 3 are also significantly larger than those in cluster 1 and cluster 2 for these hours. Table 2.14 reports the cluster probabilities of the post-CB GMHMM. As shown in Table 2.14, cluster 3 is not historically observed in state 1 and occurs with very low probability in state 2. This is consistent with the fact that DA-RT spreads in cluster 3 exhibit occasional extreme price movements

[8] A full covariance matrix is estimated in this study, but only diagonal elements are presented in Table 2.15 to convey insights.

of magnitudes that can only be observed during the summer, but rarely seen for the rest of the year.

Table 2.16 shows summary statistics for DA-RT Spreads of the states of the post-CB GMHMM in dollars per megawatt hour. The means in state 1 are higher than those in state 2, since more observations in state 1 are drawn from cluster 1 as shown in Table 2.14 and cluster 1 exhibits higher means. Similarly, the standard deviations in state 1 are smaller than those in state 2. Therefore, we can interpret state 1 as a low volatility state, and state 2 as a high volatility state. Similar implications can be seen from Figure 2.15. In Figure 2.15, the posterior probability of being in state 1 is low during the summer, and high during the rest of the year. After the inference, the posterior probability of being in state 1 is adjusted based on the empirical evidence that DA-RT spreads are most volatile during the summer to correctly reflect the updated belief that the occurrence of state 1 which exhibits low volatility is rather unlikely during this period. Finally, we note that the negative skewness shown in Table 2.16 is consistent with summary statistics in Table 2.4.

Figure 2.18 and Figure 2.19 plot the marginal distribution of the post-CB DA-RT spreads for 3 a.m. and 3 p.m., representing peak hours and off-peak hours respectively. During off-peak hours, the marginal distributions of pre-CB DA-RT spreads are almost identical in the two states. During peak hours, however, the marginal distribution of pre-CB DA-RT spreads in state 1 has more density concentrated around the mean and less in both tails, compared to that in state 2. The difference of the marginal distributions between the two states is supported by the findings we report in Table 2.7 and Table 2.8 that seasonal patterns are stronger for off-peak hours.

All of these results demonstrate that many stylized facts of the time-varying forward premium can be well captured and accommodated in the GMHMM framework.

The same statistics for the pre-CB GMHMM are presented in Table 2.9 - Table 2.12 in dollars per megawatt hour. Similar features are observed as Table 2.13 - Table 2.16. In Figure 2.9, Figure 2.16, and Figure 2.17, similar features are observed as Figure 2.15, Figure 2.18, and Figure 2.19.

Test for the Bessembinder and Lemmon (2002) Model

Bessembinder and Lemmon (2002) model the forward market as a closed system, where the only participants are producers and consumers. In their general equilibrium model, the forward premium reflects the net hedging pressure of producers and consumers, and the sign of the forward premium is indeterminate. The forward premium can be expressed as,

$$P_t^{DA} - E[P_t^{RT}] = \theta_1 Var[P_t^{RT}] - \theta_2 Skew[P_t^{RT}], \tag{2.36}$$

where $\theta_1 \leq 0$, and $\theta_2 \leq 0$, implying that the forward premium is negatively related to the variance of RT LMPs, and positively related to the skewness of RT LMPs. To express forward premia in terms of DA-RT Spreads $R_t = P_t^{DA} - P_t^{RT}$, we can rewrite (2.36) as,

$$E[R_t] = \theta_1 Var[R_t] + \theta_2 Skew[R_t]. \tag{2.37}$$

To further test the implications of Bessembinder and Lemmon (2002), we regress the means for each of the 24 hours in the 2 states of the post-CB GMHMM on the corresponding variance and skewness measures in Table 2.16. The regression specification can be written in the form of (2.38),

$$StateMean_i = \theta_0 + \theta_1 StateVar_i + \theta_2 StateSkew_i + \epsilon_i. \tag{2.38}$$

As shown in Table 2.18, θ_1 is negative with a t-statistic of -13.4369, and θ_2 is negative with a t-statistic of -4.2229. Both of θ_1 and θ_2 are significant at 1% level and the R-squared value for the regression is 0.8246, which strongly supports the empirical implications of the Bessembinder and Lemmon (2002) model.

These test results provide evidence against the efficiency of the current CAISO DA and RT markets. The theoretical framework of Bessembinder and Lemmon (2002) essentially describes the characteristics of the electricity forward premium in an inefficient market, where the risks are borne within the industry by a few producers and consumers due to a lack of risk-sharing mechanisms. As financial mechanisms are implemented to allow risk neutral outside traders to enter the market and share the risks, the risk premium should decline and these characteristics are expected to disappear for the market to be fully efficient. Nevertheless, in the post-CB period, we demonstrate that the electricity forward premium still displays characteristics similar to what Bessembinder and Lemmon (2002) describe for an inefficient market in the absence of risk neutral outside traders, which to some extent implies market inefficiency.

The same statistics for the pre-CB GMHMM are presented in Table 2.17. Similar features are observed as Table 2.18.

Pre-CB and Post-CB Performance

To test for market efficiency, we backtest the trading strategy on the last 120 days in the pre-CB and post-CB period respectively, and all the rest of the data are used in training. We adopt several popular metrics for performance assessment. The annualized expected return and the annualized standard deviation directly measure the reward and risk of the trading strategy converted to an annual basis. The Sharpe ratio, also known as the reward-to-variability ratio, is a risk-adjusted measure used to evaluate the quality of the return. The ratio is calculated by using excess return and standard deviation to determine reward per unit of risk.[9] These standard measures of risk, however, do not account for the risk exposure associated with skewness, kurtosis, and serial correlation of the return distribution. In such cases, we include the maximum drawdown, that measures the greatest loss from a historical peak in the cumulative return, as an additional measure of the worst-case risk.

In the backtest, the predetermined upper bound γ for both the VaR and CVaR constraints is set to 0.02. To investigate the robustness of the trading strategy, we vary the choice of confidence levels η. As the Chebyshev bound (2.12) in (VAR2(γ, η))

[9] We assume the risk-free interest rate is 3% in the calculation of excess return.

is a conservative approximation of the VaR constraint (2.6), we tend to use lower confidence levels for the VaR constraint than for the CVaR constraint to ensure the risks of the two portfolios obtained from (VAR2(γ, η)) and (CVAR1(γ, η)) comparable. Therefore we vary η from 0.90, 0.85 to 0.80 for the VaR constraint, and from 0.99, 0.98 to 0.95 for the CVaR constraint. The costs τ are assumed to be \$0.085 for 1 MWh of cleared virtual position and the reference price C for 1 MWh of cleared virtual positionand is calculate by the 95th percentile value of the historical price differences between DA and RT LMPs.[10]

Figure 2.10 - Figure 2.14 depict the evolution of post-CB dynamic posterior state probability through time. On day t, the dynamic posterior state probability is inferred from the sequence of available DA-RT spreads up to day t, $r_1, \ldots, r_{t-2}$. These probabilities are used to compute the prediction probabilities in the out-of-sample test. Figure 2.4 - Figure 2.8 display the evolution of pre-CB dynamic posterior state probability. Similar features are observed as Figure 2.10 - Figure 2.14.

Table 2.19 and Figure 2.20 - Figure 2.23 reports the trading performance under a VaR constraint in the pre-CB and post-CB period. To begin with, we investigate the behavior of the trading strategy under different confidence levels η. In Table 2.19, both the annualized standard deviation and the maximum drawdown are negatively related to the confidence level, as a higher confidence level imposes a tighter bound for probability of tail events and hence lower risks are undertaken in the portfolio. The annualized expected return is positively related to the annualized standard deviation. This is what one might expect based on economic theory that high potential returns are associated with high levels of uncertainty. In terms of risk-adjusted performance measures, the low risk trading strategy exhibits a high Sharpe ratio in all cases except for the out-of-sample performance in the pre-CB period, as the Sharpe ratio penalizes the trading strategy that generates high but volatile returns.

We further compare the performance in the pre-CB and post-CB periods. There is little disparity between the in-sample and out-of-sample tests in their relative performance before and after the implementation of CB. In particular, to compare the post-CB metrics against the pre-CB metrics, we see the annualized expected returns and the Sharpe ratios in both of the tests drop dramatically. It is plausible because in the post-CB period virtual traders who engage in arbitrage trades tend to use the trading strategy, which proves to be profitable in the pre-CB period. As these arbitrage trades have the effect of causing price convergence between the DA and RT markets, the profitability is significantly eroded in the post-CB period, which serves to be convincing evidence for the improvement of market efficiency brought about by CB.

We now proceed to explore whether the current CAISO DA and RT markets are efficient, and if not, the extent to which the implementation of CB enhances market efficiency in the post-CB period. For this purpose, we primarily focus on the out-of-sample test. Examining the out-of-sample performance metrics in Table 2.19 reveals

[10] The upper bound of the estimated costs allocated to 1 MWh of cleared virtual position is used to ensure the robustness of our results.

that the trading strategy generates profits in the presence of transaction costs in the post-CB period. The out-of-sample Sharpe ratios under different parameters range from 2.13 to 2.35. For medium frequency strategies, the Sharpe ratio of the S&P 500 is commonly used as a benchmark, which F. Modigliani and L. Modigliani (1997) estimate to be about 0.30 based on quarterly returns ten years ending the second quarter of 1996.[11] All the out-of-sample Sharpe ratios exceed this benchmark by substantial margins in the post-CB period. In addition, the maximum drawdowns are small, if not negligible, in comparison with the corresponding annualized expected returns, which indicates that daily losses tend to be small and the occurrence of consecutive losses is uncommon. Taken together, these results provide compelling evidence that profitable trading opportunities still exist and consistent returns can be generated by exploiting these trading opportunities. Hence, market efficiency is not fully restored in the current CAISO DA and RT markets in the sense of Jensen (1978).

Combining the evidence against the efficiency of the current CAISO DA and RT markets with the evidence for the improvement of market efficiency brought about by CB, we are inclined to conclude that the current CAISO DA and RT markets lie somewhere between the two extremes, the inefficient markets as they were and the fully efficient markets that we pursue.[12] During this transition phase of CB, trading experience and market knowledge are accumulated among market participants within the industry, which serves as a necessary condition for the development of fully efficient DA and RT markets.

Table 2.20 and Figure 2.24 - Figure 2.27 reports the trading performance under a CVaR constraint in the pre-CB and post-CB period. Similar features are observed as Table 2.19 and Figure 2.20 - Figure 2.23 .

2.8 Market Power, Risk Averse Speculation and Implications

The efficient market hypothesis, which implicitly assumes that economic agents are risk neutral and have no market power, is called the simple efficiency hypothesis in Hansen and Hodrick (1980). In the forward market, the simple efficiency hypothesis implies that forward prices are unbiased predictors of expected spot prices. These risk neutral and competitive market conditions are also implicitly assumed in the statement by Jensen (1978) that no trading strategy can consistently profit from an efficient market.

However, if the market is not competitive, economic agents can exercise market power by withholding their bidding quantities below the competitive levels to maxi-

[11] Generally, low, medium, and high trading frequencies are defined as position holding periods of months, days, and hours, respectively.

[12] This is consistent with Jha and Wolak (2013) that after the implementation of CB the implied trading costs decrease but the difference between the implied trading costs before and after the implementation of CB is relatively small at the NP15 trading hub for all three hypothesis tests.

mize their profits. Thus, as a result, price discrepancies are not fully arbitraged away and the zero-profit competitive equilibrium as described by Jensen (1978) is no longer attained. We argue this is an unlikely case in the current CAISO DA and RT markets. There are currently over 70 market participants registered with the CAISO to participate in CB, including electricity producers and consumers, their trading subsidiaries, investment banks, and energy trading firms.[13] The latter two are sophisticated virtual traders, who do not own physical resources and engage in arbitrage activities for pure financial incentives. They are generally large corporations, and have sufficient access to capital to perform intended trading strategies. Therefore, in the presence of low transaction costs and full nodal granularity, it is reasonable to assume a high degree of competition among these well-informed and well-financed virtual traders that reduces the possibility of market manipulation and prevents the possession of excessive market power.

If, on the other hand, we extend the assumption to allow for risk averse economic agents, forward prices can systematically deviate from expected spot prices, which compromises the statement of Jensen (1978). Some intuitions are provided by Keynes (1923). He explains that, in a commodity market where only hedgers and speculators can take positions, the forward premium is determined by the net hedging demand.[14] As consumers traditionally show no interest in participation possibly due to informational setup costs, hedgers in this forward market are typically producers who are endowed with initial long positions in goods.[15] When facing price uncertainty, hedgers are net short to offset the exposures to their initial long positions, and therefore speculators have to be net long. Speculators are only willing to bear the risks if expected returns to speculation are positive, that is, forward prices are downward biased relative to expected spot prices. In contrast, Rolfo (1980), Anderson and Danthine (1983), and Hirshleifer (1990) argue that forward prices can be upward-biased predictors of expected spot prices, when hedgers are subject to both price and quantity uncertainties. If demand is elastic, quantity uncertainty has a more pronounced effect than price uncertainty from the perspective of hedgers, since small price fluctuations lead to large quantity fluctuations. Hedgers are then net long to reduce their quantity risks. Speculators are only willing to be net short, if forward prices constantly lie above expected spot prices. Hirshleifer (1990) shows that, apart from quantity uncertainty, the participation of consumers can also result in upward-biased forward prices, because the hedging incentives of consumers are opposite to those of producers. This way, we can think of both the upward and downward deviations of forward prices from expected spot prices as the costs of hedging, or the returns to

[13] CAISO List of Scheduling Coordinators (SCs), Congestion Revenue Rights (CRR) Holders, CB Entities as updated on July 8th, 2014. http://www.caiso.com/Documents/ISOListofSCsCRRsCBEs_July_2014pdf.pdf. Accessed July 23rd, 2014.

[14] To follow the convention in the finance literature, we use the term "speculators" referring to informed traders who explore price deviations and stabilize prices. The term "speculators" and "traders" are interchangeable in this study.

[15] Informational setup costs is the implicit costs of collecting and analyzing market information.

speculation.

In this sense, rationally, risk averse virtual traders only employ trading strategies that are capable of generating returns high enough to compensate for the risks undertaken, to arbitrage cautiously between the DA and RT markets. For virtual traders with relatively low risk-tolerance, they might require a higher risk-adjusted return than that of the trading strategy we develop to enter the forward market. If that is the case, the DA and RT markets can still be efficient in the presence of profitable trading strategies, and the profitability of these trading strategies only reflects the competitive returns to induce the participation of those risk averse virtual traders.

We tend to believe this is not the case for three reasons. Firstly, virtual traders in the current CAISO DA and RT markets are investment banks and trading firms, who are by nature less risk averse, if not risk neutral. Secondly, the Sharpe ratios of our trading strategy in Table 2.19 are significantly higher than that of the S&P 500, we can reasonably assume that the trading strategy indeed provides a decent risk-adjusted return. Thirdly, when there exists sufficient competition among virtual traders, the price deviation between the DA and RT markets is expected to be kept small, even if virtual traders are risk averse. The small DA-RT spreads should certainly lead to the the demise of the profitability in the post-CB period, which is contrary to what we observe in Table 2.19.

Although our profitable trading strategy indicates market inefficiency, it is not in itself sufficient evidence for us to fully reject the efficiency of the current CAISO DA and RT markets, with these unjustified concerns on market power and risk aversion in mind. A thorough investigation of these alternative hypotheses requires the estimation of risk aversion parameters of speculators and the level of competition, which is beyond the scope of this study, and is left for future research.

2.9 Conclusion

In this study, we investigate whether the current CAISO DA and RT markets are efficient, and whether markets efficiency is improved by CB, based on the zero-profit condition of Jensen (1978). In the backtest, our results show that our trading strategy continues to be profitable in the post-CB period, but the profitability is at a lower magnitude, compared to the profitability in the pre-CB period. Clearly, the deteriorated profitability in the post-CB period provides compelling evidence for the improved market efficiency, which demonstrates the benefit of CB. The profitability in the post-CB period, however, conveys empirical implications that can be interpreted differently, depending on the level of competition and the level of risk aversion of virtual traders. If virtual traders are risk-neutral and the competition among virtual traders is intense, the profitability in the post-CB period is convincing evidence against the fully efficient DA and RT markets. Otherwise, the profitability in the post-CB period might only rationally reflect the economic profit to incentivize the participation of risk averse virtual traders, which has nothing to do with market inefficiency and the mispricing of financial instruments.

Last but not least, market efficiency does not come for free. A market becomes or remains efficient as a result of the persistent efforts of market participants, who conduct research, identify inefficiencies, and trade until these inefficiencies disappear. In this sense, we encourage market participants to search for profitable trading strategies, make profits, and ultimately improve the efficiency of electricity forward markets.

2.10 Appendix

Appendix A

Based on a subset of data r_t, for $t = 1, \ldots, T'$ with $T' \leq T$, maximum likelihood estimators $\Theta = \{\pi_k, \mu_{k,h}, \Sigma_{k,h}, a_{k,l}, c_{k,h} : k, l = 1, \ldots, M, h = 1, \ldots, N\}$ can be derived by expectation-maximization algorithm in the following steps.[16] Assuming the noise term ϵ_t follows a standard multivariate Gaussian distribution $\epsilon_t \sim \mathbf{N}(0, I_{24})$, r_t follows a multivariate Gaussian distribution $\epsilon_t \sim \mathbf{N}(\mu_{s_t,z_t}, \Sigma_{s_t,z_t})$. The conditional probability density of r_t given s_t and z_t is

$$\begin{aligned} b_{k,h}(r_t) &= P(r_t|s_t = k, z_t = h) && (2.39)\\ &= \frac{1}{\sqrt{(2\pi)^{24}|\Sigma_{k,h}|}} \exp(-\frac{1}{2}(r_t - \mu_{k,h})^T \Sigma_{k,h}^{-1}(r_t - \mu_{k,h})). && (2.40) \end{aligned}$$

The conditional probability density of r_t given s_t is

$$\begin{aligned} b_k(r_t) &= P(r_t|s_t = k) && (2.41)\\ &= \sum_{h=1}^{N} P(r_t, z_t = h|s_t = k) && (2.42)\\ &= \sum_{h=1}^{N} P(r_t|z_t = h, s_t = k)P(z_t = h|s_t = k) && (2.43)\\ &= \sum_{h=1}^{N} P(r_t|z_t = h)P(z_t = h|s_t = k) && (2.44)\\ &= \sum_{h=1}^{N} c_{k,h} \frac{1}{\sqrt{(2\pi)^{24}|\Sigma_{k,h}|}} \exp(-\frac{1}{2}(r_t - \mu_{k,h})^T \Sigma_{k,h}^{-1}(r_t - \mu_{k,h})). && (2.45) \end{aligned}$$

The joint probability density of s_t and r_t is

$$\begin{aligned} & f(s_1, s_2, \ldots, s_{T'}, z_1, z_2, \ldots, z_{T'}, r_1, r_2, \ldots, r_{T'}|\Theta') && (2.46)\\ = \; & f(s_1, s_2, \ldots, s_{T'}, z_1, z_2, \ldots, z_{T'}|\Theta') \\ & \quad \cdot f(r_1, r_2, \ldots, r_{T'}|s_1, s_2, \ldots, s_{T'}, z_1, z_2, \ldots, z_{T'}, \Theta') && (2.47)\\ = \; & f(s_1, s_2, \ldots, s_{T'}|\Theta') f(z_1, z_2, \ldots, z_{T'}|s_1, s_2, \ldots, s_{T'}, \Theta') \\ & \quad \cdot f(r_1, r_2, \ldots, r_{T'}|z_1, z_2, \ldots, z_{T'}, s_1, s_2, \ldots, s_{T'}, \Theta') && (2.48)\\ = \; & \pi'_{s_1} \prod_{t=2}^{T'} a'_{s_{t-1},s_t} \prod_{t=1}^{T'} c'_{s_t,z_t} \prod_{t=1}^{T'} P(r_t|\mu'_{s_t,z_t}, \Sigma'_{s_t,z_t}). && (2.49) \end{aligned}$$

Then the log-likelihood function can be shown as,

$$\begin{aligned} & \log f(s_1, s_2, \ldots, s_{T'}, z_1, z_2, \ldots, z_{T'}, r_1, r_2, \ldots, r_{T'}|\Theta') && (2.50)\\ = \; & \log(\pi'_{s_1}) + \sum_{t=2}^{T'} \log a'_{s_{t-1},s_t} + \sum_{t=1}^{T'} \log c'_{s_t,z_t} + \sum_{t=1}^{T'} P(r_t|\mu'_{s_t,z_t}, \Sigma'_{s_t,z_t}). && (2.51) \end{aligned}$$

[16] π_k is the initial probability in the state k.

To take the expectation on both sides yields the expected complete log-likelihood,

$$E[\log f(s_1, s_2, \ldots, s_{T'}, z_1, z_2, \ldots, z_{T'}, r_1, r_2, \ldots, r_{T'}|\Theta')|r_1, r_2, \ldots, r_{T'}, \Theta] \quad (2.52)$$

$$= \sum_{s_1=1}^{M}\sum_{s_2=1}^{M}\cdots\sum_{s_{T'}=1}^{M}\sum_{z_1=1}^{N}\sum_{z_2=1}^{N}\cdots\sum_{z_{T'}=1}^{N} P(s_1, s_2, \ldots, s_{T'}, z_1, z_2, \ldots, z_{T'}|r_1, r_2, \ldots, r_{T'}, \Theta)$$

$$\cdot(\log(\pi'_{s_1}) + \sum_{t=2}^{T'}\log a'_{s_{t-1},s_t} + \sum_{t=1}^{T'}\log c'_{s_t,z_t} + \sum_{t=1}^{T'} P(r_t|\mu'_{s_t,z_t}, \Sigma'_{s_t,z_t})). \quad (2.53)$$

Let $\lambda_k(t)$ be the conditional probability of being in the state k at period t given $r_1, \ldots, r_{T'}$,

$$\lambda_k(t) = P(s_t = k|r_1, \ldots, r_{T'}). \quad (2.54)$$

Let $\xi_{k,l}(t)$ be the conditional probability of being in the state k at period t and being in the state l at period $t+1$ given $r_1, \ldots, r_{T'}$,

$$\xi_{k,l}(t) = P(s_t = k, s_{t+1} = l|r_1, \ldots, r_{T'}). \quad (2.55)$$

Let $\zeta_{k,h}(t)$ be the conditional probability of being in the state k at period t and being in the cluster h at period t given $r_1, \ldots, r_{T'}$,

$$\zeta_{k,h}(t) = P(s_t = k, z_t = h|r_1, \ldots, r_{T'}). \quad (2.56)$$

By substituting $\lambda_k(t)$, $\xi_{k,l}(t)$ and $\zeta_{k,h}(t)$, we have

$$E[\log f(s_1, s_2, \ldots, s_{T'}, r_1, r_2, \ldots, r_{T'}|\Theta')|r_1, r_2, \ldots, r_{T'}, \Theta] \quad (2.57)$$

$$= \sum_{s_1=1}^{M}\log(\pi'_{s_1})P(s_1|r_1, \ldots, r_{T'}) + \sum_{t=2}^{T'}\sum_{s_{t-1}=1}^{M}\sum_{s_t=1}^{M}\log a'_{s_{t-1},s_t}P(s_{t-1}, s_t|r_1, \ldots, r_{T'})$$
$$+\sum_{t=1}^{T'}\sum_{s_t=1}^{M}\sum_{z_t=1}^{N}(\log c'_{s_t,z_t} + P(r_t|\mu'_{s_t,z_t}, \Sigma'_{s_t,z_t}))P(s_t, z_t|r_1, \ldots, r_{T'}) \quad (2.58)$$

$$= \sum_{k=1}^{M}\log(\pi'_k)\lambda_k(1) + \sum_{t=2}^{T'}\sum_{k=1}^{M}\sum_{l=1}^{M}\log a'_{k,l}\xi_{k,l}(t)$$
$$+\sum_{t=1}^{T'}\sum_{k=1}^{M}\sum_{h=1}^{N}(\log c'_{k,h} + P(r_t|\mu'_{k,h}, \Sigma'_{k,h}))\zeta_{k,h}(t). \quad (2.59)$$

Maximum likelihood estimators can be derived by expectation-maximization algorithm. The parameters Θ are updated in the following form,

$$\pi'_k = \lambda_k(1) \tag{2.60}$$

$$\mu'_{k,h} = \frac{\sum_{t=1}^{T'} \zeta_{k,h}(t) r_t}{\sum_{t=1}^{T'} \zeta_{k,h}(t)} \tag{2.61}$$

$$\Sigma'_{k,h} = \frac{\sum_{t=1}^{T'} \zeta_{k,h}(t)(r_t - \mu'_{k,h})(r_t - \mu'_{k,h})^T}{\sum_{t=1}^{T'} \zeta_{k,h}(t)} \tag{2.62}$$

$$a'_{k,l} = \frac{\sum_{t=1}^{T'-1} \xi_{k,l}(t)}{\sum_{t=1}^{T'-1} \lambda_k(t)} \tag{2.63}$$

$$c'_{k,h} = \frac{\sum_{t=1}^{T'} \zeta_{k,h}(t)}{\sum_{t=1}^{T'} \lambda_k(t)}. \tag{2.64}$$

The forward-backward algorithm is used to compute $\lambda_k(t)$, $\xi_{k,l}(t)$ and $\zeta_{k,h}(t)$ efficiently. The forward probability $\alpha_k(t)$ is defined as the joint probability of observing the first t vectors r_τ, $\tau = 1, \ldots, t$, and being in the state k at time t,

$$\alpha_k(t) = P(r_1, r_2, \ldots, r_t, s_t = k). \tag{2.65}$$

This probability can be evaluated by the following recursive formula. For $t = 1$, the probability can be computed as $\alpha_k(1) = \pi_k b_k(r_1)$. For $t \geq 2$, the probability follows

$$\alpha_k(t) \tag{2.66}$$

$$= \sum_{l=1}^{M} P(r_1, r_2, \ldots, r_{t-1}, s_{t-1} = l) P(r_1, r_2, \ldots, r_t, s_t = k | r_1, r_2, \ldots, r_{t-1}, s_{t-1} = l) \tag{2.67}$$

$$= \sum_{l=1}^{M} P(r_1, r_2, \ldots, r_{t-1}, s_{t-1} = l) P(r_t, s_t = k | r_1, r_2, \ldots, r_{t-1}, s_{t-1} = l) \tag{2.68}$$

$$= \sum_{l=1}^{M} P(r_1, r_2, \ldots, r_{t-1}, s_{t-1} = l) P(r_t, s_t = k | s_{t-1} = l) \tag{2.69}$$

$$= \sum_{l=1}^{M} P(r_1, r_2, \ldots, r_{t-1}, s_{t-1} = l) P(r_t | s_t = k, s_{t-1} = l) P(s_t = k | s_{t-1} = l) \tag{2.70}$$

$$= \sum_{l=1}^{M} P(r_1, r_2, \ldots, r_{t-1}, s_{t-1} = l) P(r_t | s_t = k) P(s_t = k | s_{t-1} = l) \tag{2.71}$$

$$= b_k(r_t) \sum_{l=1}^{M} \alpha_l(t-1) a_{l,k}. \tag{2.72}$$

The backward probability $\beta_k(t)$ is defined as the conditional probability of observing the vectors after time t, r_τ, $\tau = t+1, \ldots, T'$, given the state at time t is k,

$$\beta_k(t) \quad = \quad P(r_{t+1}, \ldots, r_{T'} | s_t = k). \tag{2.73}$$

By setting $\beta_k(T') = 1$, this backward probability can be evaluated by the following recursive formula,

$$\begin{aligned}
& \beta_k(t) && (2.74)\\
= & \sum_{l=1}^{M} P(r_{t+1}, \ldots, r_{T'}, s_{t+1} = l | s_t = k) && (2.75)\\
= & \sum_{l=1}^{M} P(s_{t+1} = l | s_t = k) P(r_{t+1}, \ldots, r_{T'} | s_{t+1} = l, s_t = k) && (2.76)\\
= & \sum_{l=1}^{M} P(s_{t+1} = l | s_t = k) P(r_{t+1}, \ldots, r_{T'} | s_{t+1} = l) && (2.77)\\
= & \sum_{l=1}^{M} P(s_{t+1} = l | s_t = k) P(r_{t+2}, \ldots, r_{T'} | s_{t+1} = l) P(r_{t+1} | r_{t+2}, \ldots, r_{T'}, s_{t+1} = l) && (2.78)\\
= & \sum_{l=1}^{M} P(s_{t+1} = l | s_t = k) P(r_{t+2}, \ldots, r_{T'} | s_{t+1} = l) P(r_{t+1} | s_{t+1} = l) && (2.79)\\
= & \sum_{l=1}^{M} a_{k,l} \beta_l(t+1) b_l(r_{t+1}). && (2.80)
\end{aligned}$$

The probabilities $\lambda_k(t)$, $\xi_{k,l}(t)$ and $\zeta_{k,h}(t)$ are solved by

$$\begin{aligned}
& \lambda_k(t) && (2.81)\\
= & P(s_t = k | r_1, \ldots, r_{T'}) && (2.82)\\
= & \frac{P(r_1, \ldots, r_{T'}, s_t = k)}{P(r_1, \ldots, r_{T'})} && (2.83)\\
= & \frac{1}{P(r_1, \ldots, r_{T'})} P(r_1, \ldots, r_t, s_t = k) P(r_{t+1}, \ldots, r_{T'} | r_1, \ldots, r_t, s_t = k) && (2.84)\\
= & \frac{1}{P(r_1, \ldots, r_{T'})} P(r_1, \ldots, r_t, s_t = k) P(r_{t+1}, \ldots, r_{T'} | s_t = k) && (2.85)\\
= & \frac{1}{P(r_1, \ldots, r_{T'})} \alpha_k(t) \beta_k(i), && (2.86)
\end{aligned}$$

and

$$
\begin{aligned}
& \xi_{k,l}(t) && (2.87)\\
= \; & P(s_t = k, s_{t+1} = l | r_1, \ldots, r_{T'}) && (2.88)\\
= \; & \frac{1}{P(r_1, \ldots, r_{T'})} P(r_1, \ldots, r_{T'}, s_t = k, s_{t+1} = l) && (2.89)\\
= \; & \frac{1}{P(r_1, \ldots, r_{T'})} P(r_1, \ldots, r_t, s_t = k) P(r_{t+1}, \ldots, r_{T'}, s_{t+1} = l | r_1, \ldots, r_t, s_t = k) && (2.90)\\
= \; & \frac{1}{P(r_1, \ldots, r_{T'})} P(r_1, \ldots, r_t, s_t = k) P(r_{t+1}, \ldots, r_{T'}, s_{t+1} = l | s_t = k) && (2.91)\\
= \; & \frac{1}{P(r_1, \ldots, r_{T'})} P(r_1, \ldots, r_t, s_t = k) P(r_{t+1}, \ldots, r_{T'} | s_{t+1} = l, s_t = k) \\
& \quad \cdot P(s_{t+1} = l | s_t = k) && (2.92)\\
= \; & \frac{1}{P(r_1, \ldots, r_{T'})} P(r_1, \ldots, r_t, s_t = k) P(r_{t+1}, \ldots, r_{T'} | s_{t+1} = l) P(s_{t+1} = l | s_t = k) && (2.93)\\
= \; & \frac{1}{P(r_1, \ldots, r_{T'})} P(r_1, \ldots, r_t, s_t = k) P(r_{t+2} \ldots, r_{T'} | r_{t+1}, s_{t+1} = l) \\
& \quad \cdot P(r_{t+1} | s_{t+1} = l) P(s_{t+1} = l | s_t = k) && (2.94)\\
= \; & \frac{1}{P(r_1, \ldots, r_{T'})} P(r_1, \ldots, r_t, s_t = k) P(r_{t+2} \ldots, r_{T'} | s_{t+1} = l) \\
& \quad \cdot P(r_{t+1} | s_{t+1} = l) P(s_{t+1} = l | s_t = k) && (2.95)\\
= \; & \frac{1}{P(r_1, \ldots, r_{T'})} \alpha_k(t) \beta_l(t+1) b_l(r_{t+1}) a_{k,l}, && (2.96)
\end{aligned}
$$

and

$$\zeta_{k,h}(t) = P(s_t = k, z_t = h | r_1, \ldots, r_{T'}) \tag{2.97}$$

$$= P(s_t = k | r_1, \ldots, r_{T'}) \frac{P(z_t = h, r_t | s_t = k, r_1, \ldots, r_{t-1}, r_{r+1}, \ldots, r_{T'})}{P(r_t | s_t = k, r_1, \ldots, r_{t-1}, r_{r+1}, \ldots, r_{T'})} \tag{2.98}$$

$$= P(s_t = k | r_1, \ldots, r_{T'}) \frac{P(z_t = h, r_t | s_t = k, r_1, \ldots, r_{t-1}, r_{r+1}, \ldots, r_{T'})}{P(r_t | s_t = k)} \tag{2.99}$$

$$= \frac{P(s_t = k | r_1, \ldots, r_{T'})}{P(r_t | s_t = k)} \frac{P(z_t = h, r_t, r_1, \ldots, r_{t-1} | s_t = k, r_{r+1}, \ldots, r_{T'})}{P(r_1, \ldots, r_{t-1} | s_t = k, r_{r+1}, \ldots, r_{T'})} \tag{2.100}$$

$$= \frac{P(s_t = k | r_1, \ldots, r_{T'})}{P(r_t | s_t = k)} \frac{P(r_{r+1}, \ldots, r_{T'} | s_t = k)}{P(r_{r+1}, \ldots, r_{T'} | s_t = k, r_1, \ldots, r_{t-1}) P(r_1, \ldots, r_{t-1} | s_t = k)} \cdot P(z_t = h, r_t, r_1, \ldots, r_{t-1} | s_t = k, r_{r+1}, \ldots, r_{T'}) \tag{2.101}$$

$$= \frac{P(s_t = k | r_1, \ldots, r_{T'})}{P(r_t | s_t = k)} \frac{P(r_{r+1}, \ldots, r_{T'} | s_t = k)}{P(r_{r+1}, \ldots, r_{T'} | s_t = k) P(r_1, \ldots, r_{t-1} | s_t = k)} \cdot P(z_t = h, r_t, r_1, \ldots, r_{t-1} | s_t = k, r_{r+1}, \ldots, r_{T'}) \tag{2.102}$$

$$= \frac{P(s_t = k | r_1, \ldots, r_{T'})}{P(r_t | s_t = k) P(r_1, \ldots, r_{t-1} | s_t = k)} \frac{P(z_t = h, r_t, r_1, \ldots, r_{t-1}, r_{r+1}, \ldots, r_{T'} | s_t = k)}{P(r_{r+1}, \ldots, r_{T'} | s_t = k)} \tag{2.103}$$

$$= \frac{P(s_t = k | r_1, \ldots, r_{T'})}{P(r_t | s_t = k) P(r_1, \ldots, r_{t-1} | s_t = k) P(r_{r+1}, \ldots, r_{T'} | s_t = k)} \cdot P(z_t = h, r_t | s_t = k) P(r_1, \ldots, r_{t-1}, r_{r+1}, \ldots, r_{T'} | z_t = h, r_t, s_t = k) \tag{2.104}$$

$$= \frac{P(s_t = k | r_1, \ldots, r_{T'})}{P(r_t | s_t = k) P(r_1, \ldots, r_{t-1} | s_t = k) P(r_{r+1}, \ldots, r_{T'} | s_t = k)} P(z_t = h, r_t | s_t = k) \cdot P(r_1, \ldots, r_{t-1} | z_t = h, r_t, s_t = k) P(r_{r+1}, \ldots, r_{T'} | r_1, \ldots, r_{t-1}, z_t = h, r_t, s_t = k) \tag{2.105}$$

$$= \frac{P(s_t = k | r_1, \ldots, r_{T'})}{P(r_t | s_t = k) P(r_1, \ldots, r_{t-1} | s_t = k) P(r_{r+1}, \ldots, r_{T'} | s_t = k)} P(z_t = h, r_t | s_t = k) \cdot \frac{P(r_1, \ldots, r_{t-1}, z_t = h, r_t | s_t = k)}{P(z_t = h, r_t | s_t = k)} P(r_{r+1}, \ldots, r_{T'} | s_t = k) \tag{2.106}$$

$$= \frac{P(s_t = k | r_1, \ldots, r_{T'})}{P(r_t | s_t = k) P(r_1, \ldots, r_{t-1} | s_t = k) P(r_{r+1}, \ldots, r_{T'} | s_t = k)} P(z_t = h, r_t | s_t = k) \cdot \frac{P(z_t = h, r_t | r_1, \ldots, r_{t-1}, s_t = k) P(r_1, \ldots, r_{t-1} | s_t = k)}{P(z_t = h, r_t | s_t = k)} P(r_{r+1}, \ldots, r_{T'} | s_t = k) \tag{2.107}$$

$$= \frac{P(s_t = k | r_1, \ldots, r_{T'})}{P(r_t | s_t = k)} P(z_t = h, r_t | s_t = k) \tag{2.108}$$

$$= \frac{P(s_t = k | r_1, \ldots, r_{T'})}{P(r_t | s_t = k)} P(r_t | z_t = h, s_t = k) P(z_t = h | s_t = k) \tag{2.109}$$

$$= \frac{\lambda_k(t)}{b_k(r_t)} b_{k,h}(r_t) c_{k,h}. \tag{2.110}$$

The joint probability of observing r_t for $t = 1, \ldots, T'$ is

$$
\begin{aligned}
P(r_1, \ldots, r_{T'}) &= \sum_{k=1}^{M} P(r_1, \ldots, r_{T'}, s_t = k) && (2.111)\\
&= \sum_{k=1}^{M} P(r_1, \ldots, r_t, s_t = k) P(r_{t+1} \ldots r_{T'} | r_1, \ldots, r_t, s_t = k) && (2.112)\\
&= \sum_{k=1}^{M} P(r_1, \ldots, r_t, s_t = k) P(r_{t+1} \ldots r_{T'} | s_t = k) && (2.113)\\
&= \sum_{k=1}^{M} \alpha_k(t)\beta_k(t). && (2.114)
\end{aligned}
$$

Note that $\xi_{k,l}(t)$ can be also expressed in the following form,

$$
\begin{aligned}
& \xi_{k,l}(t) && (2.115)\\
= \; & P(s_t = k, s_{t+1} = l | r_1, \ldots, r_{T'}) && (2.116)\\
= \; & P(s_t = k | r_1, \ldots, r_{T'}) P(s_{t+1} = l | s_t = k, r_1, \ldots, r_{T'}) && (2.117)\\
= \; & P(s_t = k | r_1, \ldots, r_{T'}) \frac{P(s_{t+1} = l, r_{t+1}, \ldots, r_{T'} | s_t = k, r_1, \ldots, r_t)}{P(r_{t+1}, \ldots, r_{T'} | s_t = k)} && (2.118)\\
= \; & P(s_t = k | r_1, \ldots, r_{T'}) \frac{P(s_{t+1} = l, r_{t+1}, \ldots, r_{T'} | s_t = k)}{P(r_{t+1}, \ldots, r_{T'} | s_t = k)} && (2.119)\\
= \; & P(s_t = k | r_1, \ldots, r_{T'}) \\
& \quad \cdot \frac{P(s_{t+1} = l | s_t = k) P(r_{t+1}, \ldots, r_{T'} | s_{t+1} = l, s_t = k)}{P(r_{t+1}, \ldots, r_{T'} | s_t = k)} && (2.120)\\
= \; & P(s_t = k | r_1, \ldots, r_{T'}) \frac{P(s_{t+1} = l | s_t = k) P(r_{t+1}, \ldots, r_{T'} | s_{t+1} = l)}{P(r_{t+1}, \ldots, r_{T'} | s_t = k)} && (2.121)\\
= \; & P(s_t = k | r_1, \ldots, r_{T'}) \\
& \quad \cdot \frac{P(s_{t+1} = l | s_t = k) P(r_{t+1} | s_{t+1} = l) P(r_{t+2}, \ldots, r_{T'} | r_{t+1}, s_{t+1} = l)}{P(r_{t+1}, \ldots, r_{T'} | s_t = k)} && (2.122)\\
= \; & P(s_t = k | r_1, \ldots, r_{T'}) \\
& \quad \cdot \frac{P(s_{t+1} = l | s_t = k) P(r_{t+1} | s_{t+1} = l) P(r_{t+2}, \ldots, r_{T'} | s_{t+1} = l)}{P(r_{t+1}, \ldots, r_{T'} | s_t = k)} && (2.123)\\
= \; & \lambda_k(t) \frac{a_{k,l} b_l(r_{t+1}) \beta_l(t+1)}{\beta_k(t)}. && (2.124)
\end{aligned}
$$

Finally, if we assume $\mu_{k,h}$ and $\Sigma_{k,h}$ are the same across different states, the pa-

rameters are updated in the following form,

$$\mu'_h = \frac{\sum_{t=1}^{T'}\sum_{k=1}^{M}\zeta_{k,h}(t)r_t}{\sum_{t=1}^{T'}\sum_{k=1}^{M}\zeta_{k,h}(t)} \tag{2.125}$$

$$\Sigma'_h = \frac{\sum_{t=1}^{T'}\sum_{k=1}^{M}\zeta_{k,h}(t)(r_t-\mu'_k)(r_t-\mu'_k)^T}{\sum_{t=1}^{T'}\sum_{k=1}^{M}\zeta_{k,h}(t)}. \tag{2.126}$$

Appendix B

With $\phi(u)=(u+1)_+^2$, we can show $\phi(\frac{u}{\alpha}) \geq \mathbb{I}(u \geq 0)$ for any $\alpha > 0$. By substituting $u = -R_t^T y_t - \gamma$, we have $\phi(\frac{1}{\alpha}(-R_t^T y_t - \gamma)) \geq \mathbb{I}(-R_t^T y_t - \gamma \geq 0)$. Taking expectation on both sides yields,

$$E[\phi(\frac{1}{\alpha}(-R_t^T y_t - \gamma))] \geq P(-R_t^T y_t - \gamma \geq 0). \tag{2.127}$$

By multiplying α on both sides and replacing the positive part function, we can further show a conservative approximation of $P(-R_t^T y_t - \gamma \geq 0) \leq 1-\eta$ in the following form,

$$\alpha P(-R_t^T y_t - \gamma \geq 0) \leq \alpha E[\phi(\frac{1}{\alpha}(-R_t^T y_t - \gamma))] \tag{2.128}$$

$$= \alpha E[(\frac{1}{\alpha}(-R_t^T y_t - \gamma)+1)_+^2] \tag{2.129}$$

$$\leq \alpha E[(\frac{1}{\alpha}(-R_t^T y_t - \gamma)+1)^2] \tag{2.130}$$

$$\leq \alpha(1-\eta). \tag{2.131}$$

Rearranging $\alpha E[(\frac{1}{\alpha}(-R_t^T y_t - \gamma)+1)^2] \leq \alpha(1-\eta)$ yields,

$$\alpha E[(\frac{1}{\alpha}(-R_t^T y_t - \gamma)+1)^2] - \alpha(1-\eta) \tag{2.132}$$

$$= \frac{1}{\alpha}E[(R_t^T y_t + \gamma)^2] - 2E[(R_t^T y_t + \gamma)] + \eta\alpha \leq 0. \tag{2.133}$$

Noticing that (2.133) is a quadratic function, we can minimize the function by setting $\alpha = (\frac{1}{\eta}E[(R_t^T y_t + \gamma)^2])^{\frac{1}{2}}$.[17] By substituting $\alpha = (\frac{1}{\eta}E[(R_t^T y_t + \gamma)^2])^{\frac{1}{2}}$ into (2.133), we derived the Chebyshev bound,

$$-E[(R_t^T y_t + \gamma)] + (\eta E[(R_t^T y_t + \gamma)^2])^{\frac{1}{2}} \leq 0. \tag{2.134}$$

[17] α is nonnegative, since $\alpha = (\frac{1}{\eta}E[(R_t^T y_t + \gamma)^2])^{\frac{1}{2}} \geq 0$.

Appendix C

Table 2.1: Summary Statistics for Pre-CB DA LMPs and RT LMPs

Hour	DA Mean	DA Standard Deviation	RT Mean	RT Standard Deviation
1	31.04	7.16	34.18	30.51
2	28.08	7.60	33.45	40.89
3	25.64	8.03	28.69	43.14
4	24.74	8.50	21.79	15.41
5	26.17	9.02	20.83	17.03
6	30.39	9.89	24.86	19.34
7	31.91	11.43	28.94	28.79
8	34.19	10.88	34.75	32.15
9	36.21	8.67	34.83	33.47
10	38.11	7.25	36.60	23.67
11	39.90	6.47	42.84	35.91
12	40.52	6.50	43.14	35.42
13	40.22	6.19	40.27	22.24
14	40.37	6.88	39.29	16.89
15	41.42	7.88	41.55	30.13
16	43.07	10.92	45.78	45.71
17	44.27	11.42	45.15	45.67
18	44.25	9.20	49.60	56.92
19	44.62	9.53	53.33	66.61
20	43.93	8.05	51.69	65.17
21	43.75	6.13	52.64	62.40
22	40.28	5.33	45.76	39.19
23	37.28	5.39	48.37	42.92
24	33.05	5.64	41.59	52.68
Overall	36.82	10.44	39.17	41.45

Table 2.2: Summary Statistics for Post-CB DA LMPs and RT LMPs

Hour	DA Mean	DA Standard Deviation	RT Mean	RT Standard Deviation
1	23.07	4.31	21.26	8.19
2	21.30	4.68	19.32	10.57
3	18.85	5.53	16.51	12.77
4	18.26	6.07	15.18	14.72
5	18.95	5.65	17.63	12.41
6	21.84	5.35	21.94	15.12
7	24.45	6.73	23.00	21.43
8	26.70	6.79	27.25	38.49
9	26.89	5.71	27.43	31.81
10	27.87	5.64	30.18	43.40
11	29.25	5.66	31.92	55.90
12	29.63	5.49	29.42	36.04
13	29.93	6.00	29.79	36.57
14	30.63	6.93	28.44	32.27
15	31.98	10.92	32.28	42.70
16	34.52	17.37	36.95	83.54
17	37.72	20.64	43.39	86.43
18	38.27	17.18	43.65	77.04
19	37.11	12.44	40.46	53.27
20	35.65	10.33	36.88	47.88
21	34.08	7.67	32.51	28.13
22	30.81	6.03	32.55	43.10
23	27.66	4.85	27.59	17.96
24	24.36	4.31	23.10	24.90
Overall	28.32	10.92	28.69	43.24

Table 2.3: Summary Statistics for Pre-CB DA-RT Spreads

Hour	Mean	Standard Deviation	Skewness
1	-3.14	31.10	-9.14
2	-5.37	41.71	-10.49
3	-3.13	44.29	-11.55
4	2.77	14.42	0.54
5	5.29	13.84	0.63
6	5.35	16.31	-4.50
7	3.46	22.97	-7.70
8	-0.56	29.56	-8.95
9	1.38	31.63	-13.38
10	1.51	21.85	-6.31
11	-2.94	35.41	-6.70
12	-2.62	34.98	-7.85
13	-0.05	20.95	-6.70
14	1.08	15.95	-3.70
15	-0.14	29.48	-7.62
16	-2.71	43.38	-6.02
17	-0.88	43.38	-6.09
18	-5.34	55.43	-5.43
19	-8.70	65.40	-6.14
20	-7.77	64.63	-6.94
21	-8.89	62.01	-6.30
22	-5.48	38.77	-7.36
23	-11.09	43.37	-4.77
24	-8.55	53.93	-7.51
Overall	-2.36	39.84	-8.61

Table 2.4: Summary Statistics for Post-CB DA-RT Spreads

Hour	Mean	Standard Deviation	Skewness
1	1.81	7.01	2.93
2	1.98	9.31	2.61
3	2.34	11.24	2.03
4	3.08	13.44	2.62
5	1.32	11.05	1.90
6	-0.10	14.23	-7.33
7	1.45	19.88	-4.94
8	-0.56	38.08	-12.09
9	-0.54	30.92	-12.10
10	-2.31	43.33	-10.24
11	-2.68	56.07	-12.03
12	0.22	35.92	-12.32
13	0.14	36.41	-9.19
14	2.19	32.08	-13.23
15	-0.29	39.99	-7.67
16	-2.43	77.89	-10.70
17	-5.68	78.68	-6.23
18	-5.39	73.41	-6.24
19	-3.35	50.58	-4.61
20	-1.23	46.79	-6.91
21	1.57	26.62	-6.90
22	-1.74	42.67	-7.49
23	0.07	17.32	-4.38
24	1.26	24.67	-10.32
Overall	-0.37	40.67	-11.71

Table 2.5: Seasonal Means of Pre-CB DA-RT Spreads

Hour	November - January	February - April	May - July	August - October
1	-3.27	1.37	-12.31	1.77
2	-1.99	0.37	-20.20	0.51
3	2.19	3.58	-20.22	1.81
4	4.84	5.18	-1.38	2.28
5	2.88	6.37	9.33	2.65
6	1.25	6.71	9.37	4.15
7	0.83	2.87	8.14	2.05
8	-4.63	2.68	2.20	-2.48
9	-4.63	2.14	6.32	1.63
10	-1.12	0.90	3.54	2.66
11	-14.39	-1.23	4.39	-0.61
12	-1.72	2.33	-6.93	-4.05
13	-2.87	1.36	3.76	-2.44
14	0.82	-0.04	2.56	0.95
15	0.51	2.55	-0.74	-2.80
16	-1.94	3.02	-6.33	-5.46
17	5.25	3.64	-7.16	-5.09
18	-28.71	6.99	2.02	-1.66
19	-15.67	3.69	-1.48	-21.16
20	-0.86	-5.84	-2.40	-21.85
21	-12.84	-5.61	-12.11	-4.99
22	-2.92	-3.24	-13.38	-2.31
23	-9.12	-3.77	-24.61	-6.67
24	-2.32	1.19	-34.06	1.34
Overall	-3.77	1.55	-4.68	-2.49

Table 2.6: Seasonal Standard Deviations of Pre-CB DA-RT Spreads

Hour	November - January	February - April	May - July	August - October
1	45.31	8.07	40.01	6.61
2	35.05	11.79	72.52	6.94
3	11.87	11.40	84.74	10.40
4	14.36	12.57	17.34	12.27
5	9.84	11.74	17.55	14.09
6	22.43	9.51	18.64	9.83
7	34.01	18.34	19.48	14.97
8	46.88	8.38	19.15	29.13
9	56.20	7.45	25.73	10.09
10	24.32	20.67	29.22	6.35
11	59.93	26.83	20.50	12.09
12	16.73	7.61	55.02	38.57
13	23.81	8.15	11.20	31.21
14	16.58	13.40	16.35	17.29
15	16.55	5.84	33.43	45.15
16	44.13	5.89	53.33	51.66
17	23.10	6.61	58.73	58.23
18	98.47	7.06	28.41	32.86
19	91.13	16.17	47.18	77.46
20	29.06	41.79	56.75	103.27
21	83.50	40.51	61.86	54.78
22	17.95	34.55	57.73	33.28
23	44.05	20.86	64.04	28.58
24	20.53	4.81	101.17	6.56
Overall	44.80	18.59	49.51	38.84

Table 2.7: Seasonal Means of Post-CB DA-RT Spreads

Hour	November - January	February - April	May - July	August - October
1	1.84	1.18	2.25	1.95
2	1.98	2.71	1.63	1.61
3	1.47	4.25	2.02	1.68
4	2.93	3.46	3.19	2.78
5	1.51	1.44	1.79	0.55
6	-0.74	-1.73	1.85	0.18
7	-0.16	0.34	5.82	-0.29
8	2.32	-3.53	-3.70	2.58
9	-3.99	-0.60	2.44	-0.14
10	-1.44	-10.37	2.03	0.27
11	0.15	-11.31	-0.72	0.90
12	-0.70	-5.47	1.85	4.99
13	-2.25	-1.93	0.92	3.70
14	2.76	-0.13	-2.22	8.27
15	1.09	-2.11	-1.71	1.43
16	0.58	1.15	-8.49	-3.04
17	2.68	-0.98	-14.45	-9.92
18	3.55	2.02	-23.82	-3.18
19	0.35	2.46	-7.51	-8.79
20	3.32	-0.39	-7.79	-0.17
21	0.93	3.39	1.38	0.44
22	-1.85	1.27	-10.84	4.32
23	-0.75	0.43	-1.19	1.66
24	1.88	2.02	-2.47	3.61
Overall	0.73	-0.52	-2.41	0.64

Table 2.8: Seasonal Standard Deviations of Post-CB DA-RT Spreads

Hour	November - January	February - April	May - July	August - October
1	7.40	7.31	8.20	4.77
2	10.37	10.48	9.36	6.72
3	8.54	13.02	13.68	8.78
4	11.23	15.42	15.22	11.65
5	9.53	10.54	14.43	9.05
6	17.46	20.04	9.15	5.22
7	19.30	22.21	14.97	22.00
8	9.44	55.29	51.24	8.76
9	56.30	17.93	7.34	17.61
10	31.29	77.13	15.91	20.01
11	30.15	98.84	27.36	36.17
12	29.90	60.60	23.17	10.13
13	53.25	20.47	36.14	27.79
14	9.72	10.40	61.68	7.89
15	16.01	21.82	56.80	49.59
16	14.09	6.75	99.58	118.79
17	14.82	20.07	111.17	108.03
18	22.96	10.59	117.88	81.25
19	40.83	12.25	47.47	78.20
20	13.03	29.47	60.89	63.16
21	20.30	7.40	21.73	43.60
22	40.20	7.09	70.50	23.48
23	18.00	10.51	22.21	16.58
24	14.12	14.65	44.51	5.70
Overall	25.50	33.81	51.67	46.29

Table 2.9: Transition Probabilities of the Pre-CB GMHMM

	State 1	State 2
State1	96.67%	3.33%
State2	7.77%	92.23%

Table 2.10: Cluster Probabilities of the Pre-CB GMHMM

	Cluster 1	Cluster 2	Cluster 3
State1	81.46%	18.51%	0.00%
State2	39.13%	56.06%	4.81%

Table 2.11: Summary Statistics for DA-RT Spreads in the Clusters of the Pre-CB GMHMM

	Mean			Standard Deviation		
Hour	Cluster 1	Cluster 2	Cluster 3	Cluster 1	Cluster 2	Cluster 3
1	1.11	-13.02	-9.07	9.55	53.43	47.24
2	0.23	-18.32	-15.27	10.14	73.78	28.48
3	2.30	-12.98	-68.48	11.39	70.58	146.98
4	4.18	-0.77	3.01	14.02	14.62	7.45
5	5.94	3.51	9.44	13.39	14.44	16.62
6	6.93	1.99	-5.36	11.29	23.78	18.52
7	5.60	1.28	-60.65	11.74	23.68	121.92
8	2.61	-4.98	-68.09	10.75	32.76	171.85
9	4.15	-5.24	0.53	9.19	56.28	9.65
10	4.67	-4.82	-24.90	9.11	34.83	52.73
11	3.43	-18.47	2.75	6.75	62.03	13.78
12	2.97	-16.06	-1.86	7.00	61.85	6.79
13	3.02	-7.51	2.21	6.92	36.17	10.50
14	3.49	-3.93	-15.12	8.81	23.56	41.48
15	4.63	-11.56	-0.22	9.17	50.94	6.58
16	6.10	-23.95	-0.07	9.13	74.98	6.06
17	7.46	-17.85	-64.59	9.67	70.60	113.34
18	6.22	-29.70	-76.13	8.41	91.09	140.81
19	4.06	-25.15	-308.54	16.08	75.66	270.04
20	4.99	-23.49	-322.35	11.71	77.02	242.70
21	3.31	-21.66	-358.18	10.42	66.47	218.42
22	1.79	-17.55	-119.07	9.20	59.30	109.04
23	-3.04	-26.01	-103.40	18.13	67.35	86.84
24	1.17	-32.46	6.50	9.41	94.54	6.50

Table 2.12: Summary Statistics for DA-RT Spreads in the States of the Pre-CB GMHMM

	Mean		Standard Deviation		Skewness	
Hour	State 1	State 2	State 1	State 2	State 1	State 2
1	-1.57	-7.27	25.08	42.19	-1.15	-0.33
2	-3.14	-10.84	33.48	56.52	-1.10	-0.34
3	-0.59	-9.50	32.53	64.23	-1.04	-0.74
4	3.25	1.38	14.22	14.36	-0.02	-0.03
5	5.53	4.75	13.67	14.28	-0.01	-0.01
6	6.05	3.50	14.57	19.86	-0.30	-0.20
7	4.78	0.22	15.20	35.44	-1.38	-3.01
8	1.11	-4.87	18.14	47.41	-2.29	-2.53
9	2.58	-1.20	25.50	42.95	-0.64	-0.25
10	2.93	-1.92	17.35	29.74	-1.00	-0.55
11	-0.56	-8.77	28.78	48.31	-1.69	-0.51
12	-0.35	-8.16	28.07	47.94	-1.39	-0.47
13	1.03	-3.03	17.20	27.95	-1.17	-0.43
14	2.11	-1.55	13.23	21.06	-0.75	-0.51
15	1.75	-4.75	23.90	39.35	-1.29	-0.47
16	0.62	-11.28	35.33	58.35	-1.78	-0.62
17	2.95	-10.54	33.08	61.52	-1.50	-0.72
18	-0.44	-18.09	42.12	78.27	-1.89	-0.68
19	-1.60	-27.46	38.84	105.23	-2.87	-3.49
20	-0.52	-27.28	36.69	105.30	-2.00	-3.34
21	-1.42	-28.35	32.53	103.04	-2.78	-3.70
22	-1.70	-15.18	27.88	57.60	-1.42	-1.40
23	-7.19	-21.01	34.10	59.88	-1.02	-0.72
24	-4.76	-17.68	42.34	73.36	-1.68	-0.57

Table 2.13: Transition Probabilities of the Post-CB GMHMM

	State 1	State 2
State1	95.23%	4.77%
State2	4.00%	96.00%

Table 2.14: Cluster Probabilities of the Post-CB GMHMM

	Cluster 1	Cluster 2	Cluster 3
State1	89.65%	10.35%	0.00%
State2	56.84%	42.10%	1.05%

Table 2.15: Summary Statistics for DA-RT Spreads in the Clusters of the Post-CB GMHMM

	Mean			Standard Deviation		
Hour	Cluster 1	Cluster 2	Cluster 3	Cluster 1	Cluster 2	Cluster 3
1	2.20	0.75	1.73	7.21	6.38	2.68
2	1.95	2.08	0.83	8.98	10.22	2.25
3	2.50	1.93	0.59	11.13	11.57	1.43
4	3.54	1.91	1.21	13.55	13.21	1.88
5	2.13	-0.84	0.22	11.57	9.28	1.38
6	1.18	-3.53	-1.30	10.28	21.27	1.59
7	1.87	0.33	-2.27	20.95	16.81	3.36
8	3.18	-5.89	-236.75	7.11	53.68	240.32
9	2.67	-9.28	-1.39	5.92	57.98	3.11
10	3.70	-18.71	0.07	6.95	80.59	4.32
11	4.70	-22.88	3.69	7.67	104.85	3.55
12	4.84	-12.16	-7.55	6.37	66.95	0.87
13	4.73	-11.70	-29.70	6.62	67.73	27.41
14	5.17	-3.67	-107.51	7.91	56.28	97.00
15	6.04	-9.11	-412.31	8.12	44.78	77.20
16	7.35	-9.84	-944.17	10.75	59.77	119.64
17	9.99	-36.38	-583.82	13.61	113.61	244.14
18	9.55	-37.59	-412.65	12.06	109.88	355.19
19	6.17	-29.78	19.05	22.38	84.75	40.92
20	7.92	-26.74	28.00	9.14	83.73	32.35
21	5.95	-10.86	22.44	8.52	47.05	23.38
22	5.35	-21.47	16.41	5.77	78.43	13.56
23	1.18	-3.09	1.20	14.77	22.62	3.48
24	3.91	-6.01	4.91	5.89	45.84	2.16

Table 2.16: Summary Statistics for DA-RT Spreads in the States of the Post-CB GMHMM

	Mean		Standard Deviation		Skewness	
Hour	State 1	State 2	State 1	State 2	State 1	State 2
1	2.05	1.59	7.16	6.89	0.00	0.05
2	1.98	1.96	9.15	9.47	0.01	0.01
3	2.49	2.18	11.25	11.24	0.01	-0.01
4	3.41	2.76	13.51	13.31	0.00	0.01
5	1.86	0.85	11.36	10.73	0.03	0.07
6	0.77	-0.82	11.93	15.90	-0.27	-0.27
7	1.74	1.17	20.54	19.22	0.02	0.03
8	2.17	-2.86	18.86	48.21	-1.06	-4.50
9	1.46	-2.41	19.75	38.74	-1.41	-0.49
10	1.61	-5.69	26.90	54.06	-1.74	-0.67
11	2.06	-6.80	34.95	69.87	-1.56	-0.64
12	3.13	-2.29	22.63	44.73	-1.57	-0.54
13	3.14	-2.76	23.28	45.07	-1.55	-0.58
14	4.38	0.43	19.55	39.98	-0.93	-0.88
15	4.36	-4.34	16.95	51.33	-1.92	-5.51
16	5.50	-9.14	22.20	102.52	-1.47	-7.92
17	5.05	-15.15	41.28	98.80	-2.57	-3.18
18	4.34	-14.22	40.55	91.68	-2.81	-3.02
19	2.33	-8.59	36.32	60.44	-1.53	-0.79
20	4.22	-6.54	30.29	57.39	-2.77	-0.98
21	4.18	-1.00	18.04	32.37	-1.91	-0.80
22	2.53	-5.76	26.68	52.36	-2.40	-0.87
23	0.74	-0.60	15.83	18.63	-0.09	-0.16
24	2.94	-0.25	15.84	30.34	-1.36	-0.53

Table 2.17: Pre-CB Regression Analysis

θ_0	θ_1	θ_2	t_{θ_0}	t_{θ_1}	t_{θ_2}	R Squared	DF
0.9050	-0.0032	-1.1511	1.2250	-16.1359	-2.0904	0.8732	45

Table 2.18: Post-CB Regression Analysis

θ_0	θ_1	θ_2	t_{θ_0}	t_{θ_1}	t_{θ_2}	R Squared	DF
1.8041	-0.0021	-1.0617	4.6235	-13.4369	-4.2229	0.8246	45

Table 2.19: Performance under a VaR Constraint

Strategy Parameter	Expected Return	Standard Deviation	Sharpe	Max Drawdown
Pre-CB In-Sample Performance				
$\gamma = 0.02$ $\eta = 0.90$	153.42%	14.60%	10.34	1.12%
$\gamma = 0.02$ $\eta = 0.85$	187.50%	19.54%	9.48	1.53%
$\gamma = 0.02$ $\eta = 0.80$	210.34%	24.71%	8.43	2.09%
Pre-CB Out-of-Sample Performance				
$\gamma = 0.02$ $\eta = 0.90$	90.36%	24.50%	3.58	6.91%
$\gamma = 0.02$ $\eta = 0.85$	118.70%	29.42%	3.95	8.96%
$\gamma = 0.02$ $\eta = 0.80$	150.92%	35.15%	4.23	9.45%
Post-CB In-Sample Performance				
$\gamma = 0.02$ $\eta = 0.90$	78.03%	11.10%	6.79	2.23%
$\gamma = 0.02$ $\eta = 0.85$	86.66%	13.08%	6.42	2.82%
$\gamma = 0.02$ $\eta = 0.80$	87.61%	15.21%	5.59	3.72%
Post-CB Out-of-Sample Performance				
$\gamma = 0.02$ $\eta = 0.90$	33.47%	13.03%	2.35	2.73%
$\gamma = 0.02$ $\eta = 0.85$	35.11%	14.35%	2.25	3.19%
$\gamma = 0.02$ $\eta = 0.80$	38.03%	16.55%	2.13	5.08%

Table 2.20: Performance under a CVaR Constraint

Strategy Parameter	Expected Return	Standard Deviation	Sharpe	Max Drawdown
Pre-CB In-Sample Performance				
$\gamma = 0.02$ $\eta = 0.99$	267.77%	37.04%	7.18	1.19%
$\gamma = 0.02$ $\eta = 0.98$	296.75%	44.60%	6.61	1.14%
$\gamma = 0.02$ $\eta = 0.95$	341.83%	59.30%	5.74	1.42%
Pre-CB Out-of-Sample Performance				
$\gamma = 0.02$ $\eta = 0.99$	245.86%	47.78%	5.10	6.59%
$\gamma = 0.02$ $\eta = 0.98$	266.79%	55.65%	4.76	7.23%
$\gamma = 0.02$ $\eta = 0.95$	284.81%	66.01%	4.29	7.80%
Post-CB In-Sample Performance				
$\gamma = 0.02$ $\eta = 0.99$	47.35%	11.54%	3.86	2.75%
$\gamma = 0.02$ $\eta = 0.98$	52.93%	13.29%	3.77	3.16%
$\gamma = 0.02$ $\eta = 0.95$	60.82%	16.58%	3.50	4.60%
Post-CB Out-of-Sample Performance				
$\gamma = 0.02$ $\eta = 0.99$	22.58%	16.56%	1.19	4.02%
$\gamma = 0.02$ $\eta = 0.98$	25.55%	17.87%	1.27	5.29%
$\gamma = 0.02$ $\eta = 0.95$	22.18%	22.83%	0.84	9.01%

Appendix D

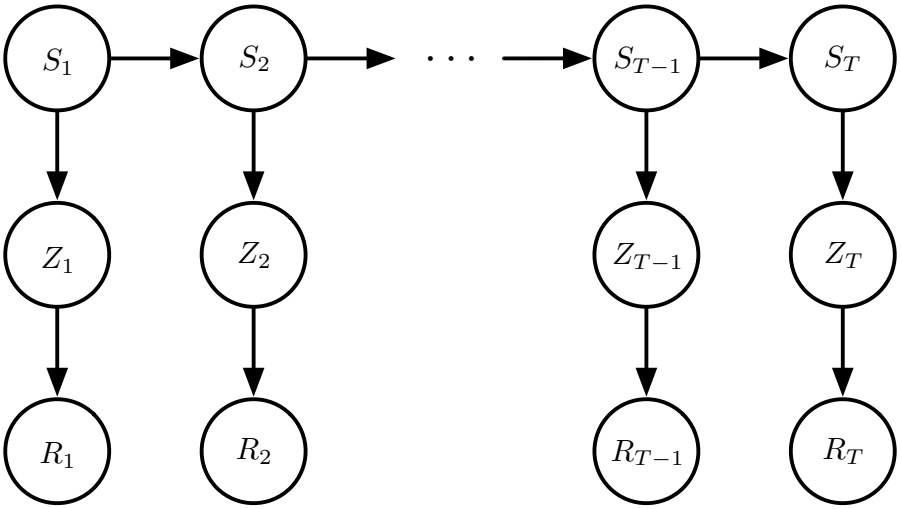

Figure 2.1: GMHMM

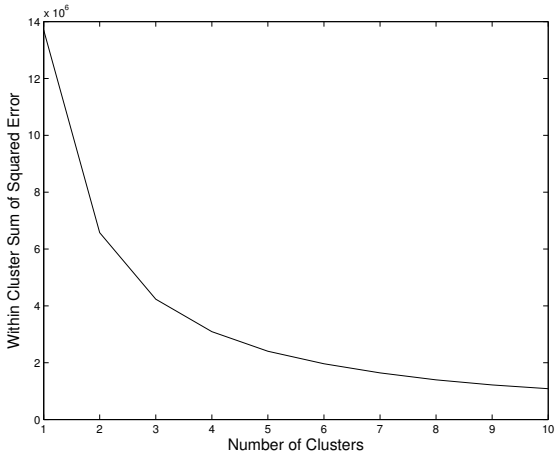

Figure 2.2: Pre-CB Within-Cluster Sum of Squared Error

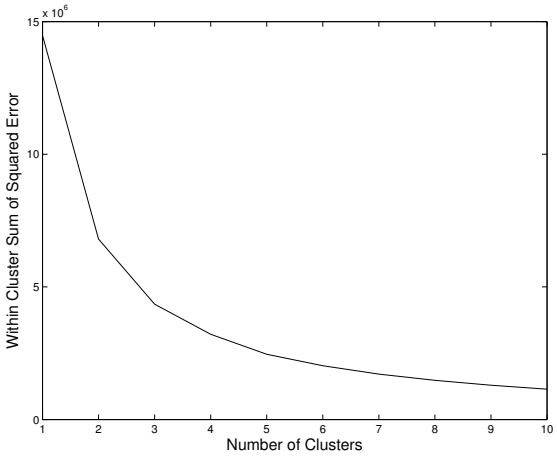

Figure 2.3: Post-CB Within-Cluster Sum of Squared Error

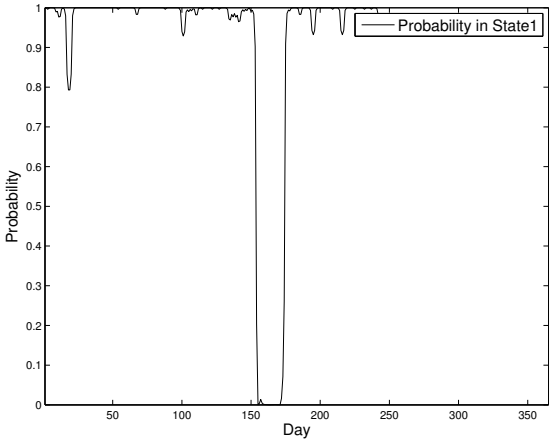

Figure 2.4: Pre-CB Dynamic Posterior State Probability 1

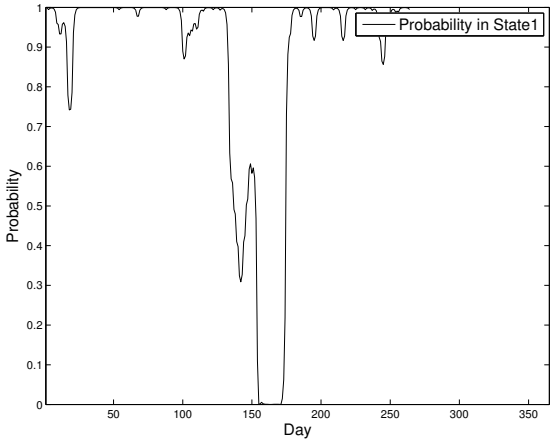

Figure 2.5: Pre-CB Dynamic Posterior State Probability 2

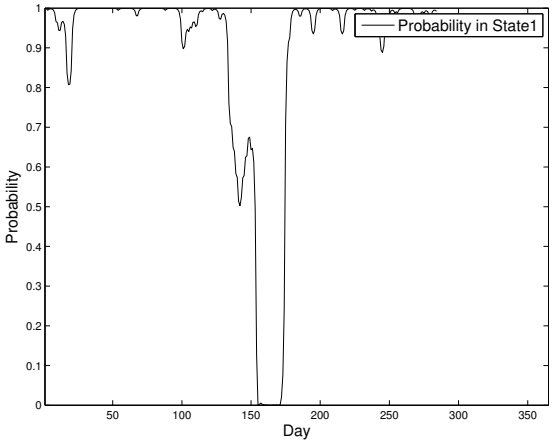

Figure 2.6: Pre-CB Dynamic Posterior State Probability 3

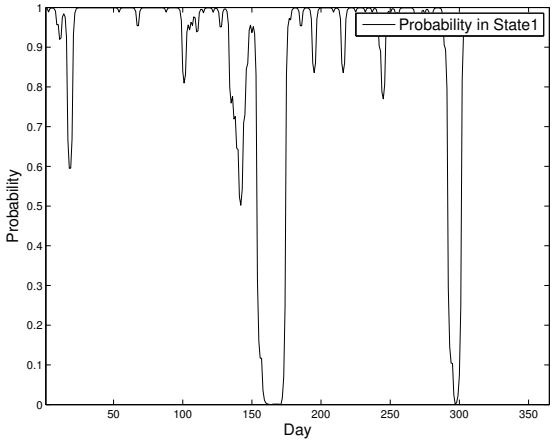

Figure 2.7: Pre-CB Dynamic Posterior State Probability 4

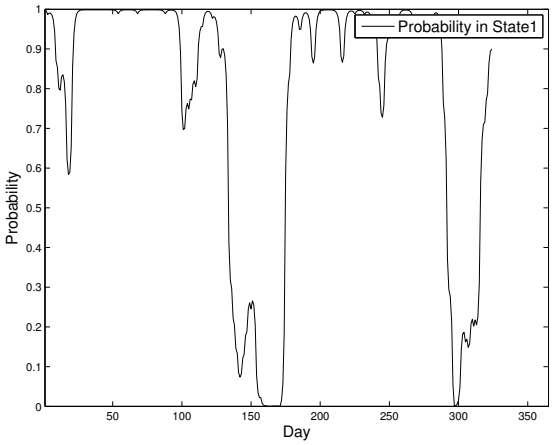

Figure 2.8: Pre-CB Dynamic Posterior State Probability 5

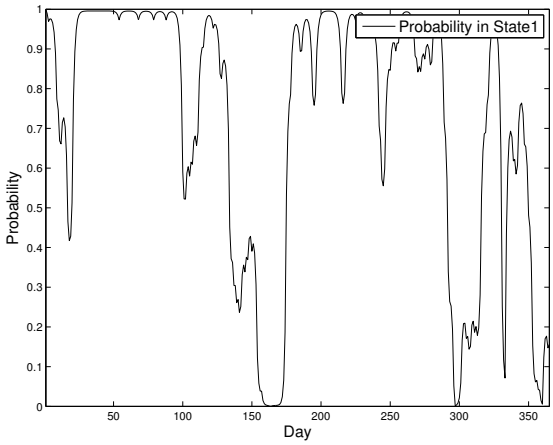

Figure 2.9: Pre-CB Posterior State Probability

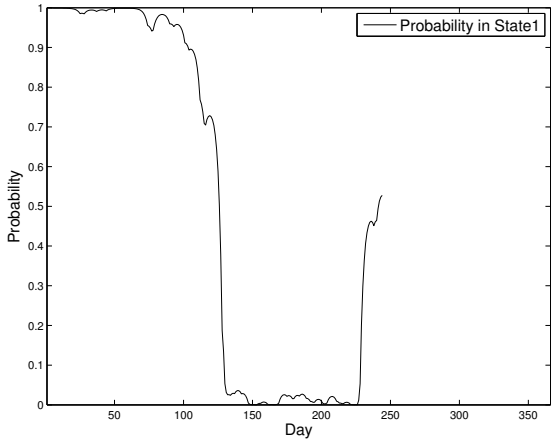

Figure 2.10: Post-CB Dynamic Posterior State Probability 1

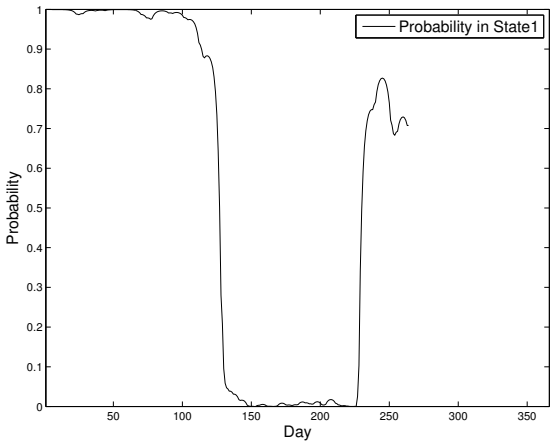

Figure 2.11: Post-CB Dynamic Posterior State Probability 2

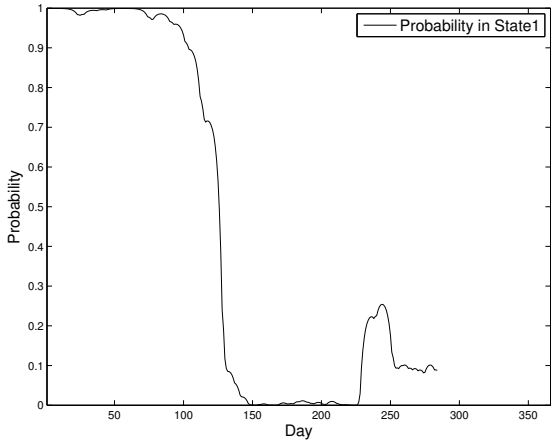

Figure 2.12: Post-CB Dynamic Posterior State Probability 3

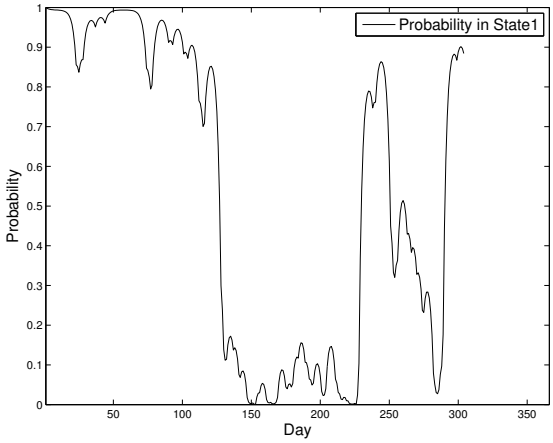

Figure 2.13: Post-CB Dynamic Posterior State Probability 4

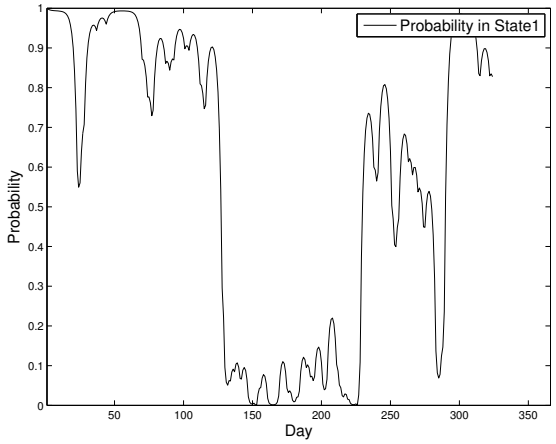

Figure 2.14: Post-CB Dynamic Posterior State Probability 5

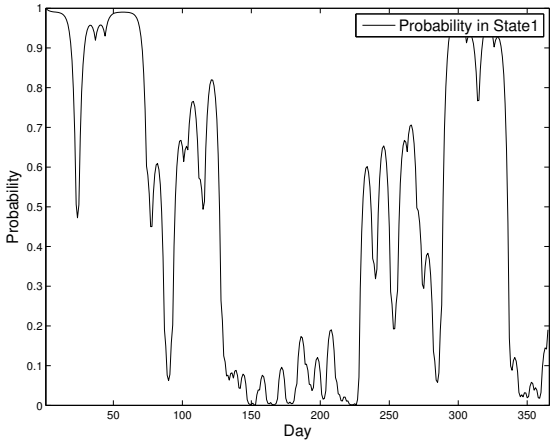

Figure 2.15: Post-CB Posterior State Probability

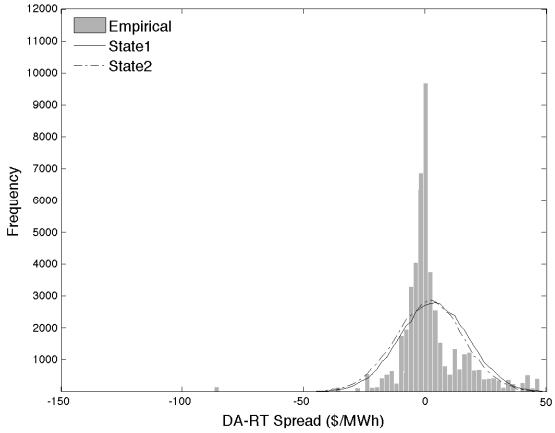

Figure 2.16: Marginal Distribution of Pre-CB DA-RT Spreads for 3 a.m.

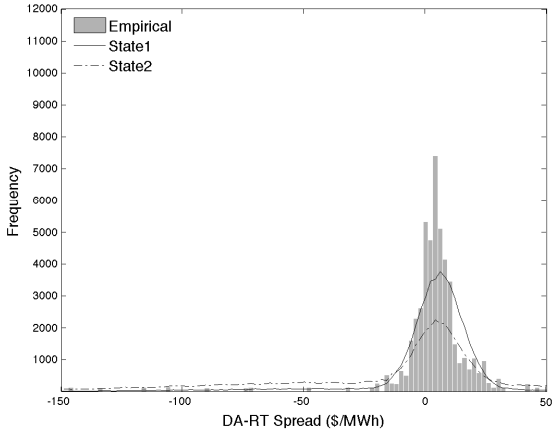

Figure 2.17: Marginal Distribution of Pre-CB DA-RT Spreads for 3 p.m.

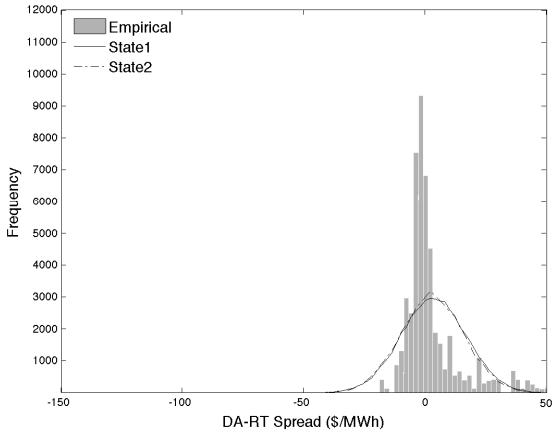

Figure 2.18: Marginal Distribution of Post-CB DA-RT Spreads for 3 a.m.

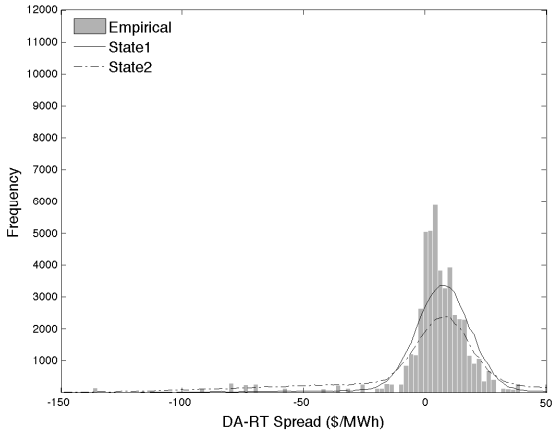

Figure 2.19: Marginal Distribution of Post-CB DA-RT Spreads for 3 p.m.

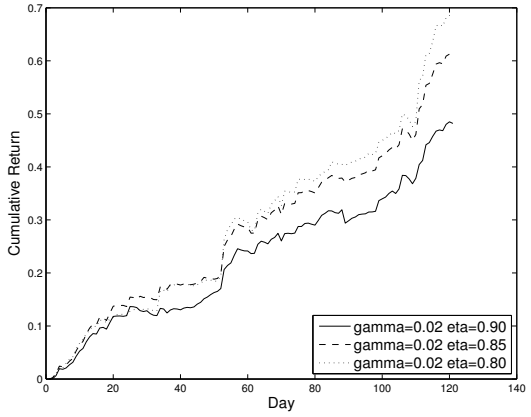

Figure 2.20: Pre-CB In-Sample Performance under a VaR constraint

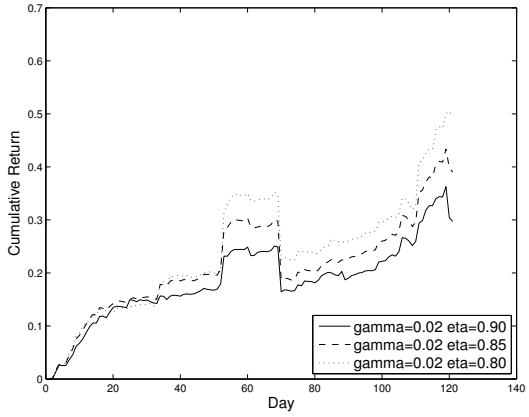

Figure 2.21: Pre-CB Out-of-Sample Performance under a VaR constraint

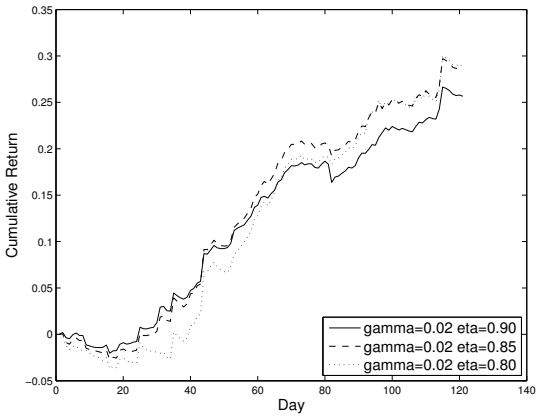

Figure 2.22: Post-CB In-Sample Performance under a VaR constraint

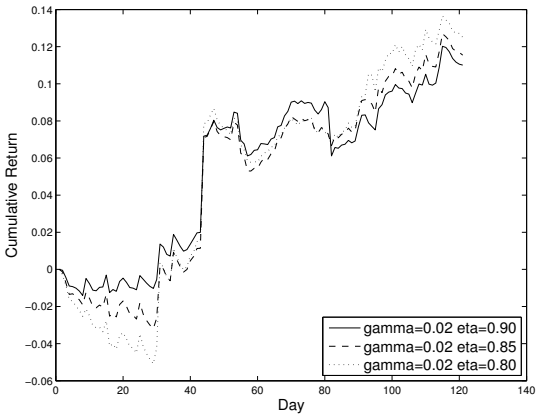

Figure 2.23: Post-CB Out-of-Sample Performance under a VaR constraint

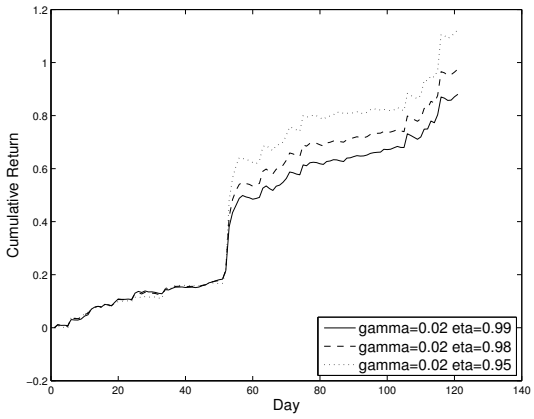

Figure 2.24: Pre-CB In-Sample Performance under a CVaR constraint

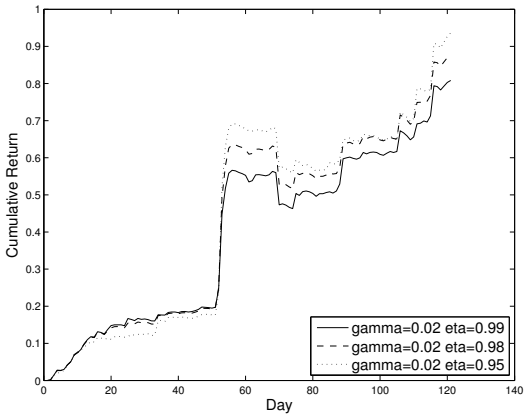

Figure 2.25: Pre-CB Out-of-Sample Performance under a CVaR constraint

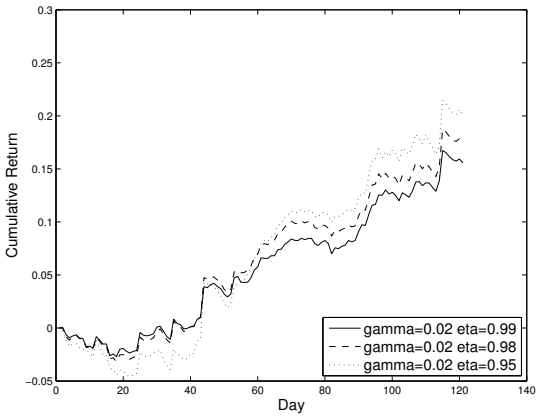

Figure 2.26: Post-CB In-Sample Performance under a CVaR constraint

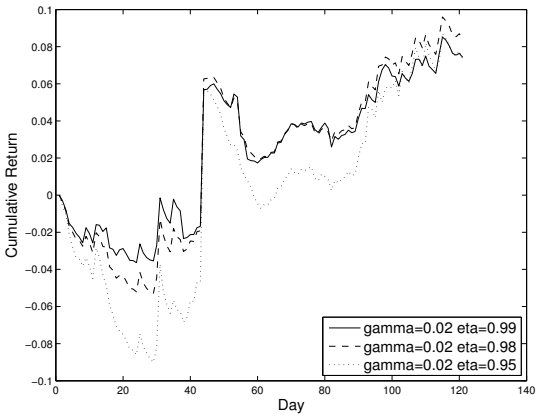

Figure 2.27: Post-CB Out-of-Sample Performance under a CVaR constraint

Chapter 3

Distribution Locational Marginal Pricing for Optimal Electric Vehicle Charging Management

3.1 Introduction

This chapter presents an integrated distribution locational marginal pricing (DLMP) method designed to alleviate congestion induced by electric vehicle (EV) loads in future power systems. In the proposed approach, the distribution system operator (DSO) determines distribution locational marginal prices (DLMPs) by solving the social welfare optimization of the electric distribution system which considers EV aggregators as price takers in the local DSO market and accounts for the price elasticity of the conventional household demand. Supply busses connecting the distribution system to the transmission grid are treated as generation nodes with marginal costs set to locational marginal prices (LMPs) for each bus. These LMPs are determined by the independent system operator (ISO), and treated in our model as exogenous inputs. Nonlinear optimization has been used to solve the social welfare optimization problem in order to obtain DLMPs which propagate the LMPs throughout the transmission network so as to alleviate distribution level congestion while meeting the conventional household demand and the EV demand. It is also shown mathematically that the socially optimal charging schedule can be implemented through a decentralized mechanism where loads respond autonomously to the posted DLMPs by maximizing their individual net surplus. We further investigate the problem of designing pricing mechanism when LMPs are uncertain. A robust DLMP method is developed for EV charging management under price uncertainty. The efficacy of the proposed use of DLMP is demonstrated by means of case studies using the Bus 4 distribution system of the Roy Billinton Test System (RBTS) and the Danish driving data. The case study results show that the DLMP and robust DLMP methods can successfully alleviate congestion caused by EV loads.

3.2 Literature Review

Environmental concerns and the quest for energy supply independence have resulted in increasing penetration of renewable energy sources (RES) and a move toward electrification of transportation. Consequently, electric vehicles (EVs) are expected to play a significant role in future power systems. Increased use of EVs will reduce the green house gas (GHG) emission from the transport sector by replacing conventional internal combustion engine (ICE) vehicles while also serving as distributed energy storage that can mitigate uncertainties arising from intermittent RES.

Numerous studies have addressed vehicle-to-grid (V2G) technology to investigate the technical and commercial feasibility of providing ancillary service to the grid from EVs. The capacity from EVs and the economic return to participate in peak power, spinning reserve and regulation markets have been explored in Kempton and Tomić (2005a), Kempton and Tomić (2005b), and Tomić and Kempton (2007). The effectiveness of using EVs to provide peak load shaving and extra flexibility has been illustrated in Sortomme and El-Sharkawi (2011) and Sortomme and El-Sharkawi (2012).

However, the deployment of a large number of EVs will challenge power system operations especially for distribution networks if there is no proper coordination of the electric vehicle (EV) charging schedule. Grid congestion results from demand patterns that induce flows exceeding design limits. Congestion from EVs can be observed at the medium voltage (MV) level, as demonstrated by a number of studies (Heydt, 1983; Clement-Nyns, Haesen, and Driesen, 2010; Dyke, Schofield, and Barnes, 2010). It was also noted that the problems are likely to originate in distribution networks, and as such, the analysis of these networks should be conducted as the primary stage of EV induced congestion (Maitra et al., 2010; Taylor et al., 2010; Lopes, Soares, and Almeida, 2011).

Grid congestion depends on a number of factors including local grid rating and topology, penetration and distribution of EVs, and charging management procedures. Coordinated charging appears to be an effective means for allowing increased penetration of EVs without violating grid constraints. There is some diversity regarding the optimal manner in which to coordinate charging, and the proposed objectives for such coordination include minimization of losses (Clement-Nyns, Haesen, and Driesen, 2010), maximization of EV penetration (Lopes, Soares, and Almeida, 2011), and minimization of customer charging costs (Rotering and Ilic, 2011; Sundstrom and Binding, 2012).

Congestion management methods can be categorized into three groups: optimal power flow (OPF) based method, price area congestion control method and transaction-based method (Christie, Wollenberg, and Wangensteen, 2000). The OPF based congestion management method is based on a centralized optimization, and it is considered to be the most accurate and effective congestion management method. The price area congestion management controls congestion by generation redispatch in response to congestion prices within an OPF framework (Glatvitsch and Alvarado, 1998). The transaction-based method determines the available transfer capability

(ATC) from the start point to the end point of a path using a power flow model described by power transfer distribution factors (PTDF).

In the existing work on load management techniques and other methods for alleviating congestions from EVs, there is no integrated method which has a closed loop solution accounting for the elasticity of the conventional household demand and the intertemporal shifting characteristics of the EV demand. In order to address this problem, the distribution locational marginal pricing (DLMP) method is proposed for distribution networks in order to alleviate congestion induced by EVs.

This chapter is arranged as follows. The nomenclature is defined in Section 3.3. The mathematical formulation of the integrated DLMP method under complete information is presented in Section 3.4. The integrated DLMP method is extended to the incomplete information case in Section 3.5. The data used in case studies is described in Section 3.6. The case study results are presented in Section 3.7 with the detailed discussion followed by the conclusion in Section 3.8.

3.3 Nomenclature

L: Set of distribution elements
N: Set of all nodes
N_c: Subset of demand nodes
T: Planning periods for optimization
g: Subset of generation node(s)[1]
$c_{i,t}$: Conventional household demand at time period t at node i
$q_{g,t}$: Generation supplied to the distribution grid at time period t
$r_{g,t}$: Net active power import/export at time period t at generation node g (positive for import)
$r_{i,t}$: Net active power import/ export at time period t at node i (positive for import)
$x_{i,t}$: EV charging energy at time period t at node i
p_t: Dual variables for the total power flow balance constraints
$\lambda^-_{l,t}, \lambda^+_{l,t}$: Dual variables for the line capacity constraints
$\xi_{i,t}$: Dual variables for the conventional household demand constraints
$\delta_{g,t}$: Dual variables for the generation node power balance constraints
$\rho_{i,t}$: Dual variables for the demand node power balance constraints
$\mu^-_{i,t}, \mu^+_{i,t}$: Dual variables for the aggregate EV charging energy constraints
$\kappa^-_{i,t}, \kappa^+_{i,t}$: Dual variables for the aggregate EV SOC constraints
$D_{l,i}$: PTDF coefficient of line l with respect to a unit injected at node i
$E_{i,t}$: Aggregate EV charging energy limit at time period t at node i
K_l: MVA capacity of line l
$P_{i,t}(\tau_{i,t})$: Benefit from using demand $\tau_{i,t}$ at time period t at node i
P^{LMP}_t: Locational marginal prices (LMPs) for the node feeding the distribution grid
$P^*_{i,t}$: Distribution locational marginal prices (DLMPs) for the distribution grid

[1]The set of all nodes N consists of two subsets, where N_c is the subset of demand nodes and g is the subset of generation node(s).

$S_{i,0}$: Initial aggregate EV battery SOC at node i
$S^{-}_{i,t}$: Minimum aggregate EV battery SOC at time period t at node i
$S^{+}_{i,t}$: Maximum aggregate EV battery SOC at time period t at node i
$d_{i,t}$: Aggregate driving energy requirement at time period t at node i

3.4 Formulation under Complete Information

Determination of DLMPs

We examine the framework intended for LMPs in the derivation of DLMPs. LMPs are determined by maximizing social welfare with the physical constraints of the transmission system respected, which expose producers and consumers to the marginal costs of electricity delivery at different locations. LMPs can be decomposed into three components: marginal cost of generation, marginal cost of losses and marginal cost of congestion (Stoft, 2002). Both the AC optimal power flow (ACOPF) and the DC optimal power flow (DCOPF) can be used to compute LMPs. The DCOPF is widely used and is considered to be sufficient for the locational marginal pricing (LMP) calculation due to its efficiency and reasonable accuracy (Li and Bo, 2007). The DCOPF has also been employed by several software tools for the chronological LMP simulation and forecasting, such as ABB GridViewTM, Siemens Promod, GE MAPSTM and PowerWorld (Yang, Li, and Freeman, 2003). The DCOPF is adopted in the derivation of DLMPs as a practical approach to address the computational complexity resulting from the large number of nodes on the distribution network.

In the proposed DLMP method, the DSO determines DLMPs by solving a constrained social welfare maximization problem for the distribution network which considers EV aggregators as price takers in the local DSO market and accounts for the price elasticity of the residential energy consumption. It is assumed that EV aggregators are economically rational, that is, their objective is to maximize their individual surplus. Supply busses connecting the distribution system to the transmission grid are treated as generation nodes with marginal costs set to LMPs for each bus.[2] These LMPs are determined by the independent system operator (ISO), and treated in our model as exogenous inputs.

DSO's Problem

The mathematical formulation in Yao, Adler, and Oren (2008), Limpaitoon, Chen, and Oren (2011), and Hogan (1992) has been modified to make it more general to allow economic allocation for both the conventional household demand and the EV

[2] In our model, we assume that there is only one generation node on the distribution network, and no demand locates at the generation node.

charging energy. The DSO's optimization problem is presented in (3.1) to (3.8),

$$\text{(P1)} \qquad \max_{r_{i,t}:i\in N,t\in T;c_{i,t},x_{i,t}:i\in N_c,t\in T;q_{g,t}:t\in T} \quad \sum_{i\in N_c}\sum_{t\in T}\int_0^{c_{i,t}} P_{i,t}(\tau_{i,t})d\tau_{i,t} - \sum_{t\in T} P_t^{LMP} q_{g,t} \tag{3.1}$$

s.t.

$$\sum_{i\in N} r_{i,t} = 0 \qquad \forall t \in T \qquad (p_t) \tag{3.2}$$

$$-K_l \le \sum_{i\in N} D_{l,i} r_{i,t} \le K_l \qquad \forall l \in L, \forall t \in T \qquad (\lambda_{l,t}^-, \lambda_{l,t}^+) \tag{3.3}$$

$$r_{g,t} + q_{g,t} = 0 \qquad \forall t \in T \qquad (\delta_{g,t}) \tag{3.4}$$

$$r_{i,t} = c_{i,t} + x_{i,t} \qquad \forall i \in N_c, \forall t \in T \qquad (\rho_{i,t}) \tag{3.5}$$

$$c_{i,t} \ge 0 \qquad \forall i \in N_c, \forall t \in T \qquad (\xi_{i,t}) \tag{3.6}$$

$$0 \le x_{i,t} \le E_{i,t} \qquad \forall i \in N_c, \forall t \in T \qquad (\mu_{i,t}^-, \mu_{i,t}^+) \tag{3.7}$$

$$S_{i,t}^- \le S_{i,0} + \sum_{t'\le t-1} x_{i,t'} - \sum_{t'\le t} d_{i,t'} \le S_{i,t}^+ \qquad \forall i \in N_c, \forall t \in T\backslash\{1\} \qquad (\kappa_{i,t}^-, \kappa_{i,t}^+) \tag{3.8}$$

The DSO's objective is to maximize social surplus (3.1)−− subject to the lossless energy-balance constraints on the distribution network (3.2), the line capacity constraints (3.3), the generation node balance constraints (3.4), the demand node balance constraints (3.5), the conventional household demand non-negative constraints (3.6), the charging energy limit constraints (3.7) and the driving requirement constraints (3.8). For the demand node balance constraints (3.5), EVs are assumed to charge energy at the locations they belong to on the distribution network, which requires that the energy import $r_{i,t}$ balances the sum of the conventional household demand $c_{i,t}$ and the EV demand $x_{i,t}$ at time period t at node i. The EV demand $x_{i,t}$ is constrained between 0 and the aggregate EV charging energy limit $E_{i,t}$ at time period t at node i in (3.7). $E_{i,t}$ varies over time to reflect the aggregate availability of EVs in different hours. The DSO is required to provide enough energy to satisfy the driving energy requirements, which is specified in (3.8). The SOC at time period t at node i is the sum of the initial SOC $S_{i,0}$ and the total charging energy $x_{i,t}$ up to time period $t-1$ minus the total driving energy requirement $d_{i,t}$ up to time period t. The SOC is constrained between the minimum aggregate EV battery SOC $S_{i,t}^-$ and the maximum aggregate EV battery SOC $S_{i,t}^+$ in (3.8). The variables in parentheses next to the constraints denote the corresponding Lagrange multipliers.

The objective function consists of two components, the social value of meeting the conventional demand, given by the area under the demand function, and the costs of satisfying both the EV demand and the conventional demand as shown in (3.1). We do not include in the objective function the benefit corresponding to the EV demand since that component is constant as long as the EV demand is met within the day and is not affected by the charging schedule. Instead, the driving requirement constraints (3.8) requiring that the EV demand is met by the schedule is included. To be more specific, the object function (3.1) can be further decomposed into three

terms as shown by,

$$\sum_{i\in N_c}\sum_{t\in T}\int_0^{c_{i,t}} P_{i,t}(\tau_{i,t})d\tau_{i,t} - \sum_{t\in T} P_t^{LMP} q_{g,t} \tag{3.9}$$

$$= \sum_{i\in N_c}\sum_{t\in T}\int_0^{c_{i,t}} P_{i,t}(\tau_{i,t})d\tau_{i,t} - \sum_{t\in T} P_t^{LMP} \sum_{i\in N_c}(c_{i,t}+x_{i,t}) \tag{3.10}$$

$$= \sum_{i\in N_c}\sum_{t\in T}\int_0^{c_{i,t}} P_{i,t}(\tau_{i,t})d\tau_{i,t} - \sum_{t\in T} P_t^{LMP} \sum_{i\in N_c} c_{i,t} - \sum_{t\in T} P_t^{LMP} \sum_{i\in N_c} x_{i,t}, \tag{3.11}$$

where $\sum_{i\in N_c}\sum_{t\in T}\int_0^{c_{i,t}} P_{i,t}(\tau_{i,t})d\tau_{i,t} - \sum_{t\in T} P_t^{LMP}\sum_{i\in N_c} c_{i,t}$is the social welfare corresponding to the conventional household demand and $\sum_{t\in T} P_t^{LMP}\sum_{i\in N_c} x_{i,t}$ is the EV charging costs.

The Karush-Kuhn-Tucker (KKT) conditions of the DSO's optimization problem (P1) are summarized below,

$$P_{i,t}(c_{i,t}) - \rho_{i,t} + \xi_{i,t} = 0 \qquad \forall i \in N_c, \forall t \in T \tag{3.12}$$

$$-p_t - \textstyle\sum_{l\in L}(\lambda_{l,t}^+ - \lambda_{l,t}^-)D_{l,i} + \rho_{i,t} = 0 \qquad \forall i \in N_c, \forall t \in T \tag{3.13}$$

$$-p_t - \textstyle\sum_{l\in L}(\lambda_{l,t}^+ - \lambda_{l,t}^-)D_{l,g} + \delta_{g,t} = 0 \qquad \forall t \in T \tag{3.14}$$

$$-P_t^{LMP} + \delta_{g,t} = 0 \qquad \forall t \in T \tag{3.15}$$

$$-\rho_{i,t} - \mu_{i,t}^+ + \mu_{i,t}^- - \textstyle\sum_{t'\geq t+1}\kappa_{i,t'}^+ + \sum_{t'\geq t+1}\kappa_{i,t'}^- = 0 \qquad \forall i \in N_c, \forall t \in T\backslash\{|T|\} \tag{3.16}$$

$$-\rho_{i,t} - \mu_{i,t}^+ + \mu_{i,t}^- = 0 \qquad \forall i \in N_c, t = |T| \tag{3.17}$$

$$\textstyle\sum_{i\in N} r_{i,t} = 0 \qquad \forall t \in T \tag{3.18}$$

$$r_{g,t} + q_{g,t} = 0 \qquad \forall t \in T \tag{3.19}$$

$$r_{i,t} = c_{i,t} + x_{i,t} \qquad \forall i \in N_c, \forall t \in T \tag{3.20}$$

$$0 \leq \lambda_{l,t}^- \quad \perp \quad \textstyle\sum_{i\in N} D_{l,i} r_{i,t} + K_l \geq 0 \qquad \forall l \in L, \forall t \in T \tag{3.21}$$

$$0 \leq \lambda_{l,t}^+ \quad \perp \quad K_l - \textstyle\sum_{i\in N} D_{l,i} r_{i,t} \geq 0 \qquad \forall l \in L, \forall t \in T \tag{3.22}$$

$$0 \leq \xi_{i,t} \quad \perp \quad c_{i,t} \geq 0 \qquad \forall i \in N_c, \forall t \in T \tag{3.23}$$

$$0 \leq \mu_{i,t}^- \quad \perp \quad x_{i,t} \geq 0 \qquad \forall i \in N_c, \forall t \in T \tag{3.24}$$

$$0 \leq \mu_{i,t}^+ \quad \perp \quad E_{i,t} - x_{i,t} \geq 0 \qquad \forall i \in N_c, \forall t \in T \tag{3.25}$$

$$0 \leq \kappa_{i,t}^- \quad \perp \quad S_{i,0} + \textstyle\sum_{t'\leq t-1} x_{i,t'} - \sum_{t'\leq t} d_{i,t'} - S_{i,t}^- \geq 0 \qquad \forall i \in N_c, \forall t \in T\backslash\{1\} \tag{3.26}$$

$$0 \leq \kappa_{i,t}^+ \quad \perp \quad S_{i,t}^+ - S_{i,0} - \textstyle\sum_{t'\leq t-1} x_{i,t'} + \sum_{t'\leq t} d_{i,t'} \geq 0 \qquad \forall i \in N_c, \forall t \in T\backslash\{1\}. \tag{3.27}$$

The KKT conditions yield optimality certificate for the primal problem and provide the economic interpretation of Lagrange multipliers. DLMPs are derived from the KKT conditions to provide financial incentives for market participants to alleviate congestion and ensure efficient load allocation. By solving (3.13), (3.14) and (3.15),

the marginal value of energy for both the EV demand and the conventional household demand at time period t at node i $\rho_{i,t}$ takes the form of

$$\rho_{i,t} = P_t^{LMP} - \sum_{l\in L}(\lambda_{l,t}^{+} - \lambda_{l,t}^{-})D_{l,g} + \sum_{l\in L}(\lambda_{l,t}^{+} - \lambda_{l,t}^{-})D_{l,i}. \tag{3.28}$$

The PTDF coefficients associated with the generation node $D_{l,g}$ are set to be 0 to enable unlimited import from the grid to the distribution network, which simplifies (3.28) and yields,

$$\rho_{i,t} = P_t^{LMP} + \sum_{l\in L}(\lambda_{l,t}^{+} - \lambda_{l,t}^{-})D_{l,i}. \tag{3.29}$$

DLMPs can be derived by combining (3.12) and (3.29) to yield

$$\begin{aligned} P_{i,t}^{*} &= \rho_{i,t} - \xi_{i,t} && (3.30)\\ &= P_t^{LMP} + \sum_{l\in L}(\lambda_{l,t}^{+} - \lambda_{l,t}^{-})D_{l,i} - \xi_{i,t}. && (3.31) \end{aligned}$$

The non-negativity constraints (3.6) can be excluded by implicitly assuming an interior solution with respect to these constraints, forcing the dual variables associated with the constraints $\xi_{i,t} = 0$. This can be explained as: every conventional household consumes at least a small positive amount of energy. Under this assumption, DLMPs become

$$P_{i,t}^{*} = P_t^{LMP} + \tilde{\varphi}_{i,t}, \tag{3.32}$$

where $\tilde{\varphi}_{i,t} = \sum_{l\in L}(\lambda_{l,t}^{+} - \lambda_{l,t}^{-})D_{l,i}$ is a sum of difference of $\lambda_{l,t}^{+}$ and $\lambda_{l,t}^{-}$ over all the lines l weighted by the i-th row of the PTDF matrix. DLMPs can be interpreted as the sum of the reference price P_t^{LMP} and the locational congestion markup $\tilde{\varphi}_{i,t}$, which is analogous to the marginal cost of congestion in LMPs. Noticing that LMPs only optimize the dispatch of instantaneous demand, DLMPs are designed to co-optimize the dispatch of both the instantaneous demand and the EV charging schedule over the planning horizon. By rearranging (3.16) and (3.17), we have $\rho_{i,t} = -(\mu_{i,t}^{+} - \mu_{i,t}^{-}) - \sum_{t'\geq t+1}(\kappa_{i,t'}^{+} - \kappa_{i,t'}^{-})$ for $\forall t \in T\backslash\{|T|\}$ and $\rho_{i,t} = -\mu_{i,t}^{+} + \mu_{i,t}^{-}$ for $t = |T|$. DLMPs $P_{i,t}^{*}$ can be written as a linear combination of the dual variables associated with the constraints of EVs,

$$\begin{aligned} P_{i,t}^{*} &= \rho_{i,t} - \xi_{i,t} && (3.33)\\ &= \begin{cases} -\mu_{i,t}^{+} + \mu_{i,t}^{-} - \sum_{t'\geq t+1}\kappa_{i,t'}^{+} + \sum_{t'\geq t+1}\kappa_{i,t'}^{-} - \xi_{i,t} & \forall i \in N_c, \forall t \in T\backslash\{|T|\} \\ -\mu_{i,t}^{+} + \mu_{i,t}^{-} - \xi_{i,t} & \forall i \in N_c, t = |T| \end{cases}. && (3.34) \end{aligned}$$

When the constraints (3.7) do not bind, it yields

$$P_{i,t}^{*} = \begin{cases} -\mu_{i,t}^{+} + \mu_{i,t}^{-} - \sum_{t'\geq t+1}\kappa_{i,t'}^{+} + \sum_{t'\geq t+1}\kappa_{i,t'}^{-} & \forall i \in N_c, \forall t \in T\backslash\{|T|\} \\ -\mu_{i,t}^{+} + \mu_{i,t}^{-} & \forall i \in N_c, t = |T| \end{cases}. \tag{3.35}$$

DLMPs defined by (3.32) and (3.35) can be interpreted as the equilibrium conditions for the market clearing of the electric distribution system. This is consistent with DLMPs derived from the dual problem of the DSO's optimization problem (D1).[3] As shown later, both efficient load allocation and distribution grid reliability can be achieved under DLMPs through a decentralized mechanism where loads respond autonomously to the posted DLMPs by maximizing their individual net surplus.

EV Aggregator's Problem

The EV charging management can take different forms: charging management controlled by individual EV user, aggregator based charging management, and the proper combination of the two mechanisms. In this study, we provide models for examining the feasibility of the aggregator based charging management. In the aggregator based charging management, the EV aggregator is a profit-seeking entity, who manages the EV fleet on behalf of EV users, ensures that the energy needs are satisfied, and provides customized service and charging solution. The objective of the EV aggregator in our model is to meet the energy needs of EV users with minimum charging costs. The shape of the DLMP curve and the driving pattern of EV users affect the optimal solution. It is also assumed that the EV aggregator does not possess market power in the DSO market, since the EV aggregator only controls a small portion of the distribution network.

The aggregator based EV optimal charging management can be described by the optimization problem that follows,

$$\text{(P2)} \qquad \min_{\hat{x}_{i,t}:t\in T} \sum_{t\in T} P^*_{i,t}\hat{x}_{i,t} \tag{3.36}$$

$$\text{s.t.} \qquad 0 \le \hat{x}_{i,t} \le E_{i,t} \qquad \forall t \in T \qquad (\hat{\mu}^-_{i,t}, \hat{\mu}^+_{i,t}) \tag{3.37}$$

$$S^-_{i,t} \le S_{i,0} + \sum_{t'\le t-1} \hat{x}_{i,t'} - \sum_{t'\le t} d_{i,t'} \le S^+_{i,t} \quad \forall t \in T\backslash\{1\} \quad (\hat{\kappa}^-_{i,t}, \hat{\kappa}^+_{i,t}). \tag{3.38}$$

The constraints (3.37) and (3.38) ensure that the EV charging energy and the EV battery SOC are within the specified limits. When DLMPs $P^*_{i,t}$ are known to the EV aggregator, the optimization problem is a linear programming problem and the EV aggregator optimally determines the amount of energy to purchase $\hat{x}_{i,t}$ to minimize the charging costs subject to the charging energy limit constraints and the driving requirement constraints.

The dual problem of the EV aggregator's optimization problem (P2) can be shown in the following form,[4]

$$\begin{aligned}\text{(D2)} \quad \max_{\hat{\mu}^+_{i,t},\hat{\kappa}^+_{i,t},\hat{\kappa}^-_{i,t}\ge 0:t\in T} & -\sum_{t\in T}\hat{\mu}^+_{i,t}E_{i,t} - \sum_{t\in T\backslash\{1\}}\hat{\kappa}^-_{i,t}(S_{i,0} - \sum_{t'\le t} d_{i,t'} - S^-_{i,t}) \\ & - \sum_{t\in T\backslash\{1\}}\hat{\kappa}^+_{i,t}(S^+_{i,t} - S_{i,0} + \sum_{t'\le t} d_{i,t'})\end{aligned} \tag{3.39}$$

[3] See Appendix A for details.

[4] See Appendix B for details.

$$\text{s.t.} \quad P^*_{i,t} - \hat{\mu}^-_{i,t} + \hat{\mu}^+_{i,t} - \sum_{t'\geq t+1} \hat{\kappa}^-_{i,t'} + \sum_{t'\geq t+1} \hat{\kappa}^+_{i,t'} = 0 \quad \forall t \in T\backslash\{|T|\} \tag{3.40}$$

$$P^*_{i,t} - \hat{\mu}^-_{i,t} + \hat{\mu}^+_{i,t} = 0 \qquad t = |T| \tag{3.41}$$

$$\hat{\mu}^-_{i,t} \geq 0 \qquad \forall t \in T \tag{3.42}$$

$$\hat{\mu}^+_{i,t} \geq 0 \qquad \forall t \in T \tag{3.43}$$

$$\hat{\kappa}^-_{i,t} \geq 0 \qquad \forall t \in T \tag{3.44}$$

$$\hat{\kappa}^+_{i,t} \geq 0 \qquad \forall t \in T. \tag{3.45}$$

The certificate of optimality of the EV aggregator's optimization problem (P2) are summarized below,

$$0 \leq \hat{x}_{i,t} \leq E_{i,t} \qquad \forall t \in T \tag{3.46}$$

$$S^-_{i,t} \leq S_{i,0} + \sum_{t'\leq t-1} \hat{x}_{i,t'} - \sum_{t'\leq t} d_{i,t'} \leq S^+_{i,t} \qquad \forall t \in T\backslash\{1\} \tag{3.47}$$

$$P^*_{i,t} - \hat{\mu}^-_{i,t} + \hat{\mu}^+_{i,t} - \sum_{t'\geq t+1} \hat{\kappa}^-_{i,t'} + \sum_{t'\geq t+1} \hat{\kappa}^+_{i,t'} = 0 \quad \forall t \in T\backslash\{|T|\} \tag{3.48}$$

$$P^*_{i,t} - \hat{\mu}^-_{i,t} + \hat{\mu}^+_{i,t} = 0 \qquad t = |T| \tag{3.49}$$

$$\hat{\mu}^-_{i,t} \geq 0 \qquad \forall t \in T \tag{3.50}$$

$$\hat{\mu}^+_{i,t} \geq 0 \qquad \forall t \in T \tag{3.51}$$

$$\hat{\kappa}^-_{i,t} \geq 0 \qquad \forall t \in T \tag{3.52}$$

$$\hat{\kappa}^+_{i,t} \geq 0 \qquad \forall t \in T \tag{3.53}$$

$$\hat{\mu}^-_{i,t}\hat{x}_{i,t} = 0 \qquad \forall t \in T \tag{3.54}$$

$$\hat{\mu}^+_{i,t}(E_{i,t} - \hat{x}_{i,t}) = 0 \qquad \forall t \in T \tag{3.55}$$

$$\hat{\kappa}^-_{i,t}(S_{i,0} + \sum_{t'\leq t-1} \hat{x}_{i,t'} - \sum_{t'\leq t} d_{i,t'} - S^-_{i,t}) = 0 \qquad \forall t \in T\backslash\{1\} \tag{3.56}$$

$$\hat{\kappa}^+_{i,t}(S^+_{i,t} - S_{i,0} - \sum_{t'\leq t-1} \hat{x}_{i,t'} + \sum_{t'\leq t} d_{i,t'}) = 0 \qquad \forall t \in T\backslash\{1\}, \tag{3.57}$$

where (3.46)-(3.47) are primal feasibility conditions, (3.48)-(3.53) are dual feasibility conditions and (3.54)-(3.57) are complementarity conditions.

Theorem 1 The efficient EV charging allocation of the DSO's problem $\{x^*_{i,t}\}$ is optimal for the EV aggregator under DLMPs $\{P^*_{i,t}\}$, if the non-negativity constraints of the conventional household demand (3.7) do not bind.

Proof of the Theorem 1: We show that the optimal solution of the DSO's problem $\{x^*_{i,t}, \mu^{+*}_{i,t}, \mu^{-*}_{i,t}, \kappa^{+*}_{i,t'}, \kappa^{-*}_{i,t'}\}$ also satisfies the optimality conditions of the EV aggregator's problem (3.46)-(3.57).

The optimal solution of the DSO's problem satisfies the KKT conditions (3.12)-(3.27). If the non-negativity constraints of the conventional household demand (3.7) do not bind, we have DLMPs $P^*_{i,t} = -\mu^{+*}_{i,t} + \mu^{-*}_{i,t} - \sum_{t'\geq t+1} \kappa^{+*}_{i,t'} + \sum_{t'\geq t+1} \kappa^{-*}_{i,t'}$ for $\forall t \in T\backslash\{|T|\}$ and $P^*_{i,t} = -\mu^{+*}_{i,t} + \mu^{-*}_{i,t}$ for $t = |T|$, which implies (3.48) and (3.49) hold. (3.46), (3.47) and (3.50)-(3.57) come directly from the KKT conditions (3.24)-(3.27). Thus, the efficient EV charging allocation of the DSO's problem satisfies the optimality conditions of the EV aggregator's problem. □

Corollary 1 The efficient allocation of the DSO's problem $\{x^*_{i,t}, c^*_{i,t}\}$ can be achieved in a decentralized system under DLMPs $\{P^*_{i,t}\}$, if the non-negativity constraints of the conventional household demand (3.7) do not bind.

Proof of the Corollary 1: The conventional household demand $\{c^*_{i,t}\}$ is deterministic under DLMPs $\{P^*_{i,t}\}$. From *Theorem 1*, it is known that, under DLMPs $\{P^*_{i,t}\}$, the optimal solution of the EV aggregator's problem is the efficient EV charging allocation of the DSO's problem $\{x^*_{i,t}\}$. Therefore, the efficient allocation of the DSO's problem can be achieved through a decentralized mechanism. □

However, *Theorem 1* only holds under the assumption of non-degeneracy. In the presence of degeneracy, the uniqueness of the solution of the EV aggregator's problem is no longer guaranteed by *Theorem 1*. Hence, in a more accurate way, the allocation of the DSO's problem can, but not necessarily always, be achieved through a decentralized mechanism (Liu and Wen, 2014). The existence of multiple optimal solutions in the EV aggregator's optimization is the result of dual degeneracy. As shown in Figure 3.2, flat DLMPs across several hours are often observed to induce intertemporal demand shifts that relieve congestion. In the dual problem, flat DLMPs across several hours cause one or more basic variables in the basic feasible solution to take zero values, which leads to degeneracy. A degenerate dual problem implies multiple optimal solutions in the primal problem and can result in infeasibility if the solution is implemented through a decentralized scheme. In such cases, pure decentralization fails and some external rationing scheme must be implemented to ensure feasibility of the primal in Huang, Wu, Oren, Li, and Liu (2014). In practice, degeneracy is a problem even at the ISO level. In the CAISO electric power markets, for instance, degeneracy occurs when the dispatch is not unique or when the prices are not unique. In such cases, heuristic procedures are employed to resolve the non-uniqueness.

DSO Market Design

The theoretical framework of DLMPs supports the implementation of a decentralized DSO market with the aim to facilitate efficient load allocation and alleviate congestion on the distribution network. The DSO market process can be described in the form of a coordinated mechanism between the DSO and market participants including retailers and EV aggregators. Based on historical data, the DSO estimates the price elasticity of the conventional household demand, and forecasts the EV demand. Once LMPs are available, the DSO calculates DLMPs that enable local welfare optimization and ensure grid reliability by accounting for the topological constraints of the distribution network. Under the assumption that retailers and EV aggregators respond rationally to the posted DLMPs by maximizing their individual net surplus, the efficient allocation of both the conventional household demand and the EV demand can be achieved by the DSO in a decentralized system under DLMPs, as

proved in *Theorem 1* and *Corollary 1*. This yields the desired outcome of DLMPs – congestion on the distribution network is properly managed, without explicit communication among the DSO and market participants. DLMPs are in themselves sufficient information to induce the consumption behavior of market participants that benefits economic efficiency and system reliability.

3.5 Formulation under Incomplete Information

Pricing and Scheduling under Uncertainty

As discussed in Section 3.4, DLMPs are solved in a deterministic environment where the DSO possesses the complete information of LMPs. The implicit assumption is that the ISO determines LMPs before the DSO calculates DLMPs. In practice, however, LMPs are determined by the ISO with an auction mechanism that economically clears the supply bids against the demand bids submitted by market participants with the transmission constraints enforced. These supply and demand bids also include the bids submitted by the DSO, which invalidates our assumption. When LMPs are unavailable, the DSO needs to determine DLMPs under uncertainty and manage associated risks, based on the forecasts of LMPs.

In wholesale electricity markets, LMPs exhibit high price volatility caused by unanticipated energy imbalances. The marginal production cost increases substantially with the aggregate demand, as the cost function of power generation becomes much steeper above a certain capacity level. The use of inventory to smooth LMPs is limited, since the non-storability of electricity makes it costly to hold inventory for price arbitrage across time periods. LMPs are most volatile during the summer, when a sudden heat wave can strain the ability of generation plants to meet the elevated demand. Without publicly known LMPs, the DSO is exposed to substantial amounts of risks, which requires effective methodologies for pricing and scheduling under uncertainty.

Optimal pricing and scheduling under uncertainty has been a central problem in the practice of power management. Various applications of linear and nonlinear stochastic optimization techniques are proposed to deal with the variability and uncertainty in power system planning. For efficient operation of reservoir systems, Pereira and Pinto (1991) propose an algorithm for multistage stochastic optimization problems based on the piecewise linear approximation of the cost-to-go functions of stochastic dynamic programming to avoid the curse of dimensionality. Takriti, Krasenbrink, and L. S.-Y. Wu (2000) present a mixed-integer program for stochastic unit commitment that can be solved by using Lagrangian relaxation and Benders decomposition. Wong and Fuller (2007) propose a stochastic linear programming model for pricing energy and reserves in power markets under N-1 reliability requirements. Garcia-Gonzalez, Muela, Santos, and González (2008) develop a two-stage stochastic programming model for renewable integration by coupling wind farms with hydro pumped-storage units.

There is a rapidly growing literature concentrated on the development of robust optimization framework to address uncertainty in diverse settings of power planning. Malcolm and Zenios (1994) develop a robust optimization model for capacity expansion under demand uncertainty. Bertsimas, Litvinov, Sun, Zhao, and Zheng (2013) propose a two-stage adaptive robust unit commitment model in the presence of supply and demand uncertainty resulting from variable generation resources, and they further demonstrate that the robust unit commitment model can be solved by a computationally tractable method based on a combination of Benders decomposition type algorithm and the outer approximation technique. Other recent work includes Q. Wang, Watson, and Guan (2013), Zhao and Guan (2013), and Zhao, J. Wang, Watson, and Guan (2013).

Both stochastic optimization and robust optimization are implemented for DLMPs, under the assumption that price uncertainty comes from a multivariate normal distribution $\mathbf{N}(\mu_{\mathbb{P}}, \Sigma_{\mathbb{P}})$ with mean values $\mu_{\mathbb{P}} \in \mathrm{R}^{|T|\times 1}$ and covariance matrix $\Sigma_{\mathbb{P}} \in \mathrm{R}^{|T|\times|T|}$.

Stochastic Optimization

The classical stochastic optimization maximizes the expected social welfare, and the scenarios are sampled from a multivariate normal distribution $\mathbf{N}(\mu_{\mathbb{P}}, \Sigma_{\mathbb{P}})$. Since the objective of the DSO's optimization problem (P1) is linear, it is equivalent to solve a deterministic optimization problem, where LMPs P_t^{LMP} are replaced by the mean values of LMPs $\mu_{\mathbb{P}}$,

$$E[\sum_{i\in N_c}\sum_{t\in T}\int_0^{c_{i,t}} P_{i,t}(\tau_{i,t})d\tau_{i,t} - \sum_{t\in T} P_t^{LMP} q_{g,t}] \tag{3.58}$$

$$= \sum_{i\in N_c}\sum_{t\in T}\int_0^{c_{i,t}} P_{i,t}(\tau_{i,t})d\tau_{i,t} - \sum_{t\in T} \mu_{\mathbb{P}} q_{g,t}. \tag{3.59}$$

We denote this natural extension as DLMPs under uncertainty.

Robust Optimization

Under the robust optimization framework, we assume the demand function at time period t at node i follows the linear dynamics $P_{i,t}(\tau_{i,t}) = a_{i,t} - b_{i,t}\tau_{i,t}$, which simplifies the objective function into a quadratic form. We further substitute in the constraints (3.4) and (3.5), and it yields

$$\text{(P1)} \max_{r_{i,t}:i\in N,t\in T;x_{i,t}:i\in N_c,t\in T} \quad \sum_{i\in N_c}\sum_{t\in T}(a_{i,t}(r_{i,t}-x_{i,t}) - \tfrac{1}{2}b_{i,t}(r_{i,t}-x_{i,t})^2) - \sum_{t\in T} P_t^{LMP}\sum_{i\in N_c} r_{i,t} \tag{3.60}$$

$$\text{s.t.} \quad -K_l \le \sum_{i\in N_c} D_{l,i} r_{i,t} \le K_l \qquad \forall l \in L, \forall t \in T \tag{3.61}$$

$$r_{i,t} - x_{i,t} \ge 0 \qquad \forall i \in N_c, \forall t \in T \tag{3.62}$$

$$0 \le x_{i,t} \le E_{i,t} \qquad \forall i \in N_c, \forall t \in T \tag{3.63}$$

$$S_{i,t}^- \le S_{i,0} + \sum_{t'\le t-1} x_{i,t'} - \sum_{t'\le t} d_{i,t'} \le S_{i,t}^+ \quad \forall i \in N_c, \forall t \in T\backslash\{1\}. \tag{3.64}$$

By putting the objective (3.60) into the constraints and introducing an auxiliary variable s, we can formulate a quadratically constrained quadratic program (QCQP),

$$\begin{aligned}
\text{(QCQP1)} \qquad & \min_{r_{i,t}:i\in N,t\in T;x_{i,t}:i\in N_c,t\in T;s} s && (3.65)\\
\text{s.t.} \quad & -\textstyle\sum_{i\in N_c}\sum_{t\in T}(a_{i,t}(r_{i,t}-x_{i,t})-\frac{1}{2}b_{i,t}(r_{i,t}-x_{i,t})^2) \\
& +\textstyle\sum_{t\in T} P_t^{LMP}\sum_{i\in N_c} r_{i,t} - s \le 0 && (3.66)\\
& -K_l \le \textstyle\sum_{i\in N_c} D_{l,i} r_{i,t} \le K_l && \forall l\in L, \forall t\in T \quad (3.67)\\
& r_{i,t}-x_{i,t}\ge 0 && \forall i\in N_c, \forall t\in T \quad (3.68)\\
& 0\le x_{i,t}\le E_{i,t} && \forall i\in N_c, \forall t\in T \quad (3.69)\\
& S_{i,t}^- \le S_{i,0}+\textstyle\sum_{t'\le t-1} x_{i,t'} - \sum_{t'\le t} d_{i,t'} \le S_{i,t}^+ && \forall i\in N_c, \forall t\in T\backslash\{1\}. \\
& && (3.70)
\end{aligned}$$

By using matrix representation for simplification, we can expressed (QCQP1) in matrix form by using notations presented in Appendix C,

$$\begin{aligned}
\text{(QCQP2)} \qquad & \min_{\mathbb{Y}} e_{2|N_c||T|+1}^T \mathbb{Y} && (3.71)\\
\text{s.t.} \quad & -\mathbb{A}^T\mathbb{U}\mathbb{Y}+\frac{1}{2}\mathbb{Y}^T\mathbb{U}^T\mathbb{B}\mathbb{U}\mathbb{Y}+\mathbb{P}^T\mathbb{V}\mathbb{Y}-e_{2|N_c||T|+1}^T\mathbb{Y}\le \mathbf{0} && (3.72)\\
& -\mathbb{K}\le \mathbb{D}\mathbb{Y}\le \mathbb{K} && (3.73)\\
& \mathbb{U}\mathbb{Y}\ge \mathbf{0} && (3.74)\\
& 0\le \mathbb{W}\mathbb{Y}\le \mathbb{E} && (3.75)\\
& \mathbb{S}^-\le \mathbb{S}+\mathbb{L}\mathbb{Y}-\mathbb{G}\le \mathbb{S}^+. && (3.76)
\end{aligned}$$

where $\mathbb{Y}\in \mathrm{R}^{(2|N_c||T|+1)\times 1}$ is the vector of decision variables and the entries of $\mathbb{Y}$ include s, $r_{i,t}$ and $c_{i,t}$ for $\forall i\in N_c, \forall t\in T$. If the uncertainty set of LMPs $\mathcal{U}=\{\mathbb{P}=\mu_{\mathbb{P}}+\zeta | \zeta^T{\Sigma_{\mathbb{P}}}^{-1}\zeta\le\alpha\}$ is ellipsoidal, Ben-Tal, Nemirovski, and Roos (2002) allow us to rewrite the quadratic constraints (3.72) as the following second-order cone constraints,

$$\begin{aligned}
& -\mathbb{Y}^T\mathbb{U}^T\mathbb{B}\mathbb{U}\mathbb{Y}+2(\mathbb{U}^T\mathbb{A}+e_{2|N_c||T|+1})^T\mathbb{Y} && (3.77)\\
\ge\ & \max_{\mathbb{P}\in\mathcal{U}} 2\mathbb{P}^T\mathbb{V}Y && (3.78)\\
=\ & \max_{\zeta^T{\Sigma_{\mathbb{P}}}^{-1}\zeta\le\alpha} 2(\mu_{\mathbb{P}}+\zeta)^T\mathbb{V}Y && (3.79)\\
=\ & 2\mu_{\mathbb{P}}^T\mathbb{V}Y+\max_{\zeta^T{\Sigma_{\mathbb{P}}}^{-1}\zeta\le\alpha} 2\zeta^T\mathbb{V}Y && (3.80)\\
=\ & 2\mu_{\mathbb{P}}^T\mathbb{V}Y+\max_{(\alpha^{-\frac{1}{2}}{\Sigma_{\mathbb{P}}}^{-\frac{1}{2}}\zeta)^T(\alpha^{-\frac{1}{2}}{\Sigma_{\mathbb{P}}}^{-\frac{1}{2}}\zeta)\le 1} 2((\alpha^{-\frac{1}{2}}{\Sigma_{\mathbb{P}}}^{-\frac{1}{2}})^{-1}\alpha^{-\frac{1}{2}}{\Sigma_{\mathbb{P}}}^{-\frac{1}{2}}\zeta)^T\mathbb{V}Y && (3.81)\\
=\ & 2\mu_{\mathbb{P}}^T\mathbb{V}Y+\max_{(\alpha^{-\frac{1}{2}}{\Sigma_{\mathbb{P}}}^{-\frac{1}{2}}\zeta)^T(\alpha^{-\frac{1}{2}}{\Sigma_{\mathbb{P}}}^{-\frac{1}{2}}\zeta)\le 1} 2(\alpha^{-\frac{1}{2}}{\Sigma_{\mathbb{P}}}^{-\frac{1}{2}}\zeta)^T\alpha^{\frac{1}{2}}({\Sigma_{\mathbb{P}}}^{\frac{1}{2}})^T\mathbb{V}Y && (3.82)\\
=\ & 2\mu_{\mathbb{P}}^T\mathbb{V}Y+2\|\alpha^{\frac{1}{2}}({\Sigma_{\mathbb{P}}}^{\frac{1}{2}})^T\mathbb{V}Y\|_2 && (3.83)\\
=\ & 2\mu_{\mathbb{P}}^T\mathbb{V}Y+2\|\alpha^{\frac{1}{2}}{\Sigma_{\mathbb{P}}}^{\frac{1}{2}}\mathbb{V}Y\|_2, && (3.84)
\end{aligned}$$

where ${\Sigma_{\mathbb{P}}}^{\frac{1}{2}}$ is the square root of covariance matrix $\Sigma_{\mathbb{P}}$, and ${\Sigma_{\mathbb{P}}}^{\frac{1}{2}}$ is a symmetric positive semidefinite matrix. Integrating with the rest of the equations, we have the robust

counterpart of (QCQP1) in the following second-order cone program (SOCP),

$$\text{(SOCP1)} \qquad \min_{\mathbb{Y}} e_{2|N_c||T|+1}^T \mathbb{Y} \tag{3.85}$$

$$\text{s.t.} \quad -\mathbb{Y}^T\mathbb{U}^T\mathbb{B}\mathbb{U}\mathbb{Y} + 2(\mathbb{U}^T\mathbb{A} + e_{2|N_c||T|+1})^T\mathbb{Y} \geq 2\mu_{\mathbb{P}}^T\mathbb{V}Y + 2\|\alpha^{\frac{1}{2}}\Sigma_{\mathbb{P}}^{\frac{1}{2}}\mathbb{V}Y\|_2 \tag{3.86}$$

$$-\mathbb{K} \leq \mathbb{D}\mathbb{Y} \leq \mathbb{K} \tag{3.87}$$

$$\mathbb{U}\mathbb{Y} \geq \mathbf{0} \tag{3.88}$$

$$0 \leq \mathbb{W}\mathbb{Y} \leq \mathbb{E} \tag{3.89}$$

$$\mathbb{S}^- \leq \mathbb{S} + \mathbb{L}\mathbb{Y} - \mathbb{G} \leq \mathbb{S}^+. \tag{3.90}$$

3.6 Data

Case studies have been conducted using the Bus 4 distribution network of the Roy Billinton Test System (RBTS) (Allan et al., 1991) and the Danish driving data. Figure 3.1 illustrates a line diagram of the distribution system used in case studies. On this medium voltage distribution network, there are 3 supply points (SPs), 38 load points (LPs) and 7 feeders. SPs are connected to the main grid by 33 kV/11 kV transformers. A summary of the customer data is presented in Table 3.1, which consist of customer type, peak and average load levels, and number of customers. There are 4779 customers in total on the distribution network. The demand function is assumed to be linear with a price elasticity of -0.1, and this is consistent with empirical evidence reported in Azevedo, Morgan, and Lave (2011). A summary of connection line types is presented in Table 3.2.

The price data for this study consist of the historical day-ahead LMPs at the California Independent System Operator (CAISO) NP15 EZ Gen Hub. For each day, the data contain day-ahead LMPs for each of the 24 hours during that day. The CAISO NP15 EZ Gen Hub is one of the trading hubs in the CAISO electric power markets, and covers the current CAISO congestion management zone NP15.

A nonhomogenous EV fleet is used in case studies. The EV battery size varies according to individual EV driving requirements. It is assumed that the maximum charging power is 1.15 kW (based on a 5A, 230V connection), and the EV energy consumption is 0.15 kWh/km (Q. Wu et al., 2010). The minimum and maximum EV battery SOCs are set as 20% and 85%, respectively. The initial EV battery SOC varies by vehicle to ensure the feasibility of individual charging and driving requirements. This is in accordance with the non-homogenous nature of EV fleet. A summary of the EV data is presented in Table 3.3.

The Danish driving data from the Danish National Travel Survey are used in case studies because the driving behavior in Denmark is representative of the driving pattern of EV users (Q. Wu et al., 2010). In Denmark, the average driving distance is about 40 km per day, and this is similar to the typical driving distance of EV users. The Danish driving data are highly detailed and provide significant insight into the driving habits of Danish drivers. The relevant data used in case studies are

driving start and stop time, distance during driving period, and day type. The EV availability for charging is defined as the period during which the EV is parked. The driving profile from the same day type as LMPs is used to ensure the consistency of case studies.

3.7 Case Study Results

Three case studies are conducted, and the details are presented in Table 3.4.[5] The results of case study 1 are shown in Figure 3.2 - Figure 3.5. Figure 3.3 and Figure 3.5 illustrate the effect of congestion alleviation on Line 1 when DLMPs are introduced. In Figure 3.5, EV aggregators minimize the charging costs under LMPs by allocating all EV loads in a single hour. Under DLMPs, however, EV loads are spread out and distributed among several hours with low LMPs, as shown in Figure 3.3. In Figure 3.2, DLMPs are higher than LMPs on the buses in the downstream areas of the congested lines, which creates intertemporal demand shifts that relieve congestion. In case study 2, without DLMPs, congestion occurs in both the morning and the afternoon when LMPs are low in Figure 3.9, but congestion is successfully alleviated under DLMPs as EV loads are shifted to the adjacent low LMP hours in Figure 3.7. The results of case study 3 are plotted in Figure 3.10 - Figure 3.13, and similar features are observed as case study 1 and case study 2.

In order to further demonstrate the effectiveness of the proposed DLMP concept in congestion alleviation, case studies with three projected futuristic EV penetration scenarios are conducted in Figure 3.14 - Figure 3.19 with 200%, 500% and 1000% EV penetration. DLMPs increase as the EV penetration level increases, but the line capacity constraints are not violated in any of the three scenarios, as shown in Figure 3.15, Figure 3.17, and Figure 3.19. It concludes that the DLMP concept is promising even in the presence of high EV penetration, which is likely to come into existence in the future.

We compare the results obtained by stochastic optimization and robust optimization. $\mu_{\mathbb{P}}$ and $\Sigma_{\mathbb{P}}$ are empirically estimated from historical LMPs with maximum likelihood estimators. Since the tail distribution can only be sampled under LMPs that yield the worst objective value, importance sampling technique is employed for the simulation of social welfare under DLMPs and robust DLMPs. Importance sampling is a statistical technique for estimating properties of a particular distribution. It generates samples from a different distribution rather than the distribution of interest to reduce variance in Monte Carlo simulation. We refer to the exposition in Hastings (1970). We draw samples from the proposal probability density function, which is centered around the worst-case LMPs, instead of the real probability density function of LMPs.

[5]The EV penetration is defined as the ratio of the maximum EV charging demand to the conventional household demand, and the maximum EV charging demand is the total EV charging demand when all EVs charge simultaneously.

As we discussed, the size of the uncertainty set is controlled by α. To demonstrate the effect of parameter α, we present the results obtained from robust optimization under different α in Figure 3.20 - Figure 3.25. $\alpha = 1$ is the smallest set which captures the lowest level of uncertainty, and conversely $\alpha = 20$ is the largest set which captures the highest level of uncertainty. Compared to the case with $\alpha = 1$, the EV demand is shifted from 2 a.m., 3 a.m. and 4 a.m. to 6 a.m., 7 a.m. and 6 p.m. in the case with $\alpha = 20$, because LMPs during 2 a.m., 3 a.m. and 4 a.m. are no longer cheap under the worst-case LMPs. Figure 3.26 compares the probability density function of social welfare under DLMPs, robust DLMPs with $\alpha = 5$ and robust DLMPs with $\alpha = 20$. They show significant improvements in reducing price risk by the robust approach, since more probability density is concentrated around the mean value under robust DLMPs. In Figure 3.27, we explore the effect of tail risk reduction by robust optimization, and importance sampling technique is used. A substantial decrease of probability density in the tail under robust DLMPs is observed. These results illustrate the differences of robust optimization from the classical stochastic optimization.

3.8 Conclusion

An integrated DLMP concept is proposed to address the problem of congestion alleviation on the distribution network faced by future power systems. By design, it can be adopted under the existing LMP framework for achieving economic allocation of both the EV demand and the conventional demand subject to line capacity constraints. In the presence of price uncertainty, a robust DLMP method is developed for EV charging management. Case studies based on the RBTS electric distribution network and the Danish driving data show the efficacy of the proposed DLMP concept. In a very extreme scenario with 1000% EV penetration, congestion on the distribution network can be alleviated by introducing DLMPs. Under robust DLMPs, both variance and tail risk reduction is achieved.

3.9 Appendix

Appendix A

From duality theory, primal and dual problems are alternative ways of characterizing market equilibrium conditions for both the EV demand and the conventional demand. If we describe our primal problem as a classical welfare maximization problem, its dual problem can be interpreted as a cost minimization problem, where dual variables are related to shadow prices that reflect the economic values of resources available to market participants. The Lagrangian dual function can be used to express the primal problem (P1) as an unconstrained one. In order to simplify the Lagrangian dual function, the PTDF coefficients associated with the generation node $D_{l,g} = 0$. The dual problem can be derived from weak duality theorem,

$$
\begin{aligned}
&\max_{r_{i,t}:i\in N,t\in T;c_{i,t},x_{i,t}:i\in N_c,t\in T;q_{g,t}:t\in T} \sum_{i\in N_c}\sum_{t\in T}\int_0^{c_{i,t}} P_{i,t}(\tau_{i,t})d\tau_{i,t} - \sum_{t\in T} P_t^{LMP} q_{g,t} \\
&+ \min_{p_t,\delta_{g,t}:t\in T;\rho_{i,t}:i\in N_c,t\in T;\lambda_{l,t}^-,\lambda_{l,t}^+\geq 0:l\in L,t\in T;\xi_{i,t},\mu_{i,t}^-,\mu_{i,t}^+\geq 0:i\in N_c,t\in T;\kappa_{i,t}^-,\kappa_{i,t}^+\geq 0:i\in N_c,t\in T\setminus\{1\}} \\
&\{-\sum_{t\in T} p_t \sum_{i\in N} r_{i,t} + \sum_{l\in L}\sum_{t\in T}\lambda_{l,t}^-(\sum_{i\in N} D_{l,i} r_{i,t} + K_l) + \sum_{l\in L}\sum_{t\in T}\lambda_{l,t}^+(K_l - \sum_{i\in N} D_{l,i} r_{i,t}) \\
&+ \sum_{t\in T}\delta_{g,t}(r_{g,t} + q_{g,t}) + \sum_{i\in N_c}\sum_{\forall t\in T}\rho_{i,t}(r_{i,t} - c_{i,t} - x_{i,t}) + \sum_{i\in N_c}\sum_{t\in T}\xi_{i,t} c_{i,t} \\
&+ \sum_{i\in N_c}\sum_{t\in T}\mu_{i,t}^- x_{i,t} + \sum_{i\in N_c}\sum_{t\in T}\mu_{i,t}^+(E_{i,t} - x_{i,t}) \\
&+ \sum_{i\in N_c}\sum_{t\in T\setminus\{1\}}\kappa_{i,t}^-(S_{i,0} + \sum_{t'\leq t-1} x_{i,t'} - \sum_{t'\leq t} d_{i,t'} - S_{i,t}^-) \\
&+ \sum_{i\in N_c}\sum_{t\in T\setminus\{1\}}\kappa_{i,t}^+(S_{i,t}^+ - S_{i,0} - \sum_{t'\leq t-1} x_{i,t'} + \sum_{t'\leq t} d_{i,t'})\}
\end{aligned}
\tag{3.91}
$$

$$
\begin{aligned}
\leq & \min_{p_t,\delta_{g,t}:t\in T;\rho_{i,t}:i\in N_c,t\in T;\lambda^-_{l,t},\lambda^+_{l,t}\geq 0:l\in L,t\in T;\xi_{i,t},\mu^-_{i,t},\mu^+_{i,t}\geq 0:i\in N_c,t\in T;\kappa^-_{i,t},\kappa^+_{i,t}\geq 0:i\in N_c,t\in T\setminus\{1\}} \\
& \max_{r_{i,t}:i\in N,t\in T;c_{i,t},x_{i,t}:i\in N_c,t\in T;q_{g,t}:t\in T} \sum_{i\in N_c}\sum_{t\in T}\int_0^{c_{i,t}} P_{i,t}(\tau_{i,t})d\tau_{i,t} - \sum_{t\in T} P_t^{LMP} q_{g,t} \\
& \{-\sum_{t\in T} p_t \sum_{i\in N} r_{i,t} + \sum_{l\in L}\sum_{t\in T}\lambda^-_{l,t}(\sum_{i\in N} D_{l,i} r_{i,t} + K_l) + \sum_{l\in L}\sum_{t\in T}\lambda^+_{l,t}(K_l - \sum_{i\in N} D_{l,i} r_{i,t}) \\
& + \sum_{t\in T}\delta_{g,t}(r_{g,t}+q_{g,t}) + \sum_{i\in N_c}\sum_{\forall t\in T}\rho_{i,t}(r_{i,t}-c_{i,t}-x_{i,t}) + \sum_{i\in N_c}\sum_{t\in T}\xi_{i,t}c_{i,t} \\
& + \sum_{i\in N_c}\sum_{t\in T}\mu^-_{i,t}x_{i,t} + \sum_{i\in N_c}\sum_{t\in T}\mu^+_{i,t}(E_{i,t}-x_{i,t}) \\
& + \sum_{i\in N_c}\sum_{t\in T\setminus\{1\}}\kappa^-_{i,t}(S_{i,0} + \sum_{t'\leq t-1} x_{i,t'} - \sum_{t'\leq t} d_{i,t'} - S^-_{i,t}) \\
& + \sum_{i\in N_c}\sum_{t\in T\setminus\{1\}}\kappa^+_{i,t}(S^+_{i,t} - S_{i,0} - \sum_{t'\leq t-1} x_{i,t'} + \sum_{t'\leq t} d_{i,t'})\} \qquad (3.92)
\end{aligned}
$$

$$
\begin{aligned}
= & \min_{p_t,\delta_{g,t}:t\in T;\rho_{i,t}:i\in N_c,t\in T;\lambda^-_{l,t},\lambda^+_{l,t}\geq 0:l\in L,t\in T;\xi_{i,t},\mu^-_{i,t},\mu^+_{i,t}\geq 0:i\in N_c,t\in T;\kappa^-_{i,t},\kappa^+_{i,t}\geq 0:i\in N_c,t\in T\setminus\{1\}} \\
& \max_{r_{i,t}:i\in N,t\in T;c_{i,t},x_{i,t}:i\in N_c,t\in T;q_{g,t}:t\in T} L(r_{i,t},c_{i,t},x_{i,t},q_{g,t};p_t,\delta_{g,t},\rho_{i,t},\lambda^-_{l,t},\lambda^+_{l,t},\xi_{i,t},\mu^-_{i,t},\mu^+_{i,t},\kappa^-_{i,t},\kappa^+_{i,t}),
\end{aligned}
$$

$$
(3.93)
$$

where

$$
\begin{aligned}
& L(r_{i,t},c_{i,t},x_{i,t},q_{g,t};p_t,\delta_{g,t},\rho_{i,t},\lambda^-_{l,t},\lambda^+_{l,t},\xi_{i,t},\mu^-_{i,t},\mu^+_{i,t},\kappa^-_{i,t},\kappa^+_{i,t}) \\
= & \sum_{i\in N_c}\sum_{t\in T}\int_0^{c_{i,t}} P_{i,t}(\tau_{i,t})d\tau_{i,t} - \sum_{t\in T} P_t^{LMP} q_{g,t} \\
& \{-\sum_{t\in T} p_t \sum_{i\in N} r_{i,t} + \sum_{l\in L}\sum_{t\in T}\lambda^-_{l,t}(\sum_{i\in N} D_{l,i} r_{i,t} + K_l) + \sum_{l\in L}\sum_{t\in T}\lambda^+_{l,t}(K_l - \sum_{i\in N} D_{l,i} r_{i,t}) \\
& + \sum_{t\in T}\delta_{g,t}(r_{g,t}+q_{g,t}) + \sum_{i\in N_c}\sum_{\forall t\in T}\rho_{i,t}(r_{i,t}-c_{i,t}-x_{i,t}) + \sum_{i\in N_c}\sum_{t\in T}\xi_{i,t}c_{i,t} \\
& + \sum_{i\in N_c}\sum_{t\in T}\mu^-_{i,t}x_{i,t} + \sum_{i\in N_c}\sum_{t\in T}\mu^+_{i,t}(E_{i,t}-x_{i,t}) \\
& + \sum_{i\in N_c}\sum_{t\in T\setminus\{1\}}\kappa^-_{i,t}(S_{i,0} + \sum_{t'\leq t-1} x_{i,t'} - \sum_{t'\leq t} d_{i,t'} - S^-_{i,t}) \\
& + \sum_{i\in N_c}\sum_{t\in T\setminus\{1\}}\kappa^+_{i,t}(S^+_{i,t} - S_{i,0} - \sum_{t'\leq t-1} x_{i,t'} + \sum_{t'\leq t} d_{i,t'})\}. \qquad (3.94)
\end{aligned}
$$

We take the derivative with respect to each primal variable, and set all the deriva-

tives equal to zero,

$$\frac{\partial L}{\partial c_{i,t}} = P_{i,t}(c_{i,t}) - \rho_{i,t} + \xi_{i,t} \qquad \forall i \in N_c, \forall t \in T \tag{3.95}$$

$$\frac{\partial L}{\partial r_{i,t}} = -p_t - \sum_{l \in L}(\lambda^+_{l,t} - \lambda^-_{l,t}) D_{l,i} + \rho_{i,t} \qquad \forall i \in N_c, \forall t \in T \tag{3.96}$$

$$\frac{\partial L}{\partial r_{g,t}} = -p_t - \sum_{l \in L}(\lambda^+_{l,t} - \lambda^-_{l,t}) D_{l,g} + \delta_{g,t} \qquad \forall t \in T \tag{3.97}$$

$$\frac{\partial L}{\partial q_{g,t}} = -P^{LMP}_t + \delta_{g,t} \qquad \forall t \in T \tag{3.98}$$

$$\frac{\partial L}{\partial x_{i,t}} = \begin{cases} -\rho_{i,t} - (\mu^+_{i,t} - \mu^-_{i,t}) - \sum_{t' \geq t+1}(\kappa^+_{i,t'} - \kappa^-_{i,t'}) & \forall i \in N_c, \forall t \in T \backslash \{|T|\} \\ -\rho_{i,t} - (\mu^+_{i,t} - \mu^-_{i,t}) & \forall i \in N_c, t = |T| \end{cases}. \tag{3.99}$$

Under these conditions, the Lagrangian dual function can be derived as,

$$\begin{aligned} & g(p_t, \delta_{g,t}, \rho_{i,t}, \lambda^-_{l,t}, \lambda^+_{l,t}, \xi_{i,t}, \mu^-_{i,t}, \mu^+_{i,t}, \kappa^-_{i,t}, \kappa^+_{i,t}) \\ = & \max_{r_{i,t}: i \in N, t \in T; c_{i,t}, x_{i,t}: i \in N_c, t \in T; q_{g,t}: t \in T} L(r_{i,t}, c_{i,t}, x_{i,t}, q_{g,t}; p_t, \delta_{g,t}, \rho_{i,t}, \lambda^-_{l,t}, \lambda^+_{l,t}, \xi_{i,t}, \mu^-_{i,t}, \mu^+_{i,t}, \kappa^-_{i,t}, \kappa^+_{i,t}) \end{aligned} \tag{3.100}$$

$$\begin{aligned} = & \sum_{i \in N_c} \sum_{t \in T} \int_0^{c_{i,t}} P_{i,t}(\tau_{i,t}) d\tau_{i,t} + \sum_{l \in L} \sum_{t \in T} \lambda^-_{l,t} K_l + \sum_{l \in L} \sum_{t \in T} \lambda^+_{l,t} K_l + \sum_{i \in N_c} \sum_{t \in T} \mu^+_{i,t} E_{i,t} \\ & + \sum_{i \in N_c} \sum_{t \in T \backslash \{1\}} \kappa^-_{i,t} (S_{i,0} - \sum_{t' \leq t} d_{i,t'} - S^-_{i,t}) + \sum_{i \in N_c} \sum_{t \in T \backslash \{1\}} \kappa^+_{i,t} (S^+_{i,t} - S_{i,0} + \sum_{t' \leq t} d_{i,t'}). \end{aligned} \tag{3.101}$$

The dual problem is presented as follows,

$$\begin{aligned} \text{(D1)} \quad & \min_{p_t, \delta_{g,t}: t \in T; \rho_{i,t}: i \in N_c, t \in T; \lambda^-_{l,t}, \lambda^+_{l,t}: l \in L, t \in T; \xi_{i,t}, \mu^-_{i,t}, \mu^+_{i,t}, \kappa^-_{i,t}, \kappa^+_{i,t}: i \in N_c, t \in T; c^*_{i,t}: i \in N_c, t \in T} \\ & \sum_{i \in N_c} \sum_{t \in T} \int_0^{c^*_{i,t}} P_{i,t}(\tau_{i,t}) d\tau_{i,t} + \sum_{l \in L} \sum_{t \in T} \lambda^-_{l,t} K_l + \sum_{l \in L} \sum_{t \in T} \lambda^+_{l,t} K_l + \sum_{i \in N_c} \sum_{t \in T} \mu^+_{i,t} E_{i,t} \\ & + \sum_{i \in N_c} \sum_{t \in T \backslash \{1\}} \kappa^-_{i,t} (S_{i,0} - \sum_{t' \leq t} d_{i,t'} - S^-_{i,t}) + \sum_{i \in N_c} \sum_{t \in T \backslash \{1\}} \kappa^+_{i,t} (S^+_{i,t} - S_{i,0} + \sum_{t' \leq t} d_{i,t'}) \end{aligned} \tag{3.102}$$

$$\text{s.t.} \quad P_{i,t}(c^*_{i,t}) = P^{LMP}_t + \sum_{l\in L}(\lambda^+_{l,t} - \lambda^-_{l,t})D_{l,i} - \xi_{i,t} \qquad \forall i \in N_c, \forall t \in \mathcal{T} \tag{3.103}$$

$$P_{i,t}(c^*_{i,t}) = -\mu^+_{i,t} + \mu^-_{i,t} - \sum_{t'\geq t+1}\kappa^+_{i,t'} + \sum_{t'\geq t+1}\kappa^-_{i,t'} - \xi_{i,t} \quad \forall i \in N_c, \forall t \in T\backslash\{|T|\} \tag{3.104}$$

$$P_{i,t}(c^*_{i,t}) = -\mu^+_{i,t} + \mu^-_{i,t} - \xi_{i,t} \qquad \forall i \in N_c, t = |T| \tag{3.105}$$

$$\lambda^-_{l,t} \geq 0 \qquad \forall l \in L, \forall t \in T \tag{3.106}$$

$$\lambda^+_{l,t} \geq 0 \qquad \forall l \in L, \forall t \in T \tag{3.107}$$

$$\xi_{i,t} \geq 0 \qquad \forall i \in N_c, \forall t \in \mathcal{T} \tag{3.108}$$

$$\mu^-_{i,t} \geq 0 \qquad \forall i \in N_c, \forall t \in \mathcal{T} \tag{3.109}$$

$$\mu^+_{i,t} \geq 0 \qquad \forall i \in N_c, \forall t \in \mathcal{T} \tag{3.110}$$

$$\kappa^-_{i,t} \geq 0 \qquad \forall i \in N_c, \forall t \in \mathcal{T} \tag{3.111}$$

$$\kappa^+_{i,t} \geq 0 \qquad \forall i \in N_c, \forall t \in T. \tag{3.112}$$

The economic interpretation of equilibrium conditions in (3.103), (3.104), and (3.105) shows the marginal value relationship between the EV charging energy and the conventional household demand, which is consistent with DLMPs derived from the KKT conditions.

Appendix B

The Lagrangian can be used to express the primal problem (P2) as an unconstrained one. The dual problem can be derived from weak duality theorem,

$$\begin{aligned}
&\min_{\hat{x}_{i,t}:t\in T}\sum_{t\in T} P^*_{i,t}\hat{x}_{i,t} + \max_{\hat{\mu}^-_{i,t},\hat{\mu}^+_{i,t},\hat{\kappa}^-_{i,t},\hat{\kappa}^+_{i,t}\geq 0:t\in T}\sum_{t\in T} -\hat{\mu}^-_{i,t}\hat{x}_{i,t} + \sum_{t\in T}\hat{\mu}^+_{i,t}(\hat{x}_{i,t} - E_{i,t}) \\
&+ \sum_{t\in T\backslash\{1\}}\hat{\kappa}^-_{i,t}(S^-_{i,t} - S_{i,0} - \sum_{t'\leq t-1}\hat{x}_{i,t'} + \sum_{t'\leq t} d_{i,t'}) \\
&+ \sum_{t\in T\backslash\{1\}}\hat{\kappa}^+_{i,t}(S_{i,0} + \sum_{t'\leq t-1}\hat{x}_{i,t'} - \sum_{t'\leq t} d_{i,t'} - S^+_{i,t})
\end{aligned} \tag{3.113}$$

$$\begin{aligned}
\geq\ &\max_{\hat{\mu}^-_{i,t},\hat{\mu}^+_{i,t},\hat{\kappa}^-_{i,t},\hat{\kappa}^+_{i,t}\geq 0:t\in T}\min_{\hat{x}_{i,t}:t\in T}\sum_{t\in T} P^*_{i,t}\hat{x}_{i,t} + \sum_{t\in T} -\hat{\mu}^-_{i,t}\hat{x}_{i,t} + \sum_{t\in T}\hat{\mu}^+_{i,t}(\hat{x}_{i,t} - E_{i,t}) \\
&+ \sum_{t\in T\backslash\{1\}}\hat{\kappa}^-_{i,t}(S^-_{i,t} - S_{i,0} - \sum_{t'\leq t-1}\hat{x}_{i,t'} + \sum_{t'\leq t} d_{i,t'}) \\
&+ \sum_{t\in T\backslash\{1\}}\hat{\kappa}^+_{i,t}(S_{i,0} + \sum_{t'\leq t-1}\hat{x}_{i,t'} - \sum_{t'\leq t} d_{i,t'} - S^+_{i,t})
\end{aligned} \tag{3.114}$$

$$= \max_{\hat{\mu}^-_{i,t},\hat{\mu}^+_{i,t},\hat{\kappa}^-_{i,t},\hat{\kappa}^+_{i,t}\geq 0:t\in T}\min_{\hat{x}_{i,t}:t\in T} L(\hat{x}_{i,t};\hat{\mu}^-_{i,t},\hat{\mu}^+_{i,t},\hat{\kappa}^-_{i,t},\hat{\kappa}^+_{i,t}), \tag{3.115}$$

where

$$L(\hat{x}_{i,t};\hat{\mu}^-_{i,t},\hat{\mu}^+_{i,t},\hat{\kappa}^-_{i,t},\hat{\kappa}^+_{i,t}) \tag{3.116}$$

$$\begin{aligned} &= P^*_{i,t}\hat{x}_{i,t} + \sum_{t\in T} -\hat{\mu}^-_{i,t}\hat{x}_{i,t} + \sum_{t\in T}\hat{\mu}^+_{i,t}(\hat{x}_{i,t}-E_{i,t}) \\ &+ \sum_{t\in T\backslash\{1\}}\hat{\kappa}^-_{i,t}(S^-_{i,t}-S_{i,0}-\sum_{t'\le t-1}\hat{x}_{i,t'}+\sum_{t'\le t}d_{i,t'}) \\ &+ \sum_{t\in T\backslash\{1\}}\hat{\kappa}^+_{i,t}(S_{i,0}+\sum_{t'\le t-1}\hat{x}_{i,t'}-\sum_{t'\le t}d_{i,t'}-S^+_{i,t}). \end{aligned} \tag{3.117}$$

We take the derivative with respect to each primal variable, and set all the derivatives equal to zero,

$$\frac{\partial L}{\partial \hat{x}_{i,t}} = P^*_{i,t}-\hat{\mu}^-_{i,t}+\hat{\mu}^+_{i,t}-\sum_{t'\ge t+1}\hat{\kappa}^-_{i,t'}+\sum_{t'\ge t+1}\hat{\kappa}^+_{i,t'}=0 \qquad \forall t\in T\backslash\{|T|\} \tag{3.118}$$

$$\frac{\partial L}{\partial \hat{x}_{i,t}} = P^*_{i,t}-\hat{\mu}^-_{i,t}+\hat{\mu}^+_{i,t} \qquad t=|T|. \tag{3.119}$$

Under these conditions, the Lagrangian dual function can be derived as,

$$g(\hat{\mu}^-_{i,t},\hat{\mu}^+_{i,t},\hat{\kappa}^-_{i,t},\hat{\kappa}^+_{i,t}) \tag{3.120}$$

$$= \max_{\hat{\mu}^-_{i,t},\hat{\mu}^+_{i,t},\hat{\kappa}^-_{i,t},\hat{\kappa}^+_{i,t}\ge 0:t\in T}\ \min_{\hat{x}_{i,t}:t\in T} L(\hat{x}_{i,t};\hat{\mu}^-_{i,t},\hat{\mu}^+_{i,t},\hat{\kappa}^-_{i,t},\hat{\kappa}^+_{i,t}) \tag{3.121}$$

$$\begin{aligned} = &\max_{\hat{\mu}^-_{i,t},\hat{\mu}^+_{i,t},\hat{\kappa}^-_{i,t},\hat{\kappa}^+_{i,t}\ge 0:t\in T} -\sum_{t\in T}\hat{\mu}^+_{i,t}E_{i,t} \\ &+ \sum_{t\in T\backslash\{1\}}\hat{\kappa}^-_{i,t}(S^-_{i,t}-S_{i,0}+\sum_{t'\le t}d_{i,t'}) + \sum_{t\in T\backslash\{1\}}\hat{\kappa}^+_{i,t}(S_{i,0}-\sum_{t'\le t}d_{i,t'}-S^+_{i,t}). \end{aligned} \tag{3.122}$$

Appendix C

The following notation is used to express (QCQP1) in matrix form,

$$\mathbb{R}^{|N_c|\times 1}_t = \{r_{1,t}, r_{2,t}, \ldots, r_{|N_c|-1,t}, r_{|N_c|,t}\}^T \tag{3.123}$$

$$\mathbb{X}^{|N_c|\times 1}_t = \{x_{1,t}, x_{2,t}, \ldots, x_{|N_c|-1,t}, x_{|N_c|,t}\}^T \tag{3.124}$$

$$\mathbb{Y}^{(2|N_c||T|+1)\times 1} = \{\mathbb{R}^T_1, \ldots, \mathbb{R}^T_{|T|}, \mathbb{X}^T_1, \ldots, \mathbb{X}^T_{|T|}, s\}^T \tag{3.125}$$

$$A^{|T|\times 1}_t = \{a_{1,t}, a_{2,t}, \ldots, a_{|N_c|-1,t}, a_{|N_c|,t}\}^T \tag{3.126}$$

$$\mathbb{A}^{|T||N_c|\times 1} = \{A^T_1, A^T_2, \ldots, A^T_{|T|-1}, A^T_{|T|}\}^T \tag{3.127}$$

$$\mathbb{U}^{|T||N_c|\times(2|T||N_c|+1)} = \begin{pmatrix} \vdots \\ e^T_i - e^T_{|T||N_c|+i} \\ \vdots \end{pmatrix} \tag{3.128}$$

$$\mathbb{P}^{|T|\times 1} = \{P_1^{LMP}, P_2^{LMP}, \ldots, P_{|T|-1}^{LMP}, P_{|T|}^{LMP}\}^T \tag{3.129}$$

$$\mathcal{K}_t^{|L|\times 1} = \{K_1, K_2, \ldots, K_{|L|-1}, K_{|L|}\}^T \tag{3.130}$$

$$\mathbb{K}^{|L||T|\times 1} = \{\mathcal{K}_1^T, \mathcal{K}_2^T, \ldots, \mathcal{K}_{|L|-1}^T, \mathcal{K}_{|L|}^T\}^T \tag{3.131}$$

$$\mathbb{W}^{|N_c||T|\times(2|T||N_c|+1)} = \begin{pmatrix} \mathbf{0}^{|N_c||T|\times|N_c||T|} & I^{|N_c||T|\times|N_c||T|} & \mathbf{0}^{|N_c||T|\times 1} \end{pmatrix} \tag{3.132}$$

$$\mathcal{E}_t^{|N_c|\times 1} = \{E_{1,t}, E_{2,t}, \ldots, E_{|N_c|-1,t}, E_{|N_c|,t}\}^T \tag{3.133}$$

$$\mathbb{E}^{|N_c||T|\times 1} = \{\mathcal{E}_1^T, \mathcal{E}_2^T, \ldots, \mathcal{E}_{|T|-1}^T, \mathcal{E}_{|T|}^T\}^T \tag{3.134}$$

$$\mathcal{G}_t^{|N_c|\times 1} = \{\sum_{t'\le t} d_{1,t'}, \sum_{t'\le t} d_{2,t'}, \ldots, \sum_{t'\le t} d_{|N_c|-1,t'}, \sum_{t'\le t} d_{|N_c|,t'}\}^T \tag{3.135}$$

$$\mathbb{G}^{|N_c||T|\times 1} = \{\mathcal{G}_1^T, \mathcal{G}_2^T, \ldots, \mathcal{G}_{|T|-1}^T, \mathcal{G}_{|T|}^T\}^T \tag{3.136}$$

$$\mathcal{S}^{|N_c|\times 1} = \{S_{1,0}, S_{2,0}, \ldots, S_{|N_c|-1,0}, S_{|N_c|,0}\}^T \tag{3.137}$$

$$\mathbb{S}^{|N_c||T|\times 1} = \{\ldots, \mathcal{S}^T, \ldots\}^T \tag{3.138}$$

$$\mathcal{S}_t^{+|N_c|\times 1} = \{S_{1,0}^+, S_{2,0}^+, \ldots, S_{|N_c|-1,0}^+, S_{|N_c|,0}^+\}^T \tag{3.139}$$

$$\mathbb{S}^{+|N_c||T|\times 1} = \{\mathcal{S}_1^{+T}, \mathcal{S}_2^{+T}, \ldots, \mathcal{S}_{|T|-1}^{+\ T}, \mathcal{S}_{|T|}^{+\ T}\}^T \tag{3.140}$$

$$\mathcal{S}_t^{-|N_c|\times 1} = \{S_{1,0}^-, S_{2,0}^-, \ldots, S_{|N_c|-1,0}^-, S_{|N_c|,0}^-\}^T \tag{3.141}$$

$$\mathbb{S}^{-|N_c||T|\times 1} = \{\mathcal{S}_1^{-T}, \mathcal{S}_2^{-T}, \ldots, \mathcal{S}_{|T|-1}^{-\ T}, \mathcal{S}_{|T|}^{-\ T}\}^T \tag{3.142}$$

$$B_t^{|T|\times|T|} = \begin{pmatrix} b_{1,t} & & & & \\ & b_{2,t} & & & \\ & & \ddots & & \\ & & & b_{|N_c|-1,t} & \\ & & & & b_{|N_c|,t} \end{pmatrix} \tag{3.143}$$

$$\mathbb{B}^{|T||N_c|\times|T||N_c|} = \begin{pmatrix} B_1 & & & & \\ & B_2 & & & \\ & & \ddots & & \\ & & & B_{|T|-1} & \\ & & & & B_{|T|} \end{pmatrix} \tag{3.144}$$

$$\mathcal{D}_t^{|L|\times|N_c|} = \begin{pmatrix} D_{1,1} & D_{1,2} & \dots & D_{1,|N_c|-1} & D_{1,|N_c|} \\ D_{2,1} & D_{2,2} & \dots & D_{2,|N_c|-1} & D_{2,|N_c|} \\ & & \vdots & & \\ D_{|L|-1,1} & D_{|L|-1,2} & \dots & D_{|L|-1,|N_c|-1} & D_{|L|-1,|N_c|} \\ D_{|L|,1} & D_{|L|,2} & \dots & D_{|L|,|N_c|-1} & D_{|L|,|N_c|} \end{pmatrix} \tag{3.145}$$

$$\mathbb{D}^{|L||T|\times(2|T||N_c|+1)} = \left(\begin{array}{ccccc|c} \mathcal{D}_1 & & & & & \\ & \mathcal{D}_2 & & & & \\ & & \ddots & & & \mathbf{0}^{|L||T|\times(|T||N_c|+1)} \\ & & & \mathcal{D}_{|T|-1} & & \\ & & & & \mathcal{D}_{|T|} & \end{array}\right) \tag{3.146}$$

$$= \left(\begin{array}{ccccc|c} \mathbf{1}^{|N_c|\times 1} & & & & & \\ & \mathbf{1}^{|N_c|\times 1} & & & & \\ & & \ddots & & & \mathbf{0}^{|T|\times(|T||N_c|+1)} \\ & & & \mathbf{1}^{|N_c|\times 1} & & \\ & & & & \mathbf{1}^{|N_c|\times 1} & \end{array}\right) \tag{3.147}$$

$$= \left(\begin{array}{c|cccc|c} & \mathbf{0}^{|N_c|\times|N_c|} & \mathbf{0}^{|N_c|\times|N_c|} & \dots & \mathbf{0}^{|N_c|\times|N_c|} & \mathbf{0}^{|N_c|\times|N_c|} & \\ & I^{|N_c|\times|N_c|} & \mathbf{0}^{|N_c|\times|N_c|} & \dots & \mathbf{0}^{|N_c|\times|N_c|} & \mathbf{0}^{|N_c|\times|N_c|} & \\ \mathbf{0}^{|N_c||T|\times|N_c||T|} & \vdots & & & & \vdots & \mathbf{0}^{|N_c||T|\times 1} \\ & I^{|N_c|\times|N_c|} & I^{|N_c|\times|N_c|} & \dots & \mathbf{0}^{|N_c|\times|N_c|} & \mathbf{0}^{|N_c|\times|N_c|} & \\ & I^{|N_c|\times|N_c|} & I^{|N_c|\times|N_c|} & \dots & I^{|N_c|\times|N_c|} & \mathbf{0}^{|N_c|\times|N_c|} & \end{array}\right). \tag{3.148}$$

Appendix D

Table 3.1: Customer Data Summary

Number of Load Points	Load Points	Customer Type	Average Load Per Load Point	Peak Load Per Load Point	Number of Customers
15	1-4, 11-13, 18-21, 32-35	Residential	0.545 MW	0.8869 MW	200
7	5, 14, 15, 22, 23, 36, 37	Residential	0.5 MW	0.8137 MW	200
7	8, 10, 26-30	Small user	1.0 MW	1.63 MW	1
2	9, 31	Small user	1.5 MW	2.445 MW	1
7	6, 7, 16, 17, 24, 25, 38	Commercial	0.415 MW	0.6714 MW	10
Total			24.58 MW	40.00 MW	4779

Table 3.2: Connection Line Types

Connection Line Type	Line Length	Line Number
1	0.6 km	2 6 10 14 17 21 25 28 30 34 38 41 43 46 49 51 55 58 61 64 67
2	0.75 km	1 4 7 9 12 16 19 22 24 27 29 32 35 37 40 42 45 48 50 53 56 60 63 65
3	0.8 km	3 5 8 11 13 15 18 20 23 26 31 33 36 39 44 47 52 54 57 59 62 66

Table 3.3: EV Data Summary

EV Parameter	EV Parameter Value
EV Battery Size	25 kWh
Charging Power	5.28 kW
EV Energy Consumption	150 Wh/km
Minimum SOC	20%
Maximum SOC	85%

Table 3.4: Case Study Scenarios

Case Study Number	Day Type	EV Penetration
1	Friday	100%
2	Saturday	100%
3	Thursday	100%, 200%, 500% and 1000%

Appendix F

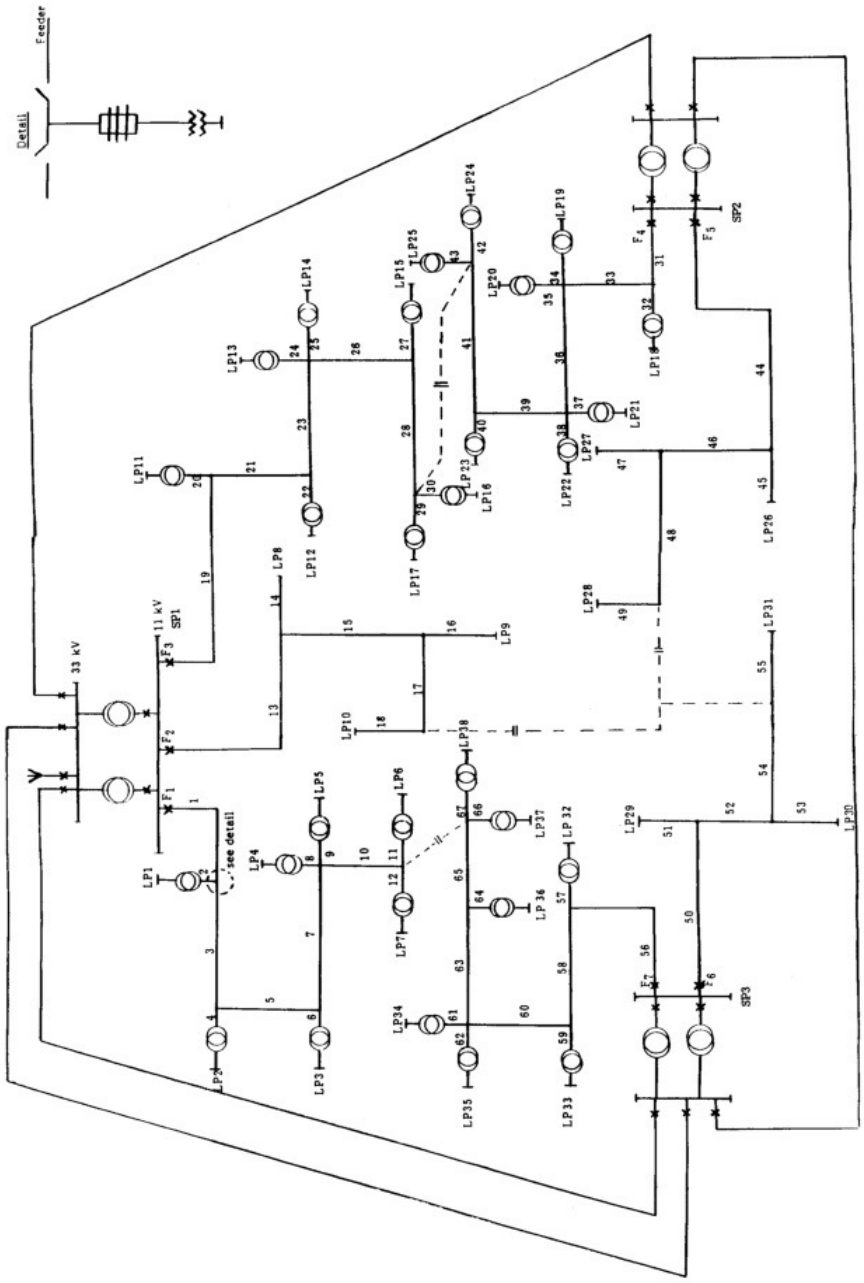

Figure 3.1: Distribution System of RBTS

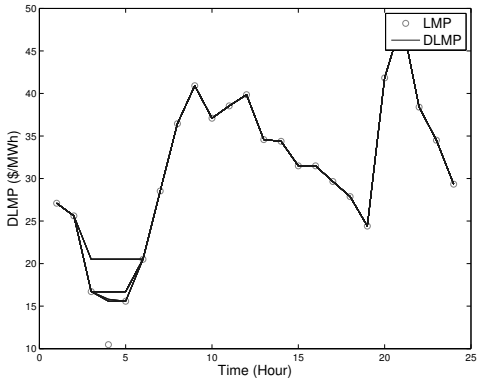

Figure 3.2: LMPs and DLMPs for Case 1 under 100% EV Load Penetration

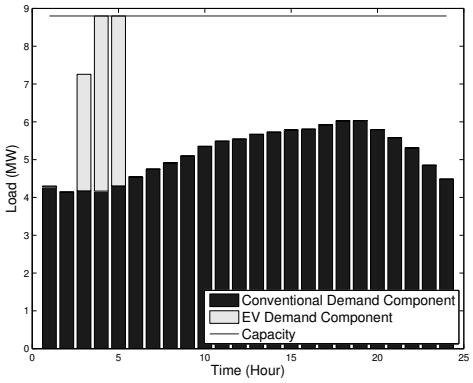

Figure 3.3: Line 1 Loading with DLMPs for Case 1 under 100% EV Load Penetration

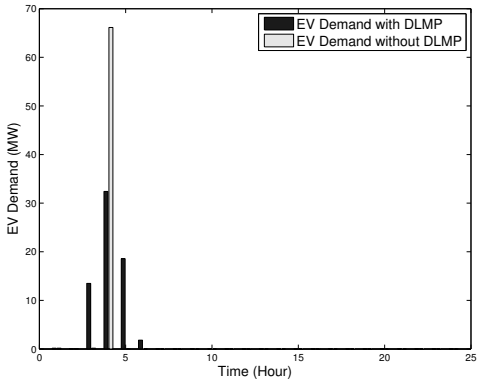

Figure 3.4: EV Demand with DLMPs for Case 1 under 100% EV Load Penetration

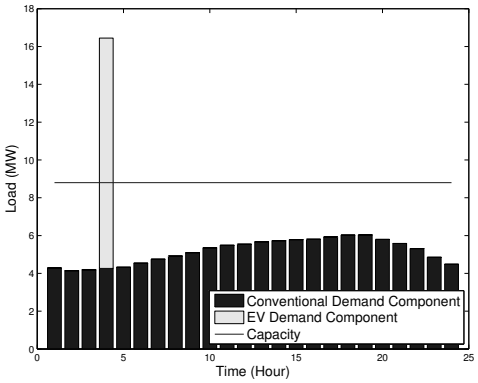

Figure 3.5: Line 1 Loading without DLMPs for Case 1 under 100% EV Load Penetration

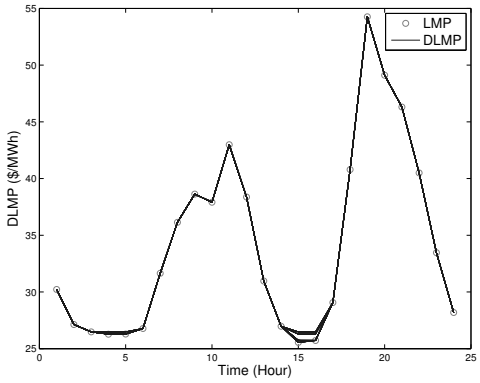

Figure 3.6: LMPs and DLMPs for Case 2 under 100% EV Load Penetration

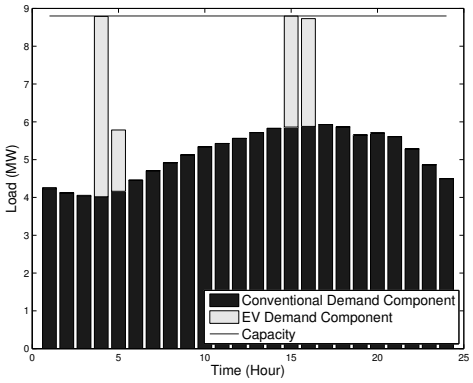

Figure 3.7: Line 1 Loading with DLMPs for Case 2 under 100% EV Load Penetration

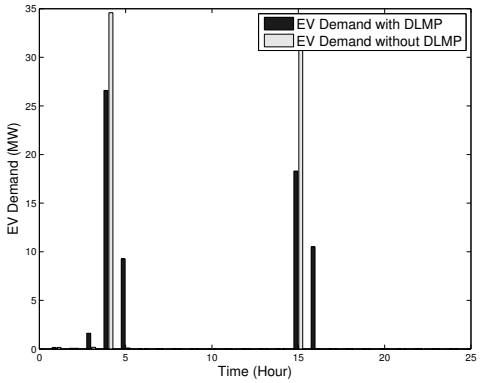

Figure 3.8: EV Demand with DLMPs for Case 2 under 100% EV Load Penetration

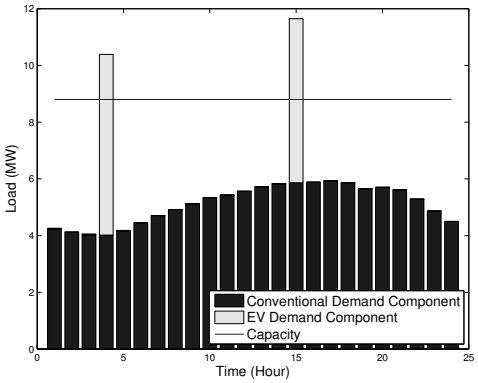

Figure 3.9: Line 1 Loading without DLMPs for Case 2 under 100% EV Load Penetration

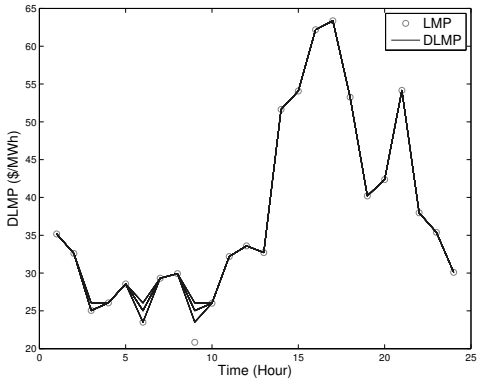

Figure 3.10: LMPs and DLMPs for Case 3 under 100% EV Load Penetration

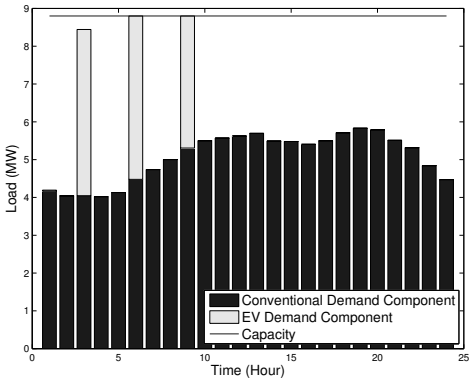

Figure 3.11: Line 1 Loading with DLMPs for Case 3 under 100% EV Load Penetration

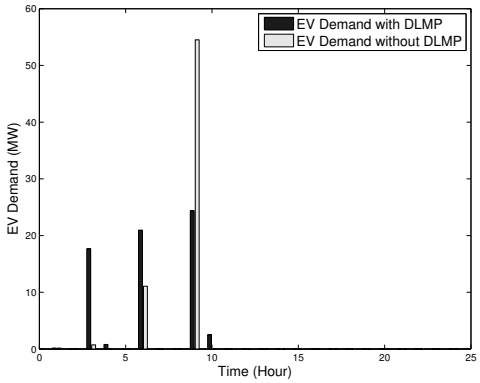

Figure 3.12: EV Demand with DLMPs for Case 3 under 100% EV Load Penetration

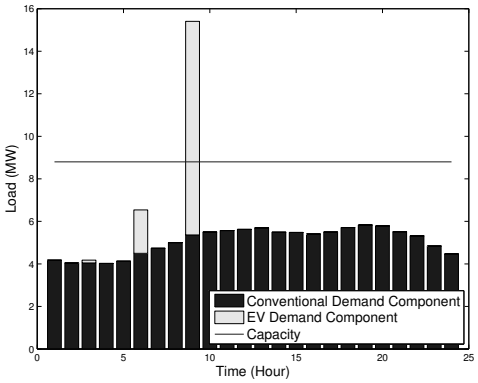

Figure 3.13: Line 1 Loading without DLMPs for Case 3 under 100% EV Load Penetration

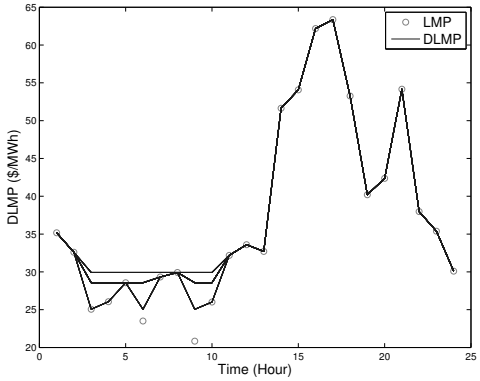

Figure 3.14: LMPs and DLMPs for Case 3 under 200% EV Load Penetration

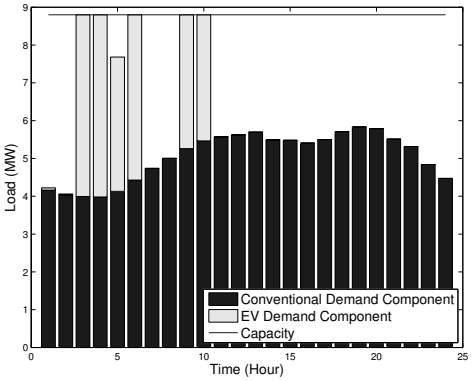

Figure 3.15: Line 1 Loading with DLMPs for Case 3 under 200% EV Load Penetration

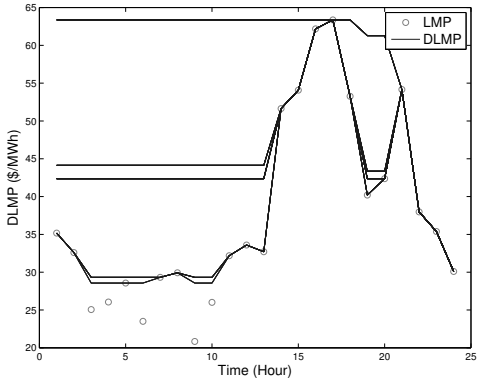

Figure 3.16: LMPs and DLMPs for Case 3 under 500% EV Load Penetration

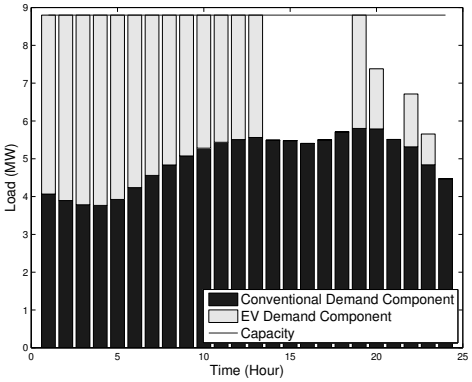

Figure 3.17: Line 1 Loading with DLMPs for Case 3 under 500% EV Load Penetration

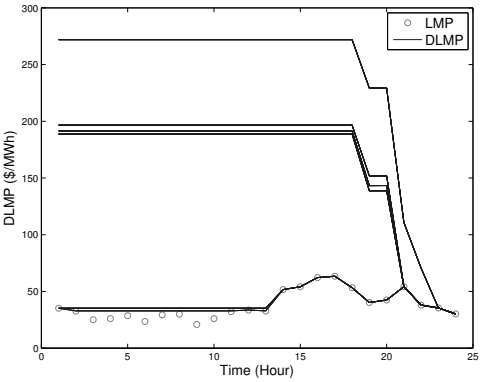

Figure 3.18: LMPs and DLMPs for Case 3 under 1000% EV Load Penetration

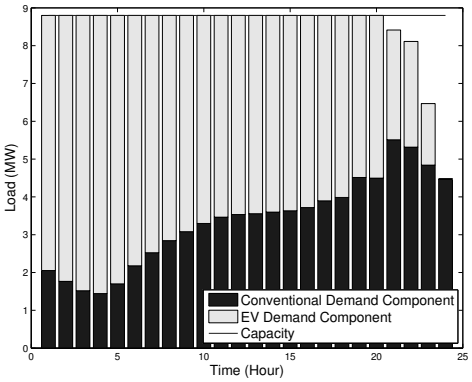

Figure 3.19: Line 1 Loading with DLMPs for Case 3 under 1000% EV Load Penetration

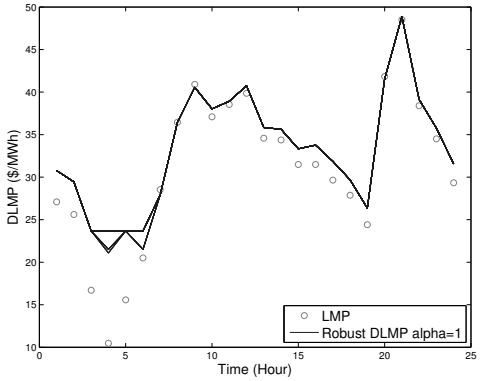

Figure 3.20: LMPs and Robust DLMPs for Case 1 with $\alpha = 1$

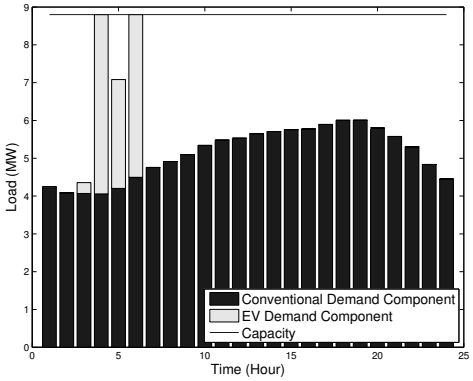

Figure 3.21: Line 1 Loading with Robust DLMPs for Case 1 with $\alpha = 1$

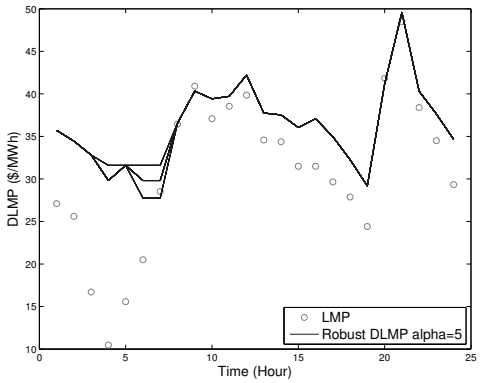

Figure 3.22: LMPs and Robust DLMPs for Case 1 with $\alpha = 5$

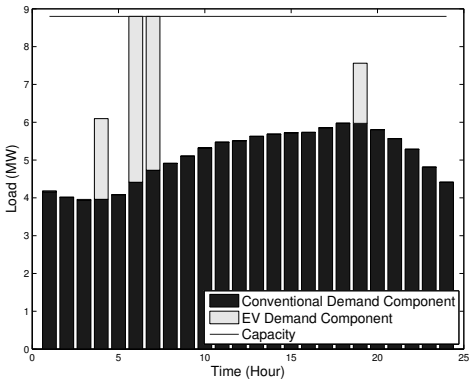

Figure 3.23: Line 1 Loading with Robust DLMPs for Case 1 with $\alpha = 5$

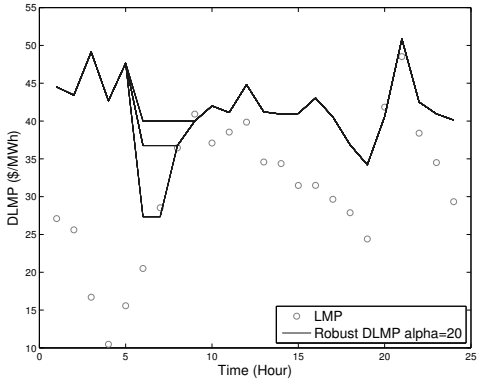

Figure 3.24: LMPs and Robust DLMPs for Case 1 with $\alpha = 20$

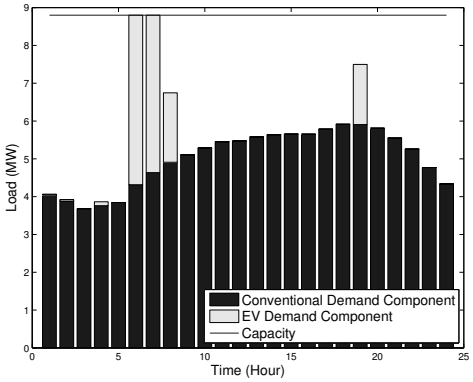

Figure 3.25: Line 1 Loading with Robust DLMPs for Case 1 with $\alpha = 20$

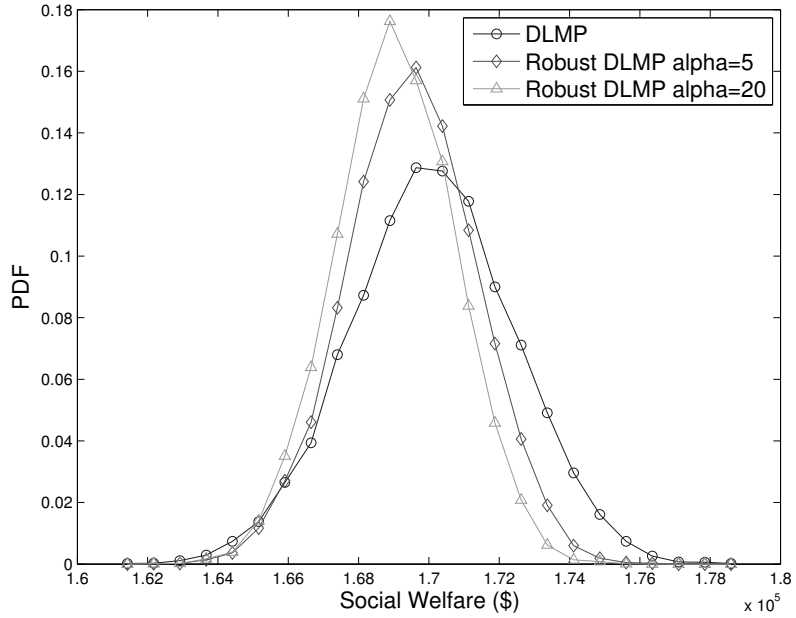

Figure 3.26: Probability Density Function of Social Welfare under DLMPs and Robust DLMPs for Case 1

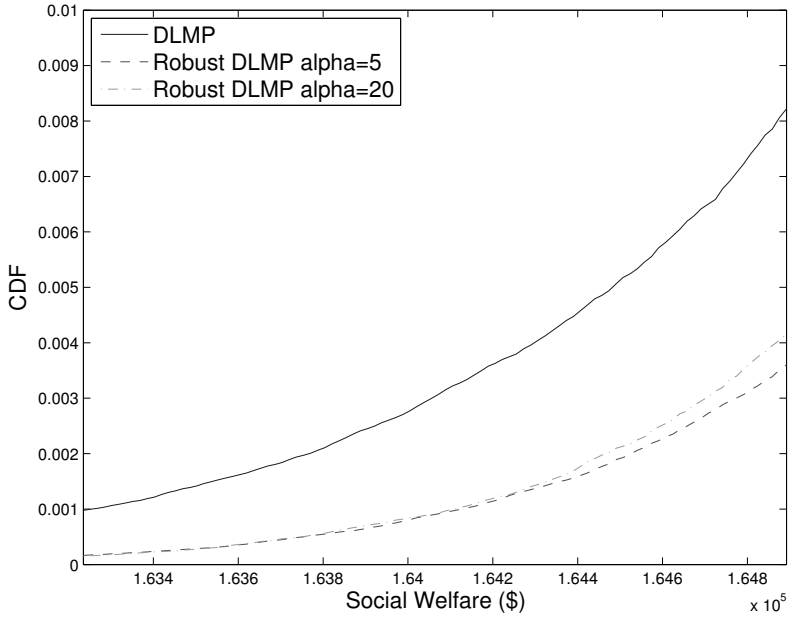

Figure 3.27: Cumulative Density Function of Social Welfare under DLMPs and Robust DLMPs for Case 1

Chapter 4

Concluding Remarks

This dissertation investigates two topics in wholesale market design for the existing and future power systems – CB and DLMP. A key link that connects these two topics is market design - determining how to create proper incentives to compensate market participants that ensures efficiency and reliability of the power grid.

In Chapter 2, we investigate whether the CAISO's existing two-settlement electricity markets are efficient, and whether markets efficiency is improved by CB, based on the zero-profit condition of Jensen (1978). Our backtest results show that our trading strategy continues to be profitable in the post-CB period, but the profitability decreases substantially. The decrease in profitability in the post-CB period indicates the improvement of market efficiency, and demonstrates the benefit of CB. The profitability in the post-CB period, however, conveys empirical implications that can be interpreted differently, depending on the level of competition and the level of risk aversion of virtual traders. Although we tend to attribute the existence of profitable arbitrage opportunities in the CAISO's existing two-settlement electricity markets to market inefficiency, we cannot exclude the possibility that the profitability simply reflects incentives to induce speculative behavior. Due to limited market data, it is difficult to distinguish whether this profitability level can persist in the long run or can be explained by some short run equilibrium. Further investigation is required to fully resolve this ambiguity.

In Chapter 3, an integrated DLMP concept is proposed to address the problem of congestion alleviation on the distribution network faced by future power systems. By design, it can be adopted under the existing wholesale market design for achieving economic allocation of both the EV demand and the conventional demand subject to line capacity constraints. Under perfect competition, we show that DLMPs provide financial incentives to achieve the socially optimal charging schedule in a decentralized system where market participants respond to DLMPs by maximizing their individual net surplus. In the presence of price uncertainty, a robust DLMP method is developed to coordinate EV charging schedule. Case studies based on the RBTS electric distribution network and the Danish driving data show the efficacy of the proposed DLMP and robust DLMP concept. However, it is still unclear whether the use of DLMPs can incentivize EV aggregators with market power, and whether DLMPs can

induce demand side flexibility for renewable integration. Further investigation might be able to shed additional light on these questions.

As many questions are still left unanswered in these topics, we sincerely hope this dissertation lays the groundwork for some further research in electricity market design.

Bibliography

Allan, Ronald N et al. (1991). "A reliability test system for educational purposes-basic distribution system data and results". In: *Power Systems, IEEE Transactions on* 6.2, pp. 813–820.

Anderson, Ronald W and Jean-Pierre Danthine (1983). "Hedger diversity in futures markets". In: *The Economic Journal*, pp. 370–389.

Azevedo, Inês M Lima, M Granger Morgan, and Lester Lave (2011). "Residential and Regional Electricity Consumption in the US and EU: How Much Will Higher Prices Reduce CO¡ sub¿ 2¡/sub¿ Emissions?" In: *The Electricity Journal* 24.1, pp. 21–29.

Backus, David K, Silverio Foresi, and Chris I Telmer (2001). "Affine term structure models and the forward premium anomaly". In: *The Journal of Finance* 56.1, pp. 279–304.

Baillie, Richard T and Rehim Kilic (2006). "Do asymmetric and nonlinear adjustments explain the forward premium anomaly?" In: *Journal of International Money and Finance* 25.1, pp. 22–47.

Bekaert, Geert and Robert J Hodrick (1993). "On biases in the measurement of foreign exchange risk premiums". In: *Journal of International Money and Finance* 12.2, pp. 115–138.

Ben-Tal, Aharon, Arkadi Nemirovski, and Cees Roos (2002). "Robust solutions of uncertain quadratic and conic-quadratic problems". In: *SIAM Journal on Optimization* 13.2, pp. 535–560.

Benth, Fred Espen, Álvaro Cartea, and Rüdiger Kiesel (2008). "Pricing forward contracts in power markets by the certainty equivalence principle: explaining the sign of the market risk premium". In: *Journal of Banking & Finance* 32.10, pp. 2006–2021.

Bertsimas, Dimitris et al. (2013). "Adaptive robust optimization for the security constrained unit commitment problem". In: *Power Systems, IEEE Transactions on* 28.1, pp. 52–63.

Bessembinder, Hendrik and Michael L Lemmon (2002). "Equilibrium pricing and optimal hedging in electricity forward markets". In: *the Journal of Finance* 57.3, pp. 1347–1382.

Bohn, Roger E, Michael C Caramanis, and Fred C Schweppe (1984). "Optimal pricing in electrical networks over space and time". In: *The Rand Journal of Economics*, pp. 360–376.

Cartea, Álvaro and Pablo Villaplana (2008). "Spot price modeling and the valuation of electricity forward contracts: The role of demand and capacity". In: *Journal of Banking & Finance* 32.12, pp. 2502–2519.

Christie, Richard D, Bruce F Wollenberg, and Ivar Wangensteen (2000). "Transmission management in the deregulated environment". In: *Proceedings of the IEEE* 88.2, pp. 170–195.

Clement-Nyns, Kristien, Edwin Haesen, and Johan Driesen (2010). "The impact of charging plug-in hybrid electric vehicles on a residential distribution grid". In: *Power Systems, IEEE Transactions on* 25.1, pp. 371–380.

De Jong, Cyriel (2006). "The nature of power spikes: A regime-switch approach". In: *Studies in Nonlinear Dynamics & Econometrics* 10.3.

Deng, Shijie (2000). *Stochastic models of energy commodity prices and their applications: Mean-reversion with jumps and spikes*. University of California Energy Institute.

Dyke, Kevin J, Nigel Schofield, and Mike Barnes (2010). "The impact of transport electrification on electrical networks". In: *Industrial Electronics, IEEE Transactions on* 57.12, pp. 3917–3926.

Fama, Eugene F (1970). "Efficient capital markets: A review of theory and empirical work*". In: *The journal of Finance* 25.2, pp. 383–417.

— (1984). "Forward and spot exchange rates". In: *Journal of Monetary Economics* 14.3, pp. 319–338.

Fama, Eugene F and Kenneth R French (1987). "Commodity futures prices: Some evidence on forecast power, premiums, and the theory of storage". In: *Journal of Business*, pp. 55–73.

Garcia-Gonzalez, Javier et al. (2008). "Stochastic joint optimization of wind generation and pumped-storage units in an electricity market". In: *Power Systems, IEEE Transactions on* 23.2, pp. 460–468.

Glatvitsch, H and Fernando Alvarado (1998). "Management of multiple congested conditions in unbundled operation of a power system". In: *Power Systems, IEEE Transactions on* 13.3, pp. 1013–1019.

Haldrup, Niels and Morten Ørregaard Nielsen (2006). "A regime switching long memory model for electricity prices". In: *Journal of Econometrics* 135.1, pp. 349–376.

Hansen, Lars Peter and Robert J Hodrick (1980). "Forward exchange rates as optimal predictors of future spot rates: An econometric analysis". In: *The Journal of Political Economy*, pp. 829–853.

Hastings, W Keith (1970). "Monte Carlo sampling methods using Markov chains and their applications". In: *Biometrika* 57.1, pp. 97–109.

Heydt, GT (1983). "The impact of electric vehicle deployment on load management straregies". In: *Power Apparatus and Systems, IEEE Transactions on* 5, pp. 1253–1259.

Hirshleifer, David (1990). "Hedging pressure and futures price movements in a general equilibrium model". In: *Econometrica: Journal of the Econometric Society*, pp. 411–428.

Hogan, William W (1992). "Contract networks for electric power transmission". In: *Journal of Regulatory Economics* 4.3, pp. 211–242.

Huang, Shaojun et al. (2014). *Distribution Locational Marginal Pricing through Quadratic Programming for Congestion Management in Distribution Networks*. Tech. rep. Working Paper.

Huisman, Ronald and Ronald Mahieu (2003). "Regime jumps in electricity prices". In: *Energy economics* 25.5, pp. 425–434.

Janczura, Joanna and Rafal Weron (2010). "An empirical comparison of alternate regime-switching models for electricity spot prices". In: *Energy Economics* 32.5, pp. 1059–1073.

Jensen, Michael C (1978). "Some anomalous evidence regarding market efficiency". In: *Journal of financial economics* 6.2, pp. 95–101.

Jha, Akshaya and Frank A Wolak (2013). *Testing for market efficiency with transactions costs: An application to convergence bidding in wholesale electricity markets*. Tech. rep. Working Paper.

Kempton, Willett and Jasna Tomić (2005a). "Vehicle-to-grid power fundamentals: calculating capacity and net revenue". In: *Journal of power sources* 144.1, pp. 268–279.

— (2005b). "Vehicle-to-grid power implementation: From stabilizing the grid to supporting large-scale renewable energy". In: *Journal of Power Sources* 144.1, pp. 280–294.

Keynes, John Maynard (1923). "Some aspects of commodity markets". In: *Manchester Guardian Commercial: European Reconstruction Series* 13, pp. 784–786.

Li, Fangxing and Rui Bo (2007). "DCOPF-based LMP simulation: algorithm, comparison with ACOPF, and sensitivity". In: *Power Systems, IEEE Transactions on* 22.4, pp. 1475–1485.

Limpaitoon, Tanachai, Yihsu Chen, and Shmuel S Oren (2011). "The impact of carbon cap and trade regulation on congested electricity market equilibrium". In: *Journal of Regulatory Economics* 40.3, pp. 237–260.

Liu, Weijia and Fushuan Wen (2014). "Discussion on "Distribution Locational Marginal Pricing for Optimal Electric Vehicle Charging Management"". In: *Power Systems, IEEE Transactions on* 29.4, pp. 1866–1866.

Longstaff, Francis A and Ashley W Wang (2004). "Electricity forward prices: a high-frequency empirical analysis". In: *The Journal of Finance* 59.4, pp. 1877–1900.

Lopes, João A Peças, Filipe Joel Soares, and Pedro Miguel Rocha Almeida (2011). "Integration of electric vehicles in the electric power system". In: *Proceedings of the IEEE* 99.1, pp. 168–183.

Lucia, Julio J and Eduardo S Schwartz (2002). "Electricity prices and power derivatives: Evidence from the nordic power exchange". In: *Review of Derivatives Research* 5.1, pp. 5–50.

Maitra, Arindam et al. (2010). "Grid impacts of plug-in electric vehicles on Hydro Quebec's distribution system". In: *Transmission and Distribution Conference and Exposition, 2010 IEEE PES*. IEEE, pp. 1–7.

Malcolm, Scott A and Stavros A Zenios (1994). "Robust optimization for power systems capacity expansion under uncertainty". In: *Journal of the operational research society*, pp. 1040–1049.

Modigliani, Franco and Leah Modigliani (1997). "Risk-adjusted performance". In: *The Journal of Portfolio Management* 23.2, pp. 45–54.

Mount, Timothy D, Yumei Ning, and Xiaobin Cai (2006). "Predicting price spikes in electricity markets using a regime-switching model with time-varying parameters". In: *Energy Economics* 28.1, pp. 62–80.

Nemirovski, Arkadi and Alexander Shapiro (2006). "Convex approximations of chance constrained programs". In: *SIAM Journal on Optimization* 17.4, pp. 969–996.

Pereira, MVF and Leontina MVG Pinto (1991). "Multi-stage stochastic optimization applied to energy planning". In: *Mathematical Programming* 52.1-3, pp. 359–375.

Rockafellar, R Tyrrell and Stanislav Uryasev (2000). "Optimization of conditional value-at-risk". In: *Journal of risk* 2, pp. 21–42.

Rolfo, Jacques (1980). "Optimal hedging under price and quantity uncertainty: The case of a cocoa producer". In: *The Journal of Political Economy*, pp. 100–116.

Rotering, Niklas and Marija Ilic (2011). "Optimal charge control of plug-in hybrid electric vehicles in deregulated electricity markets". In: *Power Systems, IEEE Transactions on* 26.3, pp. 1021–1029.

Samuelson, Paul A (1965). "Proof that properly anticipated prices fluctuate randomly". In: *Industrial management review* 6.2, pp. 41–49.

Shawky, Hany A, Achla Marathe, and Christopher L Barrett (2003). "A first look at the empirical relation between spot and futures electricity prices in the United States". In: *Journal of Futures markets* 23.10, pp. 931–955.

Sortomme, Eric and Mohamed A El-Sharkawi (2011). "Optimal charging strategies for unidirectional vehicle-to-grid". In: *Smart Grid, IEEE Transactions on* 2.1, pp. 131–138.

— (2012). "Optimal scheduling of vehicle-to-grid energy and ancillary services". In: *Smart Grid, IEEE Transactions on* 3.1, pp. 351–359.

Stoft, Steven (2002). "Power system economics". In: *JOURNAL OF ENERGY LITERATURE* 8, pp. 94–99.

Sundstrom, Olle and Carl Binding (2012). "Flexible charging optimization for electric vehicles considering distribution grid constraints". In: *Smart Grid, IEEE Transactions on* 3.1, pp. 26–37.

Takriti, Samer, Benedikt Krasenbrink, and Lilian S-Y Wu (2000). "Incorporating fuel constraints and electricity spot prices into the stochastic unit commitment problem". In: *Operations Research* 48.2, pp. 268–280.

Taylor, Jason et al. (2010). "Evaluations of plug-in electric vehicle distribution system impacts". In: *Power and Energy Society General Meeting, 2010 IEEE*. IEEE, pp. 1–6.

Tomić, Jasna and Willett Kempton (2007). "Using fleets of electric-drive vehicles for grid support". In: *Journal of Power Sources* 168.2, pp. 459–468.

Wang, Qianfan, J-P Watson, and Yongpei Guan (2013). "Two-stage robust optimization for Nk contingency-constrained unit commitment". In: *Power Systems, IEEE Transactions on* 28.3, pp. 2366–2375.

Weron, Rafał (2009). "Heavy-tails and regime-switching in electricity prices". In: *Mathematical Methods of Operations Research* 69.3, pp. 457–473.

Wong, Steven and J David Fuller (2007). "Pricing energy and reserves using stochastic optimization in an alternative electricity market". In: *Power Systems, IEEE Transactions on* 22.2, pp. 631–638.

Wu, Qiuwei et al. (2010). "Driving pattern analysis for electric vehicle (EV) grid integration study". In: *Innovative Smart Grid Technologies Conference Europe (ISGT Europe), 2010 IEEE PES*. IEEE.

Yang, Jian, Fangxing Li, and L Freeman (2003). "A market simulation program for the standard market design and generation/transmission planning". In: *Power Engineering Society General Meeting, 2003, IEEE*. Vol. 1. IEEE.

Yao, Jian, Ilan Adler, and Shmuel S Oren (2008). "Modeling and computing two-settlement oligopolistic equilibrium in a congested electricity network". In: *Operations Research* 56.1, pp. 34–47.

Zhao, Chaoyue and Yongpei Guan (2013). "Unified stochastic and robust unit commitment". In: *Power Systems, IEEE Transactions on* 28.3, pp. 3353–3361.

Zhao, Chaoyue, Jianhui Wang, et al. (2013). "Multi-stage robust unit commitment considering wind and demand response uncertainties". In: *Power Systems, IEEE Transactions on* 28.3, pp. 2708–2717.